FINAL REPORT

Improving Modeled Biogenic Isoprene Emissions under Drought Conditions and Evaluating Their Impact on Ozone Formation

AQRP Project 14-030

Prepared for: Elena

Mc-Donald-Buller
Texas Air Quality Research Program
The University of Texas at Austin

Prepared by

Qi Ying (Principal Investigator), Peng Wang,
Huilin Gao (Co-Principal Investigator)
Zachry Department of Civil Engineering
Texas A&M University

and

Gunnar W. Schade (Co-Principal Investigator), Monica Madronich
Department of Atmospheric Sciences
Texas A&M University

November, 2015

QA Requirements: Audits of Data Quality: 10% Required

Executive Summary

Emissions of isoprene during 2011 (a severe drought year) and 2007 (a relatively wet year in Texas) were estimated using an updated MEGAN (v2.10) model that considers the drought impacts on isoprene emissions. The regional soil moisture field needed for the MEGAN model was estimated using the WRF model with the Noah land surface scheme initialized with the soil moisture field from NLDAS-2 with Noah-2.8. Wilting point data needed for the drought parametrization was estimated using the Penn State CONUS-SOIL database and the soil-related hydraulic parameters from Table 2 of Chen and Dudhia [1]. While the predicted soil moisture generally agrees with observations, field measurements of soil moisture and isoprene emission at three field sites in east Texas in 2011 indicated that root zone soil moistures may not be adequately represented in the model because (i) the model may over- or under-predict grid average rainfall and/or evapotranspiration, and (ii) it does not consider differences in rooting depth between isoprene emitters. Greenhouse measurements on potted oak species revealed that there does not appear to be major physiological differences between species and that the current factor scaling isoprene emissions to drought stress adequately represents observed responses. When those are applied to the field data, differences between isoprene emitting oak species do emerge, but are more likely be related to root structure (and depth) and physiology than to average soil moisture.

The MEGAN model with its own isoprene emission factor (EF) field severely over-predicts observed isoprene concentrations from Automated gas chromatograph (Auto-GC) instruments throughout the continental United States. Alternative EF fields generated from two different versions of the Biogenic Emissions Inventory System (BEIS) models (v3.14 and v3.61) and their accompanying land use data bases (BELD3 and BELD4, respectively) from US Environmental Protection Agency were applied in the updated MEGAN model. Comparison of predicted hourly and daily averaged isoprene concentrations at all isoprene monitors in and out of Texas in a total of 14 months in 2007 and 2011 showed that the MEGAN model with EF fields from BEIS v3.61 and its input data (BELD4) could significantly improve the model capability in reproducing the observed isoprene concentrations at all locations. Predicted isoprene emissions under drought conditions considering the impact on leaf temperature alone led to increases in isoprene emissions. The magnitude of the emissions increase was reduced when the soil moisture activity factor was also considered. When both factors were considered, the resulting isoprene and ozone concentrations in both 2007 and 2011 changed only slightly (less than 1 ppb for monthly average 1-hour isoprene at locations where drought was significant, and less than 1 ppb for monthly average peak ozone concentrations).

Contents

List of Figures

List of Tables

1. Introduction

1.1 Background

Biogenic volatile hydrocarbons (BVOCs) are important precursors in atmospheric chemistry that lead to formation of ozone and secondary particulate matter in Southeast Texas [2-5]. Among the BVOCs emitted, isoprene is the most important for ozone formation in Southeast Texas due to its large emission quantities [2] and fast reaction rates with oxidants. Ozone air quality predictions thus depend on accurate isoprene and other BVOC emission estimates from regional vegetation. For either regional or global scale air quality modeling, the latter emissions, particularly isoprene, are estimated via various biogenic emission modeling systems, such as the Global Biosphere Emissions and Interactions System (GloBEIS) [6], Biogenic Emissions Inventory System version 3 (BEIS3) [7] or Model of Emissions of Gases and Aerosols from Nature (MEGAN) model [8, 9]. Modeling isoprene emissions requires various input parameters, particularly biomass distribution, leaf temperatures, and photosynthetically active radiation (PAR) levels, including their recent history. While these have been relatively well characterized, the influence of drought on isoprene emissions due to (i) effects of reduced soil water availability, and (ii) prolonged high temperatures on the photosynthetic production of the biochemical isoprene precursor inside the leaves has been less well represented in these emission models. As Texas regularly experiences drought episodes, including a severe drought in 2011, it is necessary to better understand the capability of current emission models in estimating BVOCs under drought conditions, and improve the drought effect parameterization.

A number of studies have shown that drought will affect emissions of BVOCs due to its impact on plant physiological processes[10-26], triggering responses such as reduction in stomatal conductance and photosynthesis rates. Higher ambient temperature and reduced stomatal conductance can also lead to higher leaf surface temperature, which further affects the BVOC emissions. In GloBEIS 3, the influence of drought on isoprene emissions is accounted for using a simple linear parameterization that scales the emission rates based on the widely used Palmer Drought Severity Index (PDSI). In MEGAN 2.1, the isoprene emission rate is scaled by the difference between soil moisture (volumetric water content) and the wilting point. Both approaches were derived based on limited observations and the appropriateness of these simple, linear parameterizations has not been extensively field tested yet. The most recent version of the BEIS3 model (version 3.14) does not consider drought impacts on biogenic emissions.

1.2 Objectives

The objectives of this research are to (i) evaluate the BVOC emission model, MEGAN 2.1, with a focus on isoprene predictions, using the default drought parameterization scheme; (ii) evaluate the capability of the WRF model in predicting meteorological conditions for air quality simulations under drought conditions; and (iii) evaluate the sensitivity of CMAQ ozone predictions in Southeast Texas when using different drought parameterizations for isoprene emissions.

2. Regional Isoprene and Ozone Modeling Under Drought Condition using CMAQ

2.1 Air quality modeling domain and model setup

A three-level nested domain is used in this study (See Figure 1), following the RPO Comprehensive Air Model with Extensions (CAMx) domains used by the TCEQ for ozone air quality modeling. Map projection parameters, and other details such as vertical domain structures, are described in detail in: http://www.tceq.texas.gov/airquality/airmod/rider8/modeling/domain. In summary, the 36-km, 12-km and 4-km resolution domains have sizes of 148x112, 149x110 and 191x218 grid cells. All have the same vertical layer structure, with 28 stretching layers up to approximately 15 km above surface. The first layer thickness is approximately 34 m.
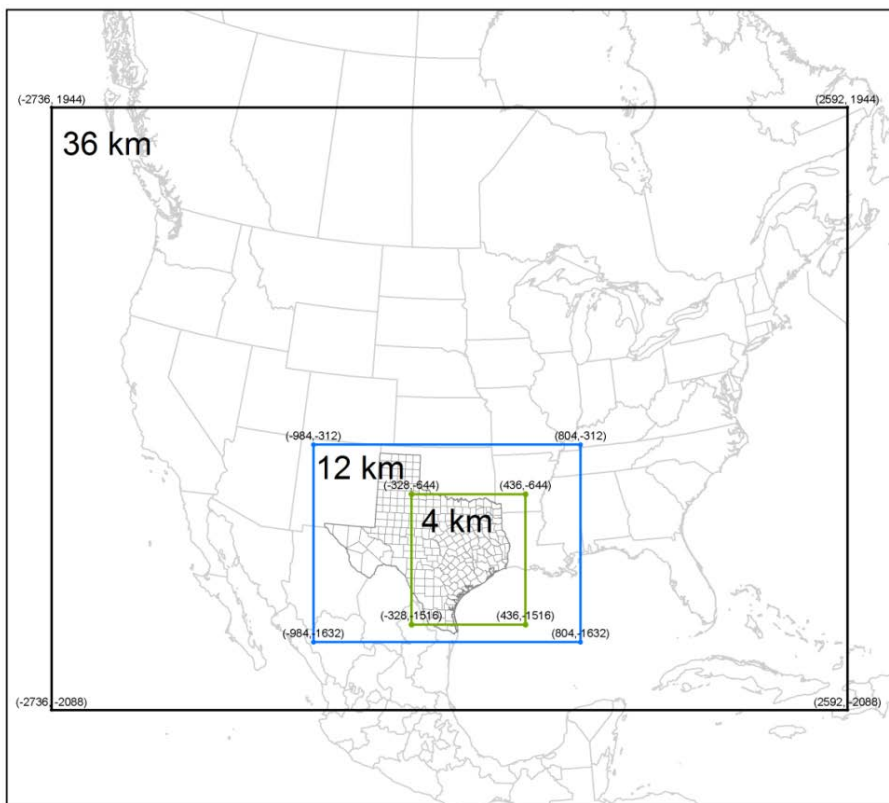
Figure 1 Three-level nested CMAQ model domain.

The CMAQ (v5.0.2) model configuration is listed in Table 1. Previously, online dust emission calculation depended on the USGS land use information used in the inline biogenic emission module. The CMAQ model was modified to allow online windblown dust emission simulation using the 20-category Moderate Resolution Imaging Spectroradiometer (MODIS) land use classification data. The equation to estimate the vertical dust flux was modified to follow that of Shaw et al. [27] and the PM_{10} fraction in total PM emissions was estimated based on Choi and Fernando [28]. The same equations were used in an offline dust module in previous applications of CMAQ in China [29, 30]. Photolysis rates are also calculated inline to correctly account for the reduction of actinic flux due to aerosol loading.

Table 1 Configuration of CMAQ

Options	Value	Notes
Mechanism	cb05tucl	CB05 mechanism, including updates in toluene chemistry, homogeneous hydrolysis rate constants for N_2O_5, and chlorine chemistry.
Aerosol	AERO6	Version 6 of the aerosol mechanism - treatment of trace metals; aging of primary organics
Solver	EBI	
Plume rise	Inline	7 point source sectors
Dry deposition	Inline	
Dust emissions	Inline	Modified to use MODIS landuse type.
Photolysis	Inline	
Vertical diffusion	ACM2	
Lighting NOx	Not included	
Surface HONO	Enabled	
Biogenic emission	Pre-calculated MEGAN	

2.2 Meteorological modeling with Weather Research and Forecast (WRF) model and anthropogenic emission processing

The meteorological inputs are generated by the Weather Research and Forecasting (WRF) model v3.6. The three-level nested WRF domains follow the same setup as those used by the TCEQ for ozone modeling (http://www.tceq.texas.gov/airquality/airmod/rider8/modeling/domain). In summary, for the North America (36-km), South US (12-km) and Texas (4-km) domains, there are 163x129, 175x139 and 217x289 grid cells in the horizontal direction. There are 43 stretching vertical layers, reaching approximately 20000 m above surface. The simulations are initialized using the North American Regional Reanalysis (NARR) data (from National Oceanic and Atmospheric Administration (NOAA), http://www.esrl.noaa.gov/psd/data/gridded/data.narr.html) with 32-km horizontal resolution and 3-h time resolution, for all variables except soil moisture, which was initialized using predictions from the North American Land Data Assimilation System (NLDAS). Sea surface temperature was initialized using daily satellite-based observation (available from http://polar.ncep.noaa.gov/sst/oper/Welcome.html). The leaf area index (LAI) was based on the 8-day MODIS LAI product (MOD15A2) for 2011, and land use/land cover classifications were also updated using the 2011 MODIS product (MOD12Q1). Land surface processes were simulated using the Noah land surface model.

A summary of the emission processing for NEI 2011 is given below. The National Emission Inventory (NEI) 2011 source sectors, as shown in Table 2, were processed using SMOKE v3.5.1. Details of the NEI 2011 as used in the EPA's 2011v6 platform can be found in ftp://ftp.epa.gov/EmisInventory/2011v6/v1platform/README_2011v6_package.txt. A short summary regarding point and on-road mobile source sectors is included in the following. In NEI 2011, emissions from electrical generating units (EGUs) are divided into three sectors: *ptegu*, *ptegu_pk* and *ptnonipm*. In older NEIs, the *ptegu* sector was called "*ptipm*" or "Integrated Planning Model". This sector incorporates Continuous Emissions Monitoring (CEM) hourly

emissions for a majority of sources. The *ptegu_pk* sector includes units that only operate during times of peak demand, rather than for most or all of the year, as defined by EPA's Clean Air Markets Division (CAMD). Peaking units are kept in a separate sector by the EPA for the purposes of source apportionment in future modeling applications. This sector incorporates CEM hourly emissions for all sources. The *ptnonipm* sector includes emissions from all other industrial point sources. The run scripts provided with the 2011v6 platform were modified so that emissions from all three CMAQ modeling domains can be generated. For the 4-km domain, spatial allocation surrogates for the United States were provided by the US EPA. However, spatial allocation surrogates for Mexico is not available but the 4-km domain does contain a small fraction of Mexico in the lower left corner. The Spatial Allocator program developed by the US EPA was used to re-grid the 12-km resolution emissions (othar and othon, see Table 2) into 4-km resolution emissions.

Table 2 Source sectors processed using SMOKE 3.5.1 for CMAQ modeling

Source sectors	Type	Notes
afdust	nonpoint	Area fugitive dust
ag	nonpoint	Agriculture ammonia sector
c1c2rail	nonroad	Class 1/Class 2 commercial marine vessels and locomotives
c3marine	nonroad	treated as point sources; Class 3 commercial marine vessels
nonpoint	nonpoint	Other non-point sources
nonroad	nonroad	Non-road mobile equipment sources
np_oilgas	nonpoint	Oil and gas extraction-related emissions
othar	nonpoint/nonr oad	Area and nonroad mobile sources from Canada and Mexico
othon	onroad	Onroad mobile sources from Canada and Mexico
othpt	point	Offshore Class 3 CMV; drilling platforms; Canada and Mexico point sources
ptegu	point	Electrical generating unit; non-peaking units
ptegu_pk	point	Electrical generating unit; peaking units
ptfire	point	Wildfire and prescribed burning
ptnonipm	point	Other industrial point sources
pt_oilgas	point	Oil and gas extraction-related emissions
rateperdistance_cat x	onroad, RPD	California and Texas on-road emissions[1]; on-network emissions[2]
rateperdistance_no RFL	onroad, RPD	On-road emissions for other states; on-network emissions
rateperdistance_Rf only	onroad, RPD	Refuling emissions[3]; all states; on-network emissions
rateperprofile_catx	onroad, RPP	California and Texas on-road emissions; off-network emissions, fuel vapor venting
rateperprofile	onroad, RPP	On-road emissions for other states; off-network emissions, fuel vapor venting
ratepervehicle_catx	onroad, RPV	California and Texas on-road emissions; off-network emissions, non-venting
ratepervehicle_noR FL	onroad, RPV	On-road emissions for other states; off-network emissions, non-venting
ratepervehicle_RF Lonly	onroad, RPV	On-road emissions for other states; off-network emissions, non-venting; refuel only
rwc	nonpoint	Residential wood combustion

[1] Total of the California and Texas emissions were adjusted to match the States' reported totals.
[2] On-network emissions include running emissions from rural and urban roads.
[3] Off-network emissions include start, evaporative and extended idle emissions.

2.3 Modeling biogenic isoprene emissions using MEGAN

2.3.1 Update of MEGAN model to include drought effect on isoprene emissions

2.3.1.1 Parameterization of activity factor γ_{SM}

The MEGAN model (FORTRAN version v2.10, hereafter v2.10 for simplicity) was updated to include the parameterization of activity factor γ_{SM} as a function of soil moisture and wilting point soil moisture, as documented in Guenther et al.[8]:

$$
\begin{aligned}
\gamma_{SM,isoprene} &= 1, & &\text{for } \theta > \theta_1 \\
\gamma_{SM,isoprene} &= (\theta - \theta_w)/\Delta\theta_1, & &\text{for } \theta_w < \theta < \theta_1 \,,\; \theta_1 = \Delta\theta_1 + \theta_w \\
\gamma_{SM,isoprene} &= 0, & &\text{for } \theta < \theta_w
\end{aligned}
\tag{1}
$$

where θ is volumetric soil moisture, θ_w is soil moisture at the wilting point, and $\Delta\theta_1$ is an empirical soil moisture amount of 4% ($\Delta\theta_1$=0.04). According to this scheme, no isoprene is emitted after soil moisture drops below the wilting point, as shown in Figure 2.
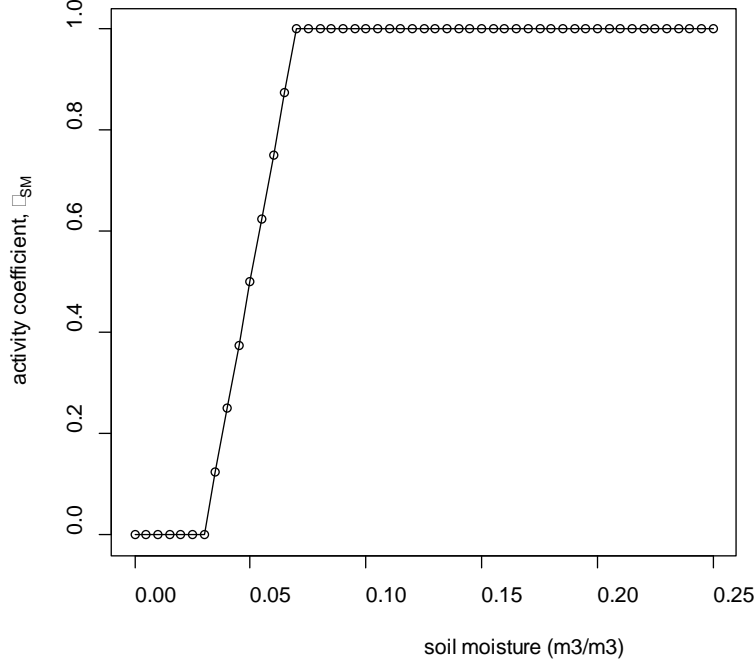
Figure 2 Illustration of the default drought parameterization of γ_{SM} using θ_w=3%.

The Noah land surface model provides soil moisture at 4 different levels. The MEGAN processors were modified to read and process the additional soil moisture data. The EMPROC module in MEGAN v2.10 was modified to calculate γ_{SM} for each grid cell. The overall γ_{SM} at grid cell (i,j) is calculated using the following equation:

$$
\gamma_{SM}^{i,j} = \sum_{n=1}^{N_{PFT}} \sum_{z=1}^{N_{layer}} PFT^{i,j}(n)\xi(z,n)\max\left(0,\min\left(1,\frac{\theta^{i,j}(z)-\theta_w^{i,j}(z)}{\Delta\theta_1}\right)\right)
\tag{2}
$$

where N_{PFT} and N_{layer} are number of plant functional types (PFTs) and soil layers, respectively. PFT(n) is fractional plant functional type for the nth PFT. ξ is the root zone fraction in the zth soil

14

layer for the nth PFT. The root zone fraction data are based on the global root zone distribution data as reported by Zeng[31].

The modified MEGAN is backward compatible with the original MEGAN and can be run without additional soil moisture data. The parameterization of γ_{SM} can also be turned off to use a default value of 1 during MEGAN execution by an environmental variable defined in the run script.

Modifications were also made to the Meteorology Chemistry Interface Processor (MCIP) program, the CMAQ utility program to process WRF meteorology outputs and generate meteorology input files for CMAQ. The modified MCIP program now saves soil moisture at all four Noah levels, instead of the first layer.

A 1x1 km resolution wilting point data set was prepared using gridded soil texture from the Penn State CONUS-SOIL database and the soil-related hydraulic parameters from Table 2 of Chen and Dudhia [1]. Wilting point in other regions was based on the Global Gridded Surfaces of Selected Soil Characteristics (IGBP-DIS) data set from ORNL (http://webmap.ornl.gov/wcsdown/dataset.jsp?ds_id=569), which as a resolution of 5'. Figure 3 shows the regional distribution of the first (a, 0-0.1 m), second (b, 0.1-0.4 m), third (c, 0.4-1 m) and fourth (d, 1-2 m) layer wilting points in the 4-km domain.
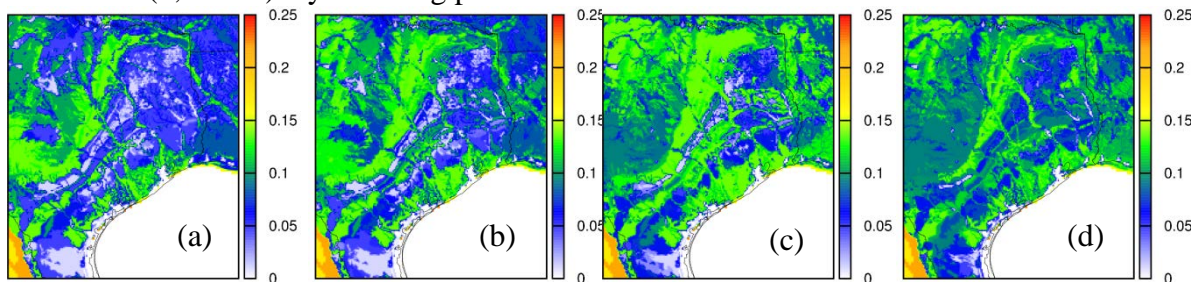
Figure 3 Regional distribution of wilting point in the 4-km domain. Units are m^3 m^{-3}.

2.3.1.1 Drought impact on stomatal resistance and left temperature

Reduced soil moisture could also affect the leaf surface temperature by increasing stomatal resistance thus reducing plant transpiration. Increased leaf temperature can lead to higher emission rates of isoprene. The canopy model in MEGAN v2.10 already includes a parameterization of the drought effect on leaf temperature using the Palmer Drought Severity Index (PDSI). However, the original MEGAN v2.10 does not require PDSI as its input and the PDSI array is not assigned an initial value (a detailed discussion of the problem in MEGAN is included in Appendix A). In this study, MEGAN v2.10 is updated to read a gridded monthly PDSI field[32]. The PDSI fields are downloaded from the National Center for Atmospheric Research (NCAR) website (http://www.cgd.ucar.edu/cas/catalog/climind/pdsi.html). Figure 4 and Figure 5 show the re-projected PDSI to the 36-km resolution domain for April to October 2007 and 2011, respectively. In 2007, drought occurred mainly in the southeast states of Alabama and Georgia while Texas was fairly wet. In 2011, severe drought persisted in Texas throughout the months while the northeast states were wet. In future studies, higher resolution gridded PDSI data should be used.
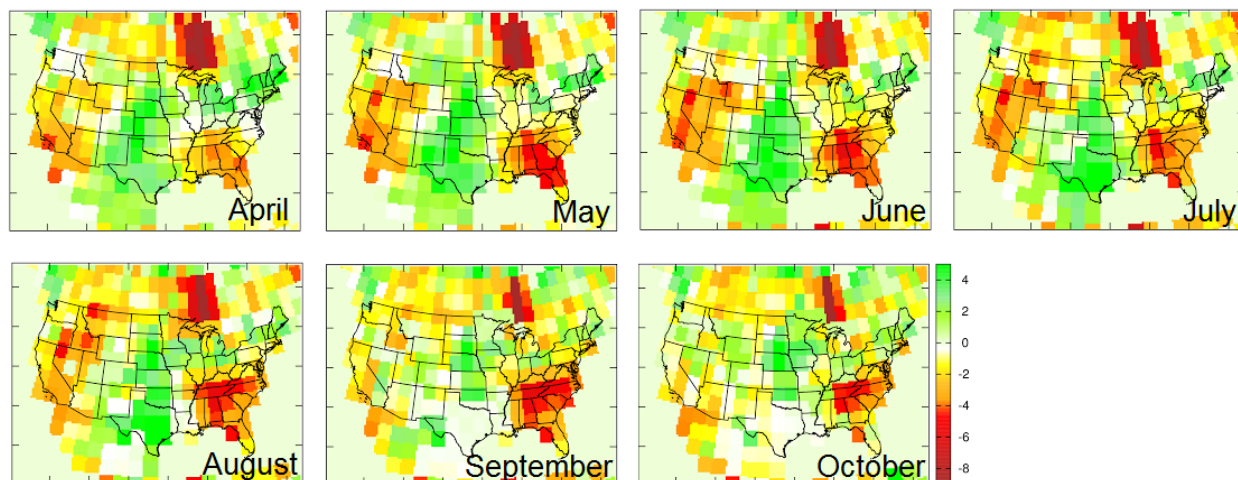
Figure 4 Gridded Palmer Drought Severity Index (PDSI) in 2.5°x2.5° re-gridded and re-projected to the 36-km model domain for April – October, 2007.
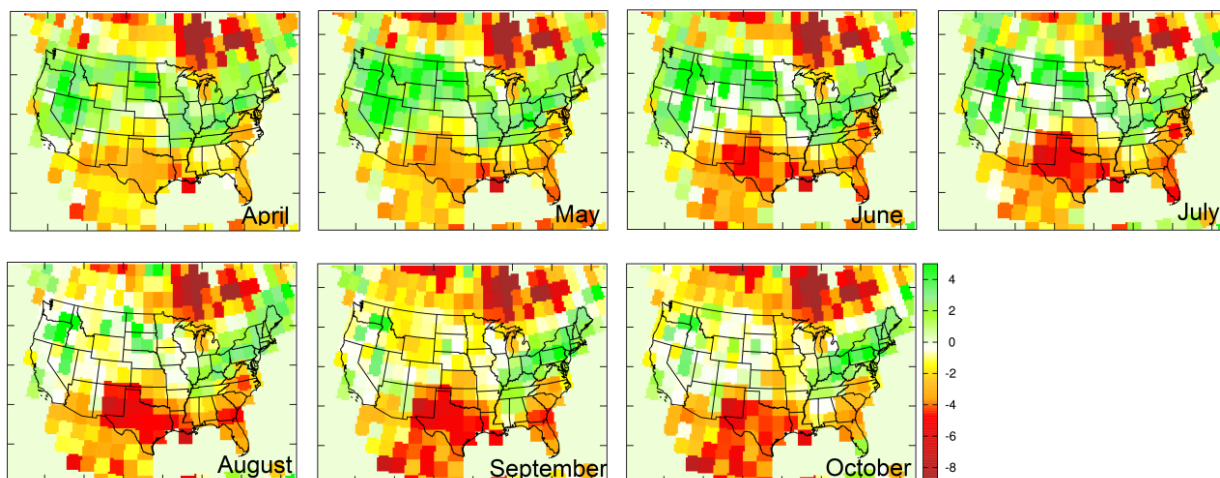
Figure 5 Same as Figure 3 but for April – October, 2011.

2.3.2 Gridded emission factor fields for MEGAN

In a simplified representation, the emission rate (F) of isoprene in MEGAN in each model grid cell ($\mu g\ h^{-1}$) can be calculated by Equation (3):

$$F = \gamma \times LAI_v \times EF \times A \tag{3}$$

where γ is a lumped correction factor (unit-less) that includes corrections for radiation, temperature, soil moisture, leaf age, and CO_2 level; LAI_v is the leaf area index for the vegetated surface (m^2 of leaf area per m^2 of vegetated surface area); EF is the emission factor of isoprene at standard conditions ($\mu g\ m^{-2}\ h^{-1}$, or more explicitly, μg VOC per m^2 of leaf surface area per hour multiplied by the vegetation cover fraction, see definition of EF below); and A is the area of the grid cell (m^2). In the default configuration, MEGAN2.1 uses a gridded EF map for isoprene emissions. The EF map was prepared based on fractional areal coverage of vegetation species in a grid cell as shown in Equation (4):

$$EF = \sum_{i=1}^{N} \chi_i \varepsilon_i \qquad (4)$$

where i is the vegetation type index, ε is the species specific emission factors (µg VOC per hour per m^2 of leaf surface area) at standard condition, χ is the fractional of the cell covered by a given vegetation emission type (m^2 vegetated surface per m^2 of ground surface), and N and is the total number of vegetation types in a grid cell. Note that the units of EF are neither µg VOC per unit ground area nor µg VOC per unit vegetation surface area.

Previous modeling studies have shown that the MEGAN model significantly over-predicted isoprene concentrations[33-36] in various locations in the United States while the ambient isoprene concentrations based on BEIS-generated emissions agree better with observations [33, 34]. In order to improve the baseline isoprene emission estimation so that the drought impact on ozone air quality can be better evaluated, two alternative emission factor fields were generated using the input data for BEIS v3.14 (with Biogenic Emissions Landcover Database, version 3, or BELD3) and BEIS v3.61 (with BELD version4, or BELD4). The BELD3 includes a 230-type land use database, which is generated from the USGS 1-km data (1992), and county-level tree and crop species information from forest and agricultural datasets. The BELD4 includes a preprocessing program (computeGridLandUse_beld4.exe in the Spatial Allocator) that can utilize user specified National Land Cover Database (NLCD) land cover data as well as tree and crop fraction table at county level to generate a BEISv3.61 compatible BELD4 database for a given air quality model domain.

In this study, NLCD 2006 and NLCD 2011 were used in the preprocessing program to generate the BELD4 data for year 2007 and 2011, respectively. The tree fraction table used in BELD3 was still used for BELD4. For both 2007 and 2011, crop fraction data based on National Agricultural Statistics Service (NASS) crop fraction tables at county level for year 2006 were used. The BEIS v3.14 program distributed with SMOKE version 2.5 and the BEIS v3.61 program distributed with SMOKE version 3.7 were modified to generate the gridded isoprene EF fields for use in MEGAN. Figure 6 shows the isoprene EF fields from the original MEGAN database (Figure 6a), and based on BEIS3.14 (Figure 6b) and BEIS3.61 (Figure 6c). The original MEGAN database gives much higher emission factors than both versions of the BEIS, and BEIS3.14 gives the lowest EF. The spatial distributions of the EF generated by BELD4/BEIS3.61 are similar to those from the original MEGAN.
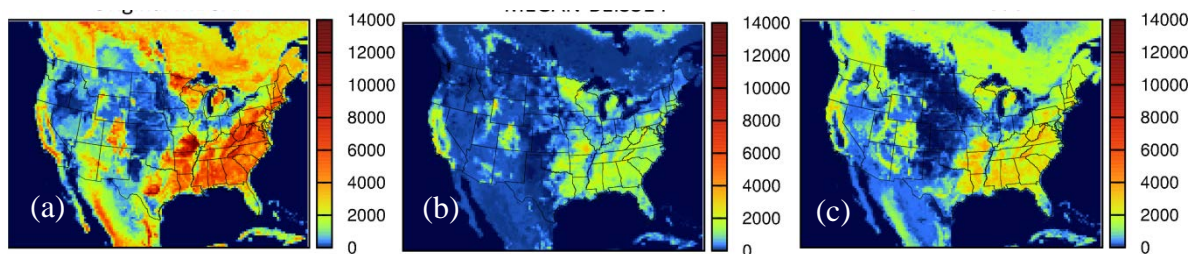
Figure 6 Emission factor (EF) of isoprene at standard condition: (a) original MEGAN database, (b) BELD3 as used in BEIS3.14 and (c) BELD4 as used in BEIS3.61 for year 2011 (summer). Units are (vegetation area/ground area)*(µg/hr/leaf area).

Isoprene emissions generated from all three sets of EF fields will be used in a preliminary CMAQ study for July 2011 to determine which EF fields generate the most reasonable isoprene emissions (see Section 2.5). In addition, isoprene emissions generated directly from BEIS3.14 and BEIS3.61 are also used in the preliminary study. Details of the preliminary study and conclusion from that study are discussed in Section 2.5.

2.3.3 Updates to the LAI fields

MODIS LAI data for the entire years of 2007 and 2011 have been downloaded and processed for MEGAN v2.10. LAI in 2011 in most part of Texas (especially western Texas) were much lower compared to the values in 2007, as shown in Figure 7 for a one-week period in August. This suggests that the importance of using correct LAI data for biogenic emission modeling, especially under drought conditions.
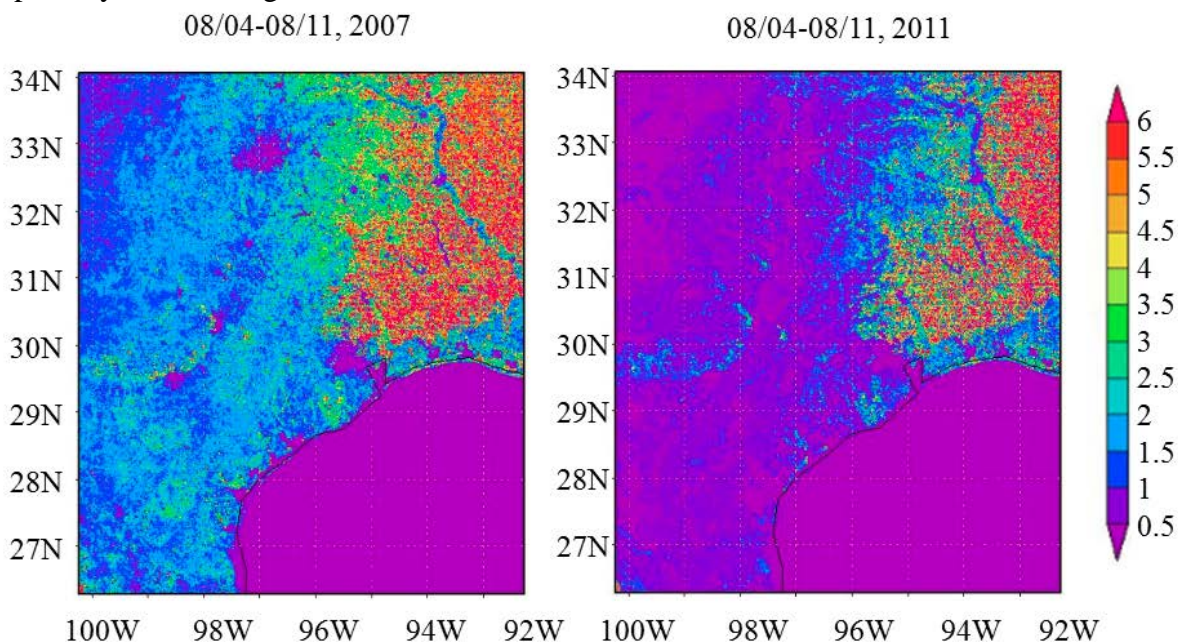
Figure 7 MODIS Leaf Area Index (LAI) for August 4-11, 2007 and 2011 for the 4-km domain.

LAI in the urban grid cells is based on the TCEQ approach, as describe by Kota et al.[36], and summarized in the following. LAI for the urban grid cells were estimated based on four urban classes from National Land Cover Database (NLCD) with predesignated maximum LAI and a season variation profile. Year specific NLCD data were used (NLCD 2006 was used for 2007 emissions). The four urban categories and the maximum LAI values are: developed open area (maximum LAI=3.3), developed low density (maximum LAI=2.3), developed medium density (maximum LAI=1.3) and developed high density (maximum LAI=0.3). The LAI values are then normalized by the fractional vegetation cover in a grid cell to calculate LAIv.

2.4 Isoprene observation data

2.4.1 Auto-GC data in Texas

Isoprene observation data were acquired from two sources. For Texas, the hourly ambient isoprene concentrations measured by a number of Automatic Gas Chromatography (Auto-GC) monitors were acquired from the Texas Commission of Environmental Quality (TCEQ). Figure 8 shows the locations of the Auto-GC sites in the 4-km domain where 2011 data are available. Some of the 23 sites were not operational in 2007. Table 3 shows the geographical coordinates of all the Auto-GC sites in Texas.

Table 3 Auto-GC sites in Texas

#	AIRScode	Latitude	Longitude	Region	Name
1	484970088	33.2217	-97.5844	Dallas/Fort Worth	Decatur Thompson
2	481211013	33.1309	-97.2977	Dallas/Fort Worth	Dish Airfield
3	481211007	33.0459	-97.1300	Dallas/Fort Worth	Flower Mound Shiloh
4	481130069	32.8201	-96.8601	Dallas/Fort Worth	Dallas Hinton
5	484391002	32.8058	-97.3566	Dallas/Fort Worth	Fort Worth Northwest
6	484391009	32.6211	-97.2904	Dallas/Fort Worth	Everman Johnson Park
7	484390075	32.9879	-97.4772	Dallas/Fort Worth	Eagle Mountain Lake
8	483550041	27.8292	-97.5436	Corpus Christi	Solar Estates
9	483550035	27.7989	-97.4339	Corpus Christi	Oak Park
10	483550083	27.8029	-97.4199	Corpus Christi	Corpus Christi Palm
11	482450009	30.0364	-94.0711	Beaumont	Beaumont Downtown
12	482451035	29.9789	-94.0109	Beaumont	Nederland High School
13	480390618	29.1489	-95.7650	Houston	Danciger
14	480391016	29.0438	-95.4729	Houston	Lake Jackson
15	481670056	29.4057	-94.9471	Houston	Texas City 34th Street
16	482011035	29.7337	-95.2576	Houston	Clinton
17	482010069	29.7062	-95.2611	Houston	Milby Park
18	482016000	29.6844	-95.2536	Houston	Cesar Chavez
19	482010617	29.8214	-94.9900	Houston	Wallisville Road
20	482010026	29.8027	-95.1255	Houston	Channelview
21	482011039	29.6700	-95.1285	Houston	Houston Deer Park
22	482010803	29.7648	-95.1785	Houston	HRM #3 Haden Rd
23	482011015	29.7617	-95.0814	Houston	Lynchburg Ferry
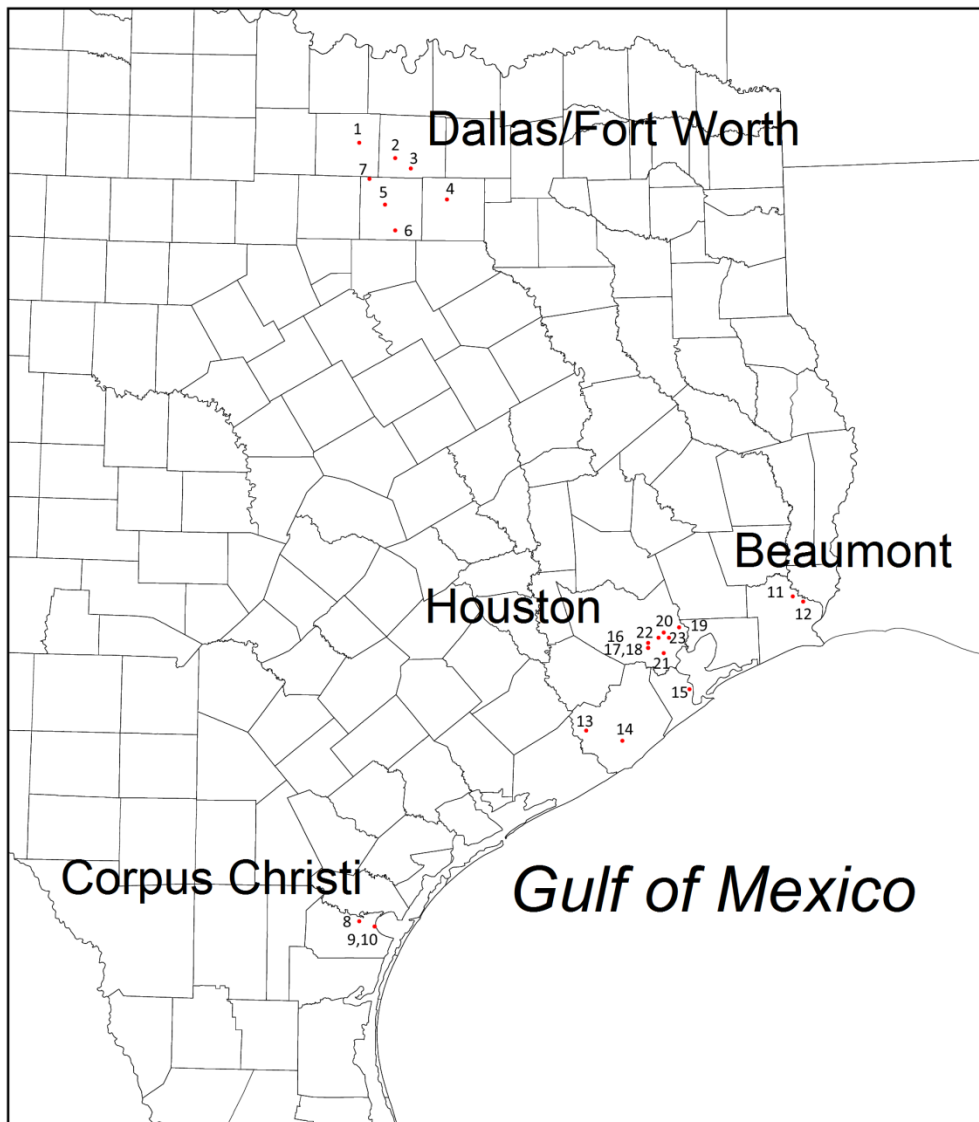
Figure 8 Location of the Auto-GC sites in the 4-km domain in Texas.

2.4.2 Isoprene data in other states

Observations of isoprene outside Texas were acquired from the AIRS database prepared by the US EPA. Figure 9 shows the locations of the isoprene monitors in other states. Most of the isoprene monitors are along the east coast of US. Additionally, there is one site in California (Livermore, a commercial urban site near San Francisco) and three sites in Georgia near Atlanta. The geographical coordinates of these monitors are shown in Table 4.

Table 4 Location of the isoprene monitors in other states

#	AIRS Code	Name	State	Longitude	Latitude	Land Use	Location type
1	060010007	Livermore	CA	-121.7842	37.6875	Commercial	Urban
2	090019003	Sherwood Island, Fairfield	CT	-73.3367	41.1183	Forest	Rural
3	090031003	Maculiffee Park, East Hartford	CT	-72.6317	41.7847	Residential	Suburban
4	110010043	S.E. End Mcmillian Reservoir	DC	-77.0132	38.9218	Commerical	Urban
5	130890002	South Dekalb, Decatur	GA	-84.2905	33.6880	Residential	Suburban
6	132230003	Yorkville	GA	-85.0453	33.9285	Agricultural	Rural
7	132470001	Conyers Monastery	GA	-84.0653	33.5911	Agricultural	Rural
8	180890022	Iitri Bunker, Gary	IN	-87.3047	41.6067	Industrial	Urban
9	230090102	Top of Cadillac Moutain	ME	-68.2270	44.3517	Mobile	Rural
10	240053001	Essesx	MD	-76.4744	39.3108	Residential	Suburban
11	250092006	Lynn	MA	-70.9708	42.4746	Commercial	Urban
12	250094005	Newburyport	MA	-70.8178	42.8144	Industrial	Urban
13	250130008	Anderson Road Air Force Base	MA	-72.5551	42.1944	Commercial	Suburban
14	250154002	Quabbin Summit, Ware	MA	-72.3341	42.2985	Forest	Rural
15	330111011	Gilson Road, Nashua	NH	-71.5224	42.7189	Residential	Suburban
16	330115001	Pack Monadnock Summit	NH	-71.8784	42.8618	Forest	Rural
17	340230011	R.U. Veg Research Farm	NJ	-74.4294	40.4622	Agricultural	Rural
18	360050133	NYBG Pfizer Plant Research Lab	NY	-73.8781	40.8679	Residential	Urban
19	420010001	Narsto Site - Arendtsville	PA	-77.3097	39.9200	Residential	Rural
20	510330001	US Geogetic Survey, Corbin	VA	-77.3774	38.2009	Forest	Rural
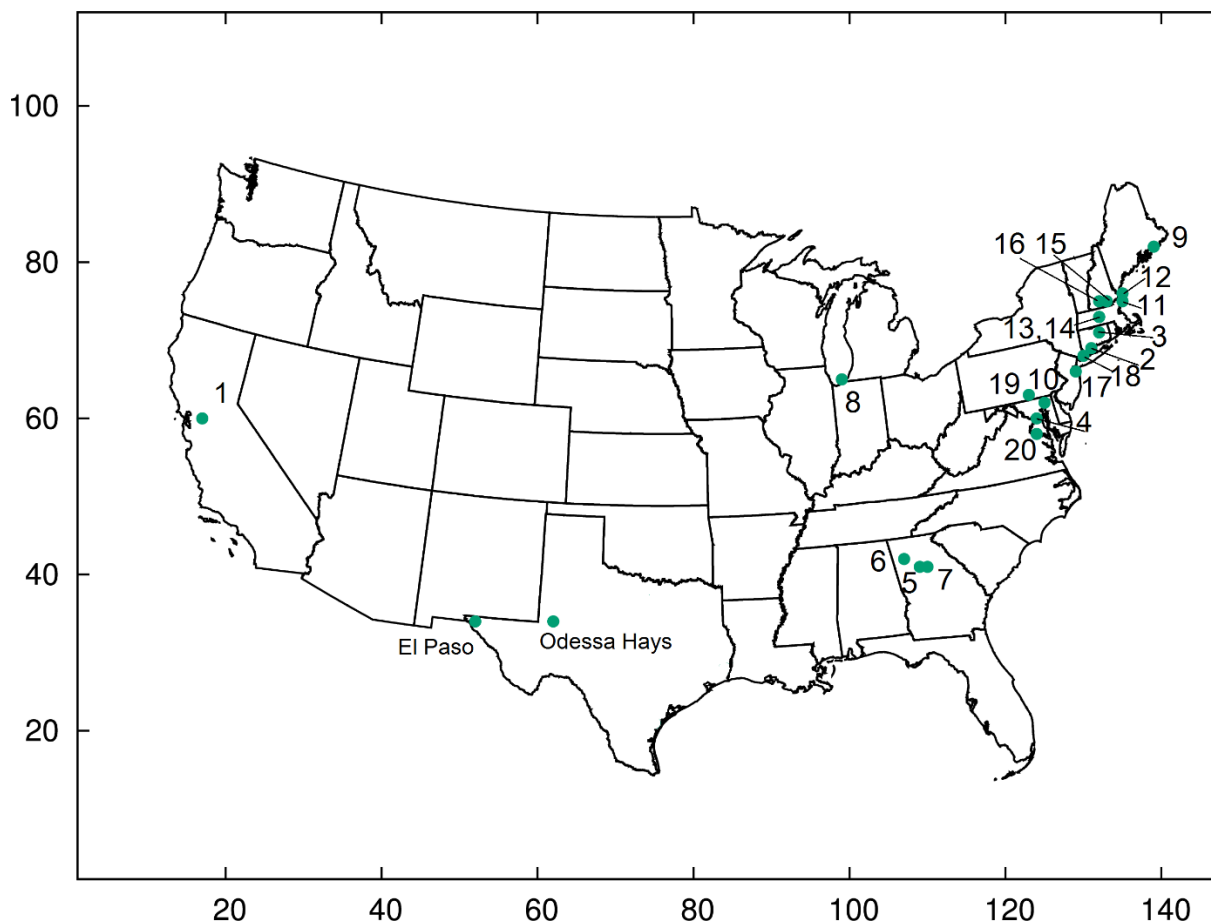
Figure 9 Location of the isoprene monitors in other states. El Paso and Odessa Hay have Auto-GC measurements but are not in the 4-km domain.

2.5 Preliminary isoprene modeling study with different EF fields

In order to select a baseline isoprene emission that yields best agreement between modeled and predicted isoprene concentrations so that the effect of drought on isoprene emissions and ozone air quality can be evaluated, four sets of isoprene emissions were generated using the MEGAN v2.10 model. In addition, two sets of emissions based on two different BEIS models were also generated for July 2011. Six preliminary CMAQ simulations were conducted using these emissions, as shown in Table 5. In simulations 4 and 6, the original gridded isoprene EF field used in the MEGAN model was replaced with EF fields generated using the BEIS input data. The BEIS input data includes gridded land use databased (BELD3 and BELD4) as described Section 2.3.2 and tabulated leaf-level emission factors and representative LAI for the vegetation. For simulations 3 and 5, isoprene emissions generated using the BEIS models were used to replace the isoprene emissions from MEGAN in the final model ready emissions for CMAQ. As the original MEGAN EF shown in Figure 6(a) is much higher than EF from BEIS, it was suspected that the original EF fields might have a unit conversion problem (i.e. in unit of µg/hr/ground area). In simulation 2, the original MEGAN EF at each grid was divided by the overall LAIv to get the correct units. The original MEGAN fields for other VOC species remained unchanged so simulations 1-6 only differ in isoprene emissions.

22

Table 5 List of isoprene emissions used in the preliminary CMAQ modeling study

Simulation #	Isoprene Emission	Notes
1	MEGAN	Original isoprene EF field; MEGAN v2.10
2	Modified MEGAN	Original EF field was divided by LAIv in each grid; MEGAN v2.10
3	BEIS314	Emission were generated using the BEIS3.14 and BELD3 land use database
4	MEGAN-BEIS314	Gridded isoprene EF based on BELD3 and leaf level emission factors used in BEIS3.14; MEGAN v2.10
5	BEIS361	Emission were generated using the BEIS3.61 and BELD4 land use database
6	MEGAN-BEIS361	Gridded isoprene EF based on BELD3 and leaf level emission factors used in BEIS3.14; MEGAN v2.10

Figure 10 shows the predicted monthly average isoprene emissions in July 2011 for the 36-km domain. Although spatial distributions of isoprene are generally similar, with highest isoprene emissions occuring in the southeast states of Alabama and Georgia, the emission rates differ significantly. As expected, the original MEGAN predicted the highest emission rates of isoprene due to large EF fields. The MEGAN-BEIS314 predicted the lowest emission rates. The MEGAN-BEIS predicted emissions are generally higher than their BEIS counterparts. While the BEIS3.14/BELD3 predicted lower isoprene emission rates, the emissions from BEIS3.61/BELD4 are significantly higher, and in some areas higher than the original MEGAN predictions. The total July 2011 isoprene emissions are 9.7Tg, 5.3Tg, 3.7Tg, 2.5Tg, 8.4Tg and 4.2Tg, for simulations (a)-(f), respectively. Figure 11 shows the predicted monthly average isoprene concentrations for the six cases. The original MEGAN emission leads to high concentrations of isoprene greater than 10 ppb over vast areas in the south and southeast US.

Figure 12 shows the comparison of predicted and observed daily average isoprene concentrations at all monitoring sites in Texas and other states. Model performance, measured by the mean fractional bias (MFB) and mean fractional error (MFE), are shown in Table 6.
The original MEGAN model greatly over-predicted the isoprene concentrations at most locations (MFB=0.98, MFE=1.06). This suggests an average over-prediction by a factor of 3. Based on the model performance statistics, BEIS314 (overall MFB=-0.22 and MFE=0.67) and MEGAN-BEIS361 (overall MFB=-0.34 and MFE=0.72) are the two of the best among the six sets of simulations. The MEGAN-BEIS361 did an obviously better job than BEIS314 in predicting isoprene concentrations in rural forest and agriculture areas (MFB and MFE are -0.31 and 0.62 for MEGAN-BEIS361, and are -0.48 and 0.75 for BEIS314), where isoprene concentrations were highest (~1.8 ppb). Isoprene concentrations are much lower in Texas. The low concentration may also contribute to larger error in the model predictions.
Based on model performance, the MEGAN-BEIS361 was used to generate baseline emissions for drought impact analysis
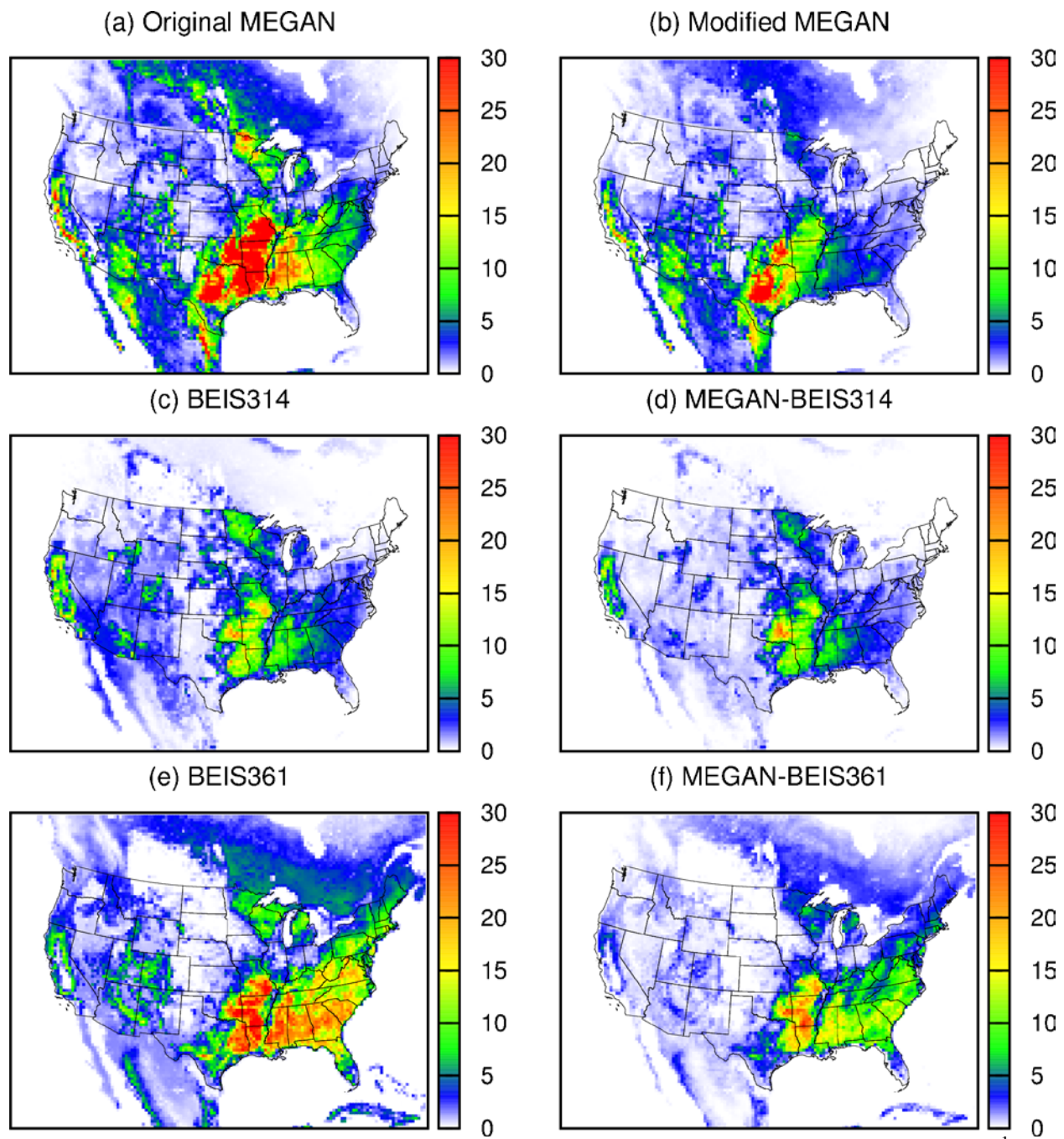
Figure 10 Predicted monthly average emissions of isoprene for July 2011. Units are moles s^{-1}.
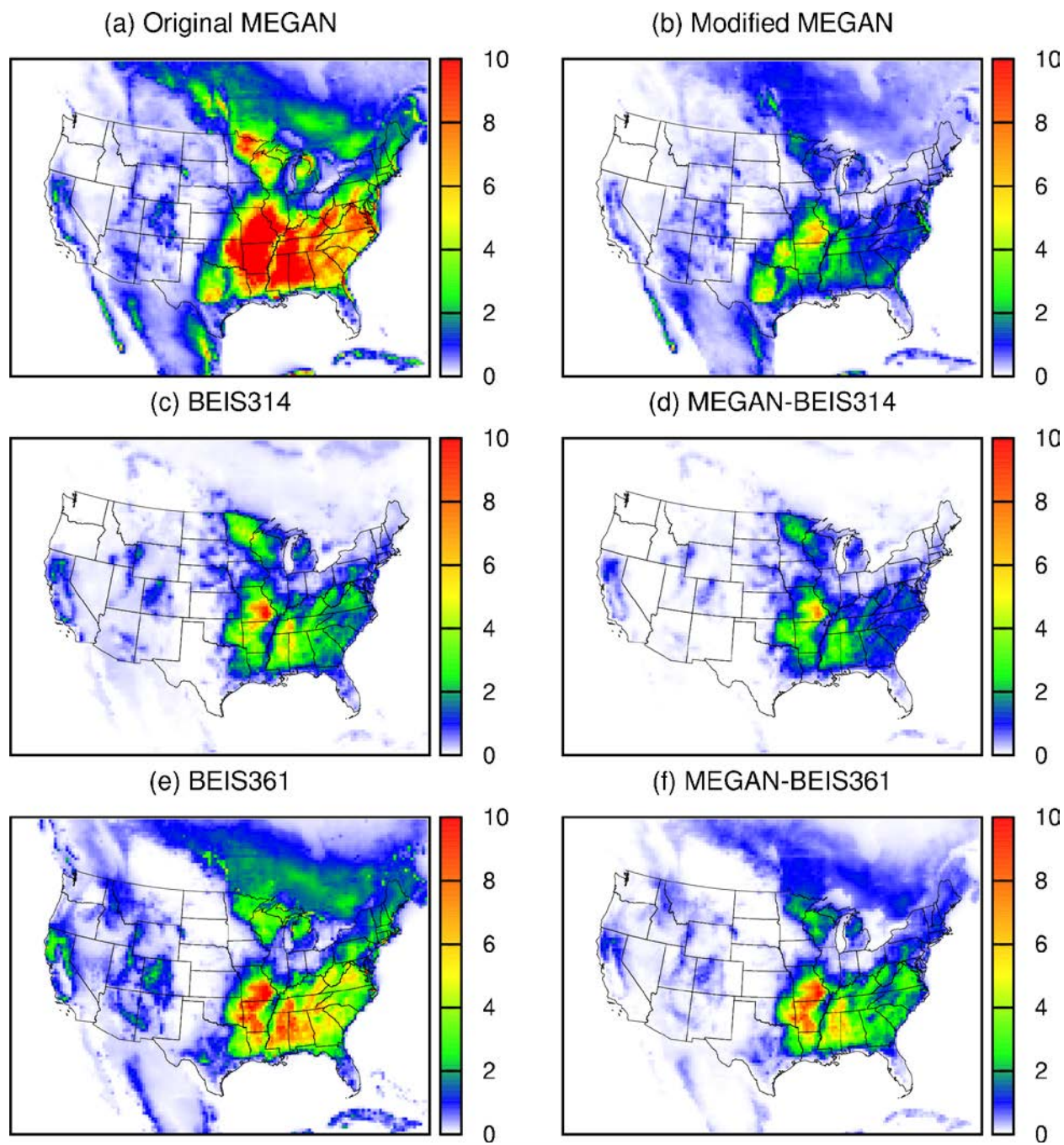
Figure 11 Predicted monthly average isoprene concentrations for July 2011. Units are ppb.
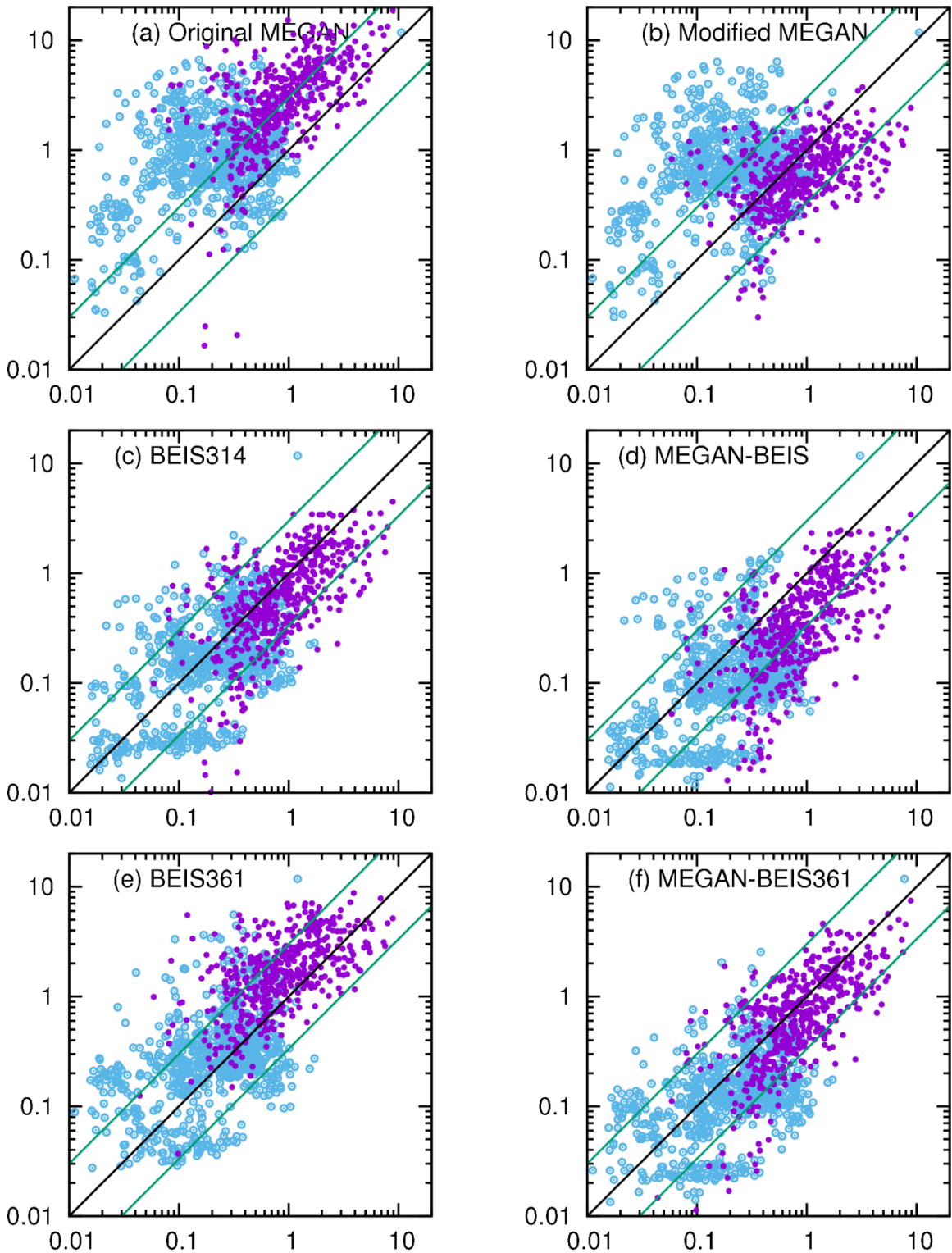
Figure 12 Predicted vs. observed daily average isoprene at all stations with valid measurements in July 2011. (Units are ppb). The green lines are 1:3 and 3:1 ratios. The blue dots are observations made in Texas and the magenta dots are observations made in other states.

Table 6 Mean fractional bias (MFB) and mean fractional error (MFE) of isoprene for July 2011. The units for predictions and observations are ppb.

		Other States	OS_Rural	Texas	TX_Rural	Overall
MEGAN	MFB	0.91	0.66	1.02	1.11	0.98
	MFE	0.99	0.81	1.11	1.16	1.06
	Pred.	3.63	4.04	1.18	1.46	2.14
Modified-MEGAN	MFB	-0.34	-0.63	0.88	1.02	0.40
	MFE	0.68	0.81	1.03	1.08	0.89
	Pred.	0.73	0.84	0.96	1.21	0.87
BEIS314	MFB	-0.29	-0.48	-0.17	-0.25	-0.22
	MFE	0.62	0.75	0.70	0.57	0.67
	Pred.	0.88	1.10	0.25	0.22	0.50
MEGAN-BEIS314	MFB	-0.79	-0.94	-0.51	-0.45	-0.62
	MFE	0.91	1.01	0.87	0.74	0.88
	Pred.	0.52	0.65	0.18	0.17	0.31
BEIS361	MFB	0.56	0.51	0.21	0.16	0.35
	MFE	0.71	0.72	0.74	0.74	0.73
	Pred.	2.11	2.72	0.44	0.40	1.10
MEGAN-BEIS361	MFB	-0.11	-0.31	-0.42	-0.49	-0.34
	MFE	0.67	0.62	0.79	0.78	0.72
	Pred.	0.94	1.30	0.17	0.16	0.49
	Obs.	1.17	1.80	0.30	0.36	0.66
	# Points	503	196	737	154	1213

2.6 Base case model performance evaluation

2.6.1 Evaluation of meteorological variables and soil moisture

Two sets of WRF simulations were conducted. The first set of simulation divided all the days into multiple groups of 7 days with the first-day as spin up. The other set of simulation modeled each day separately, with a 3-hour spin up. It is expected in particular that the second set of simulation will improve model results, especially on soil moisture due to more frequent reload of the NLDAS gridded soil moisture.

As shown in Table 7, the 1-day with 3-hr restart run improves model performance of 2-m temperature and relative humidity with lower MB, RMSE and MNGE values, and reduces the RMSE and MNGE of 10-m wind speed. In addition, prediction of soil moisture at the surface layers is also improved. Average observed volumetric soil moisture in July 2011 at 0.05 m and 0.10 m are 0.165 and 0.141 m^3m^{-3}, respectively. The predictions are 0.131and 0.109 m^3m^{-3} for the first set of simulation and 0.139 and 0.133 m^3m^{-3} for the second set of simulations. MB, RMSE, GE and MNB values are also slightly reduced. Thus, model results from the 1-day with 3-hr restart are further analyzed and used as input to drive the CMAQ model simulations.

Table 7 Comparison of July 2011 model performance of 10-m wind speed (WSPD), 2-m temperature (TEMP) and relative humidity (RH) for the 4-km inner domain.

| | 7 days, 1-day spin-up | | | 1-day, 3h-spin up | | |
	TEMP	WSPD	RH	TEMP	WSPD	RH
avg_obs	303.49	3.92	55.87	303.49	3.92	55.87
avg_pre	305.59	4.43	50.71	304.97	4.45	54.03
MB	2.08	0.51	-4.95	1.56	0.52	-1.83
RMSE	3.46	2.23	16.12	3.14	2.01	12.32
MNGE	2.63	1.71	12.12	2.25	1.54	8.92

WRF model performance for each modeled month in 2007 and 2011 in the 4-km domain is shown in Figure 13. Model performance of wind speed at 10 meters (WSPD) generally meets the performance criteria (MB≤ ±0.5, GE and RMSE ≤ 2.0; all definitions of the model performance criteria are listed in Appendix D). MB values for wind direction (WDIR) generally meet the model performance criteria of MB≤ ±10°, although the GE values slightly exceed the benchmark value of GE≤ 30° for a few months. However, this is similar to model performance of WDIR in other studies that did not apply observation nudging [30]. Temperature at 2 meters (TEMP) is significantly over-predicted with MB values near 1.5K. The model performance benchmarks are MB≤ ±1K and GE≤3K. The larger MB value indicates an obvious over-prediction in the temperature that could lead to over-prediction of isoprene emissions. The GE values are generally within the model performance criteria, and agree with the values reported in other studies, such as Zhang et al. [30]. Relative humidity is under-predicted in both years with MB values range from -2 to -12%, and GE values range from 8 to 16%. As shown in Figure 14 and Figure 15, temperature in summer 2011is higher than that in 2007 and relative humidity is lower. Wind speed is also higher in 2011 and lower in 2007. Wind direction is relatively unchanged between the two years. The year-to-year differences, as well as month-to-month differences are well captured by the WRF model.
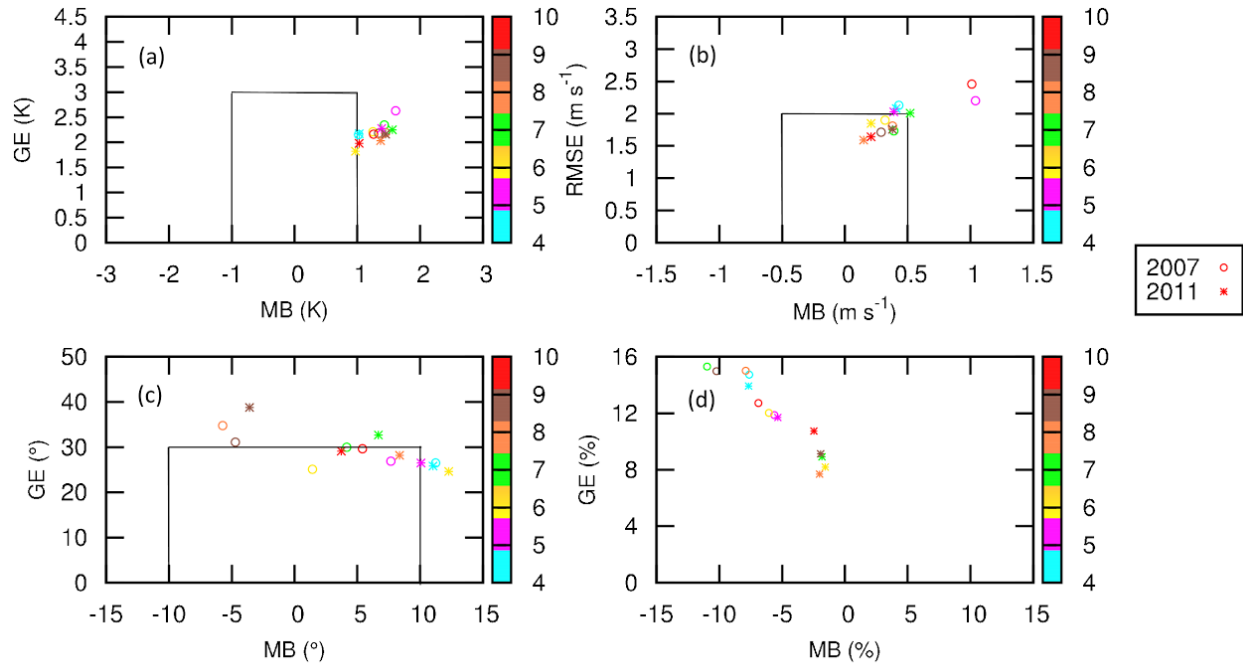
Figure 13 Model performance of (a) 2-m temperature, (b) 10-m wind speed, (c) 10-m wind direction and (d) 2-m relative humidity.
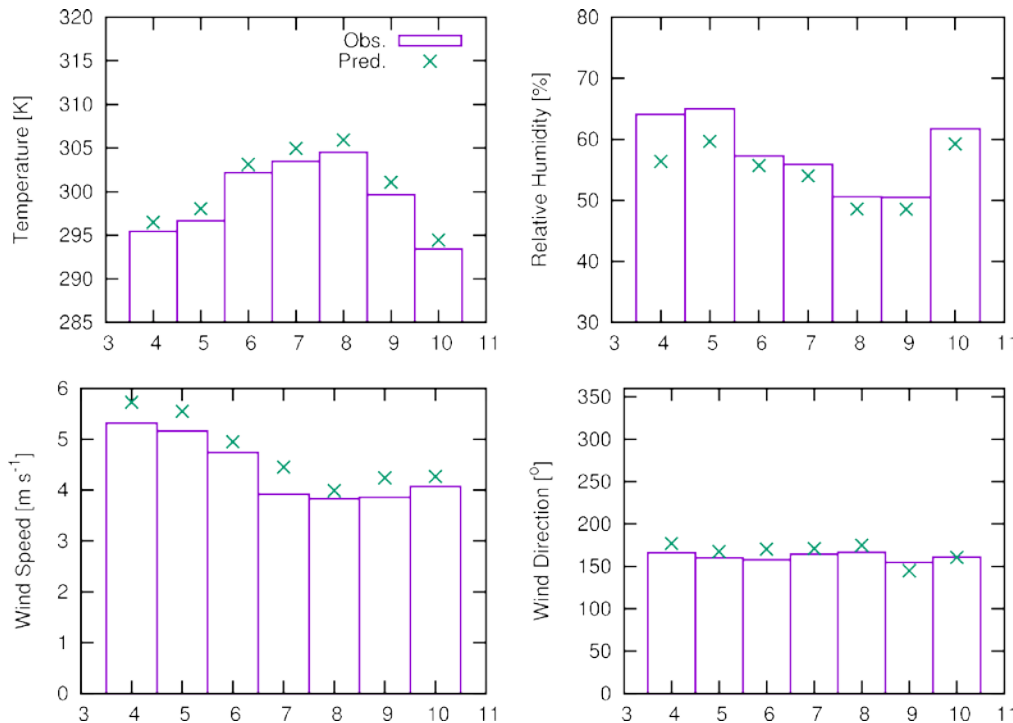
Figure 14 Monthly averaged 2-m temperature, relative humidity, and 10-m wind speed and direction based on all weather monitors in the 4-km domain for year 2011.
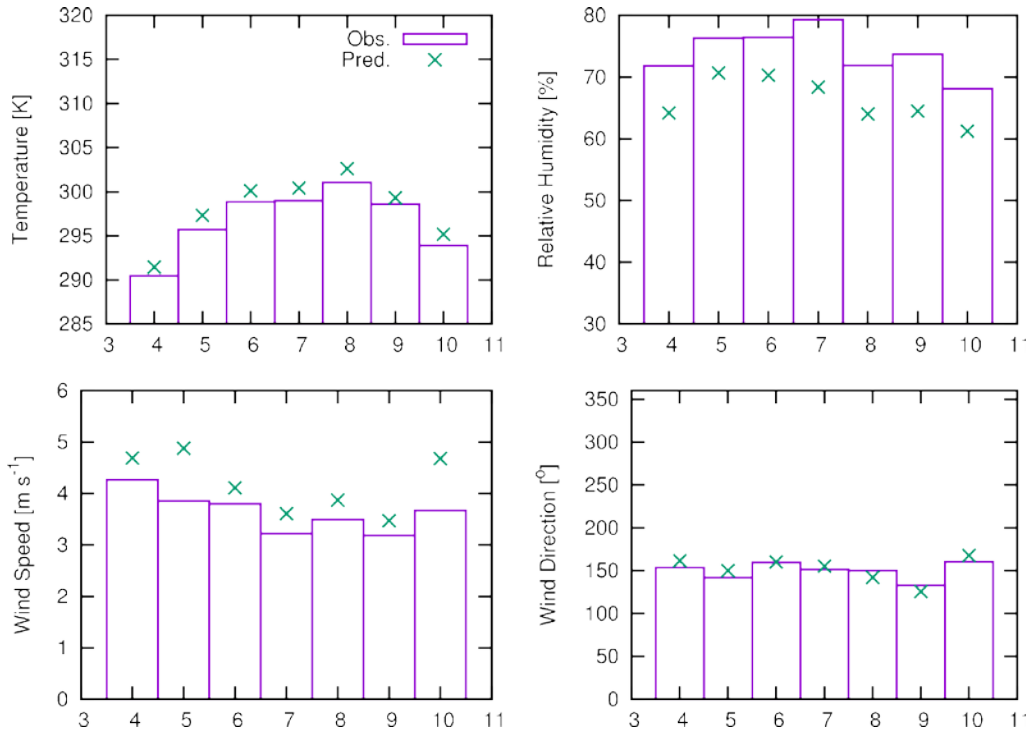
Figure 15 Monthly averaged 2-m temperature, relative humidity, and 10-m wind speed and direction based on all weather monitors in the 4-km domain for year 2007.

Soil moisture measurements were taken from the TAMU North American Soil Moisture Database (soilmoisture.tamu.edu). The WRF/Noah predictions were interpolated to the points where the measurements were made using piecewise linear interpolation. Most of the measurements are available at 7 depth levels (0.05, 0.10, 0.20, 0.25, 0.50, 0.60, 1.00 m). The model performance statistics for daily soil moisture July 2011 are shown in Table 8, as an example. The data for other months are similar and included in Appendix F. It should be noted that most of the measurement sites are in Oklahoma, and there are fewer data points available in Texas. Thus, the evaluation might not fully describe the bias in the predicted soil moisture. Overall the predicted soil moisture values at monitoring sites are lower than observations. This is likely due to the fact that rainfall amount was under-predicted in the current WRF simulation.

Table 8 Model performance statistics for daily soil moisture for July 2011 at all available sites in the TAMU North American Soil Moisture Database.

Depth	0.05m	0.1m	0.2m	0.25m	0.5m	0.6m	1m
avg_obs ($m^3 m^{-3}$)	0.165	0.141	0.135	0.243	0.161	0.199	0.169
avg_pre ($m^3 m^{-3}$)	0.139	0.133	0.128	0.157	0.119	0.140	0.116
MB	-0.03	-0.01	-0.01	-0.09	-0.04	-0.06	-0.05
RMSE ($m^3 m^{-3}$)	0.052	0.045	0.063	0.093	0.055	0.059	0.105
GE ($m^3 m^{-3}$)	0.046	0.040	0.056	0.086	0.050	0.058	0.093
MNB	-0.10	0.09	0.24	-0.34	-0.22	-0.29	-0.08

2.6.2 Evaluation of isoprene concentrations

Predicted base case (with MEGAN-BEIS361 emission) isoprene concentrations were compared with observations at all monitors. Figure 16 shows a detailed comparison of predicted (36-km domain results) and observed hourly isoprene for each monitoring site outside Texas. Isoprene concentrations spans three orders of magnitude in many of the 20 sites, and the predictions are generally in good agreement with the observations. To the best of the authors' knowledge, this is the first time hourly isoprene concentrations are extensively evaluated with observations. Ozone concentrations are highest (up to 20 ppb in July) at the US Geodetic Survey site in VA (AIRS code 510330001), which is a rural forest site, and the predicted isoprene concentrations agree with the observations generally within a factor of 5. Good predictions with observations are also found most of the other monitors. The worst model performance occurs at the NYBG Pfizer Plant Research Lab in New York (360050133). This lab is located in the urban center in downtown New York. The other urban site (Livermore, 060010007) has the lowest isoprene concentrations but the observations and predictions agree well for September and October, which have the most of number of available observations. Figure 17 shows that the model does a better job in predicting daily average isoprene concentrations at the non-Texas stations. A number of stations show agreements within a factor of 2. Figure 18 and Figure 19 show hourly and daily average isoprene concentrations at non-Texas monitors for 2007. Six of the sites do not have available data in 2007. In general, the predicted hourly concentrations still show positive correlation with the predictions but the errors are larger.

Table 9 shows the detailed model performance statistics in terms of MFB and MFE for monitors outside Texas based on 36-km model results. The model performance is best in July (MFB=-0.22 and MFE=0.89) 2011 when the isoprene concentrations are the highest, with average observed and predicted concentrations of 1.28 and 1.03 ppb, respectively. Model performance in June and August is also relatively good, with MFB<0.3 and MFE ~0.9. Model performance decreases for spring and fall months, as the observed concentrations drop significantly to below 0.2 ppb. For 2007, the model performance is also best for June to August, however, the MFB for the three months range from -0.35 to -0.53, which is much larger than MFB values for 2011 (-0.22 to -0.28). The predicted and observed highest isoprene concentrations both occur in July for 2011, and in August for 2007. For the summer months June and July, observed concentrations in 2011 are higher than those in 2007 while for July concentrations are lower in 2011. Table 10 demonstrates that both MFB and MFE are generally lower for daily average isoprene concentrations.

Table 9 Model performance of isoprene for year 2011 and 2007 (April to October) based on hourly 36-km results at non-Texas monitors. The isoprene emissions are based on MEGAN-BEIS361.

	2011					2007				
	MFB	MFE	Obs.	Pred.	# points	MFB	MFE	Obs.	Pred.	# points
April	-0.34	1.02	0.04	0.04	344	-1.37	1.59	0.12	0.04	22
May	-0.34	1.49	0.14	0.27	611	-0.04	1.01	0.17	0.24	564
June	-0.23	0.91	0.86	0.80	9960	-0.35	0.86	0.65	0.51	6675
July	-0.22	0.89	1.28	1.03	11161	-0.52	0.98	0.79	0.52	8382
August	-0.28	0.91	0.77	0.72	9928	-0.53	0.99	1.07	0.69	7726

September	-0.43	1.07	0.20	0.22	3477	-0.76	1.05	0.24	0.12	1093
October	-0.73	1.14	0.06	0.05	1249	-1.23	1.37	0.15	0.05	412

Table 10 Model performance of isoprene for year 2011 and 2007 (April to October) based on daily average 36-km results at non-Texas monitors. The isoprene emissions are based on MEGAN-BEIS361.

	2011					2007				
	MFB	MFE	Obs.	Pred.	# points	MFB	MFE	Obs.	Pred.	# points
April	0.89	1.00	0.01	0.03	28	NA	NA	NA	NA	0
May	0.64	1.60	0.03	0.11	70	0.37	1.09	0.16	0.27	71
June	-0.06	0.75	0.74	0.70	450	-0.23	0.63	0.57	0.47	368
July	-0.11	0.67	1.17	0.94	503	-0.41	0.77	0.72	0.50	456
August	-0.09	0.72	0.69	0.65	468	-0.47	0.72	0.93	0.61	428
September	0.03	0.88	0.15	0.18	182	-0.36	0.68	0.22	0.17	101
October	-0.05	0.88	0.04	0.04	69	-0.78	1.01	0.08	0.03	26

Figure 16 Predicted (36-km) vs. observed hourly average isoprene at all non-Texas stations with valid measurements in April to October 2011. (Units are ppb). The green lines are 1:1, 1:5 and 5:1 ratios. The isoprene emissions are based on MEGAN-BEIS361.

Figure 17 Predicted (36-km) vs. observed daily average isoprene at all non-Texas stations with valid measurements in April to October 2011. (Units are ppb). The green lines are 1:1, 1:2 and 2:1 ratios.

Figure 18 Predicted (36-km) vs. observed hourly average isoprene at all non-Texas stations with valid measurements in April to October 2007. (Units are ppb). The green lines are 1:1, 1:5 and 5:1 ratios. The isoprene emissions are based on MEGAN-BEIS361.

Figure 19 Predicted (36-km) vs. observed daily average isoprene at all non-Texas stations with valid measurements in April to October 2007. (Units are ppb). The green lines are 1:1, 1:2 and 2:1 ratios. The isoprene emissions are based on MEGAN-BEIS361.

Figure 20 and Figure 21 show the comparison of hourly and daily isoprene concentrations at all Auto-GC sites in Texas for 2011 based on 36-km results and the detailed model performance statistics are shown in Table 11 and Table 12. The concentrations at the Auto-GC sites are low, with hourly concentrations less than 1 ppb. Average monthly 1-hour concentration ranges from 0.09 ppb (in October) to 0.33 (in June) for 2011 and from 0.07 ppb (in April) to 0.42 ppb (in August) for 2007. The model performance statistics are similar to those at non-Texas stations under similar average isoprene concentrations, as shown in Figure 22. For example, MFB=-0.49 and MFE=1.07 for July 2011 based on hourly concentrations, and the average concentration is 0.3 ppb. Similarly, average hourly concentrations at non-Texas station in September 2011 is 0.2 ppb, and the MFB and MFE values are 0.43 and 1.07, respectively. Thus, the low model performance at the Auto-GC sites in Texas is likely due to uncertainty in both measurements of low isoprene concentrations and emissions estimations.

Table 11 Model performance of isoprene for year 2011 and 2007 (April to October) based on hourly 36-km results at all Auto-GC monitors in Texas.

| | 2011 | | | | | 2007 | | | | |
	MFB	MFE	Obs.	Pred.	# points	MFB	MFE	Obs.	Pred.	# points
April	-0.41	1.02	0.12	0.09	9760	-0.43	1.04	0.07	0.07	5534
May	-0.38	0.99	0.19	0.13	11605	-0.46	1.00	0.16	0.13	6059
June	-0.51	1.07	0.33	0.19	12942	-0.41	1.03	0.31	0.29	6369
July	-0.49	1.07	0.30	0.18	14253	-0.48	0.97	0.32	0.30	6358
August	-0.47	1.12	0.29	0.22	14324	-0.47	1.02	0.42	0.58	6245
September	-0.38	1.10	0.17	0.22	12398	-0.37	1.08	0.25	0.35	6790
October	-0.71	1.09	0.09	0.06	9177	-1.05	1.35	0.15	0.07	6235

Table 12 Model performance of isoprene for year 2011 and 2007 (April to October) based on daily average 36-km results at all Auto-GC monitors in Texas.

| | 2011 | | | | | 2007 | | | | |
	MFB	MFE	Obs.	Pred.	# points	MFB	MFE	Obs.	Pred.	# points
April	-0.19	0.65	0.11	0.08	637	-0.09	0.69	0.05	0.05	324
May	-0.24	0.70	0.18	0.12	721	-0.19	0.61	0.12	0.10	335
June	-0.37	0.79	0.32	0.18	696	-0.23	0.77	0.24	0.23	331
July	-0.42	0.79	0.30	0.17	737	-0.35	0.68	0.26	0.25	314
August	-0.28	0.76	0.28	0.21	758	-0.26	0.71	0.35	0.50	303
September	-0.18	0.75	0.16	0.20	716	-0.22	0.77	0.21	0.30	328
October	-0.54	0.78	0.09	0.06	587	-0.85	1.14	0.12	0.06	325
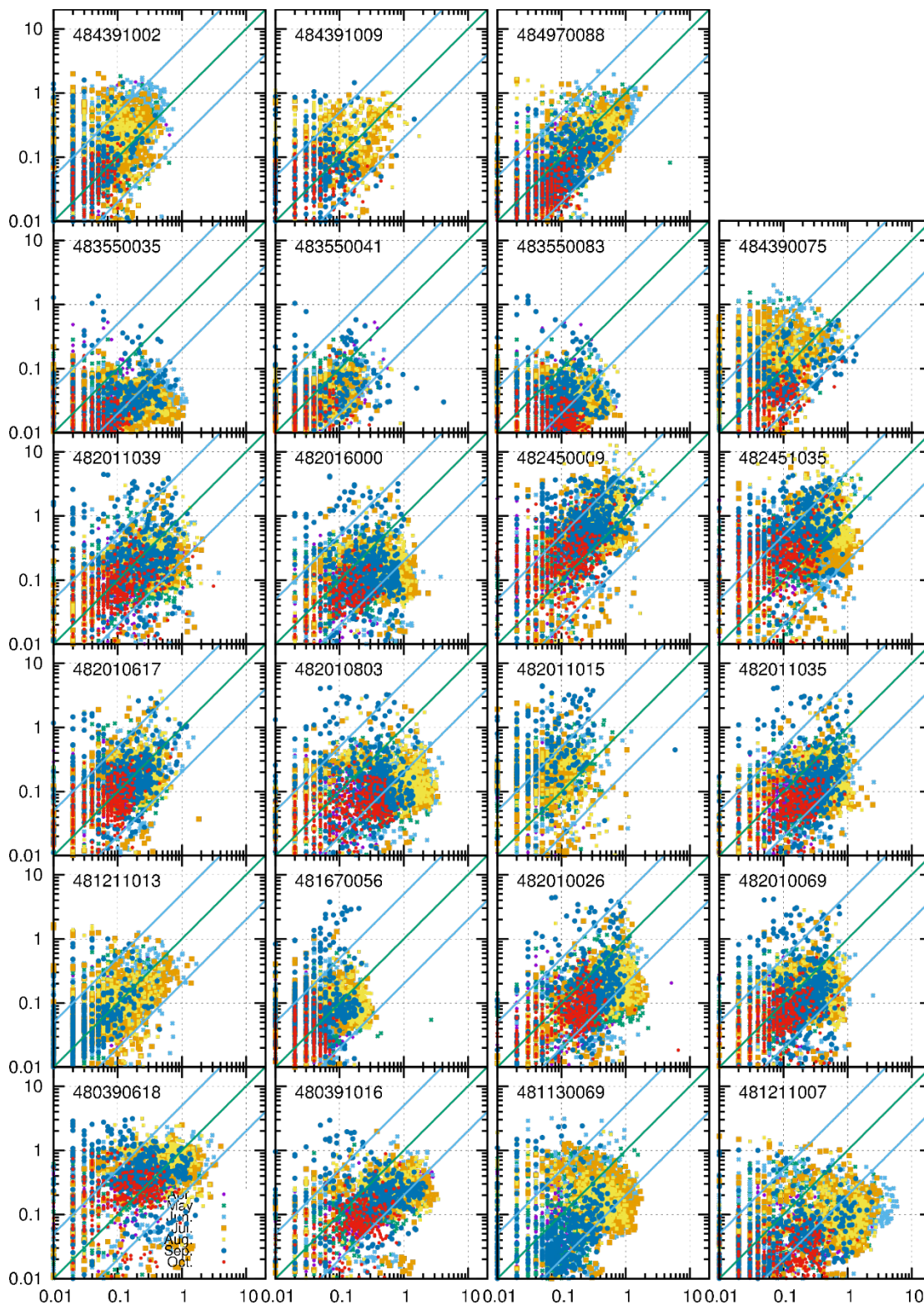
Figure 20 Predicted (36-km) vs. observed hourly average isoprene at all Texas Auto-GC sites with valid measurements in April to October 2011. (Units are ppb). The green lines are 1:1, 1:5 and 5:1 ratios.
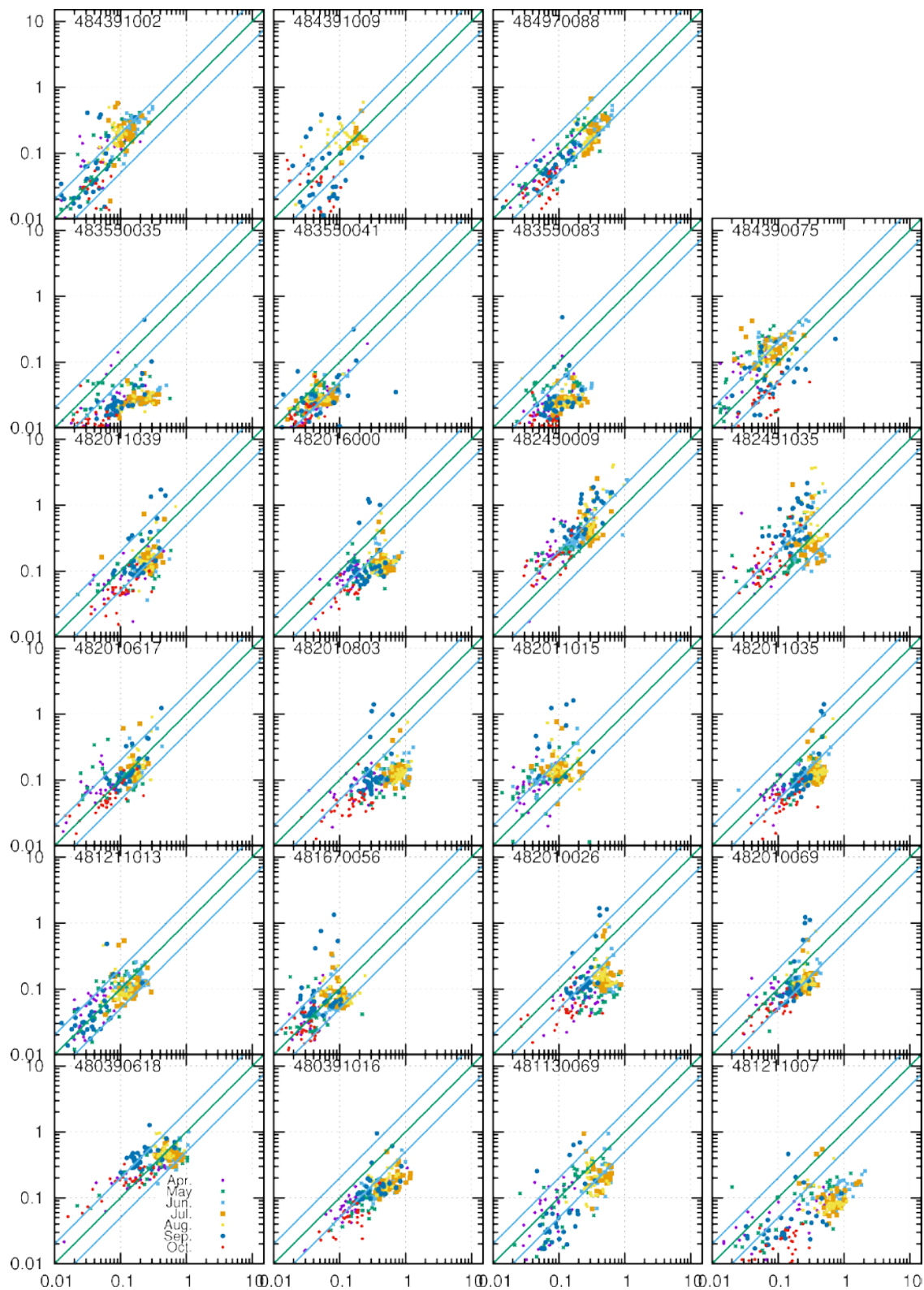
Figure 21 Predicted (36-km) vs. observed daily average isoprene at all Texas Auto-GC sites with valid measurements in April to October 2011. (Units are ppb). The green lines are 1:1, 1:5 and 5:1 ratios.
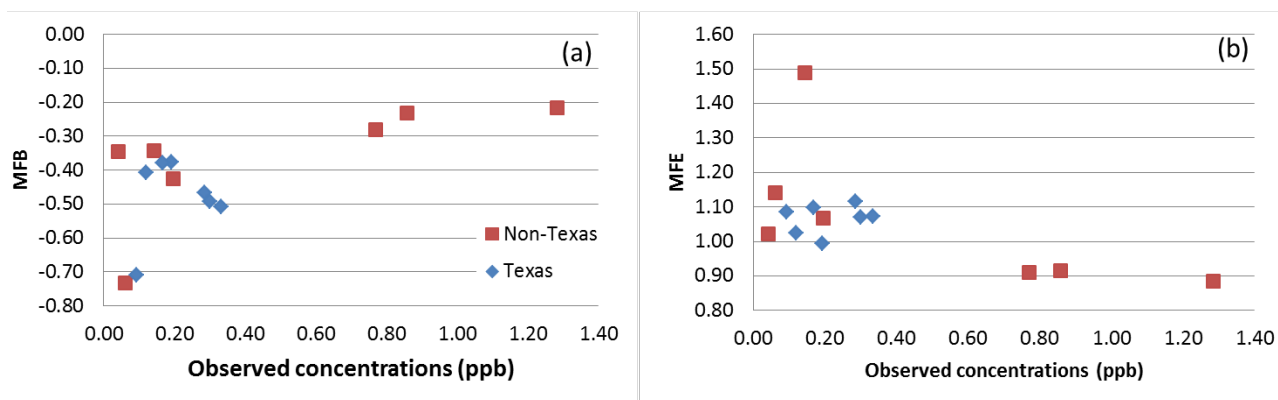
Figure 22 Comparison of MFB and MFE based hourly concentrations at monitors in Texas and other states.

In order to evaluate if higher grid resolution improves isoprene predictions at monitor sites, predicted concentrations from the 4-km resolution domain are also compared with predictions, as shown in Figure 23 and Figure 24 for hourly and daily average concentrations, respectively. While the daily averaged concentrations still show strong correlations, more scattering can be observed from the hourly scatter plots. Model performance statistics in Table 13 and Table 14 shows that the predicted concentrations from the 4-km domain are lower than those from the 36-km domain, thus leading to more negative MFB values and larger MFE values.

In BEIS361, emissions of isoprene from urban areas (NLCD sectors 21, 22, 23 and 24, and MODIS sector 13) have a uniform basal emission factor of 10 gC km^{-2}hr^{-1}. This uniform emission factor is likely too low for urban areas in Texas where oak trees are prevalent. For example, a field survey in 2009 of a 3-km radius area in downtown Houston show that temperate broadleaf deciduous trees account for approximately 25% of the ground coverage[37]. In a number of locations in urban Houston, broadleaf deciduous trees account for 10-20% of the ground coverage[36]. Based on the emission factor for the deciduous trees in BEIS361 (6707 gC km^{-2}hr^{-1}; MODIS type 4 and NLCD type 41). When the 36-km resolution domain is used, the monitors are likely located in a grid cell with less urban fraction and more tree fraction, thus with higher isoprene emissions. The grid cells where the urban monitors are located in the 4-km domain have higher urban fractions and lower vegetation fractions, thus with lower isoprene emissions. To rectify this problem, the isoprene emission factor for urban land use type(s) in Texas should be increased in future simulations. Ideally, city specific tree coverage should be applied to better reflect the difference in the tree coverage and types among different urban areas.

40

Table 13 Model performance of isoprene for year 2011 and 2007 (April to October) based on hourly 4-km results at Auto-GC monitors in Texas.

	2011					2007				
Other	MFB	MFE	Obs.	Pred.	# points	MFB	MFE	Obs.	Pred.	# points
April	-0.63	1.19	0.12	0.10	9513	-0.77	1.19	0.08	0.05	4701
May	-0.64	1.15	0.20	0.13	11015	-0.90	1.24	0.19	0.09	5173
June	-0.81	1.20	0.36	0.17	12022	-0.88	1.31	0.35	0.23	5505
July	-0.81	1.24	0.32	0.18	13199	-0.92	1.29	0.35	0.24	5726
August	-0.77	1.27	0.31	0.22	13232	-0.82	1.29	0.46	0.53	5592
September	-0.60	1.26	0.18	0.24	11356	-0.63	1.32	0.29	0.32	5645
October	-0.98	1.28	0.10	0.06	8313	-1.68	1.78	0.17	0.01	5243

Table 14 Model performance of isoprene for year 2011 and 2007 (April to October) based on daily average 4-km results at Auto-GC monitors in Texas.

Texas	2011					2007				
Other	MFB	MFE	Obs.	Pred.	# points	MFB	MFE	Obs.	Pred.	# points
April	-0.39	0.89	0.11	0.09	618	-0.50	0.89	0.06	0.03	265
May	-0.50	0.86	0.19	0.13	663	-0.77	0.93	0.14	0.07	274
June	-0.75	0.93	0.34	0.17	636	-0.77	1.04	0.28	0.18	276
July	-0.75	1.00	0.32	0.18	678	-0.78	1.01	0.29	0.20	283
August	-0.62	0.94	0.30	0.21	696	-0.58	0.99	0.39	0.45	272
September	-0.40	0.93	0.17	0.22	656	-0.41	0.95	0.25	0.27	271
October	-0.79	1.02	0.09	0.06	534	-1.64	1.72	0.14	0.01	267
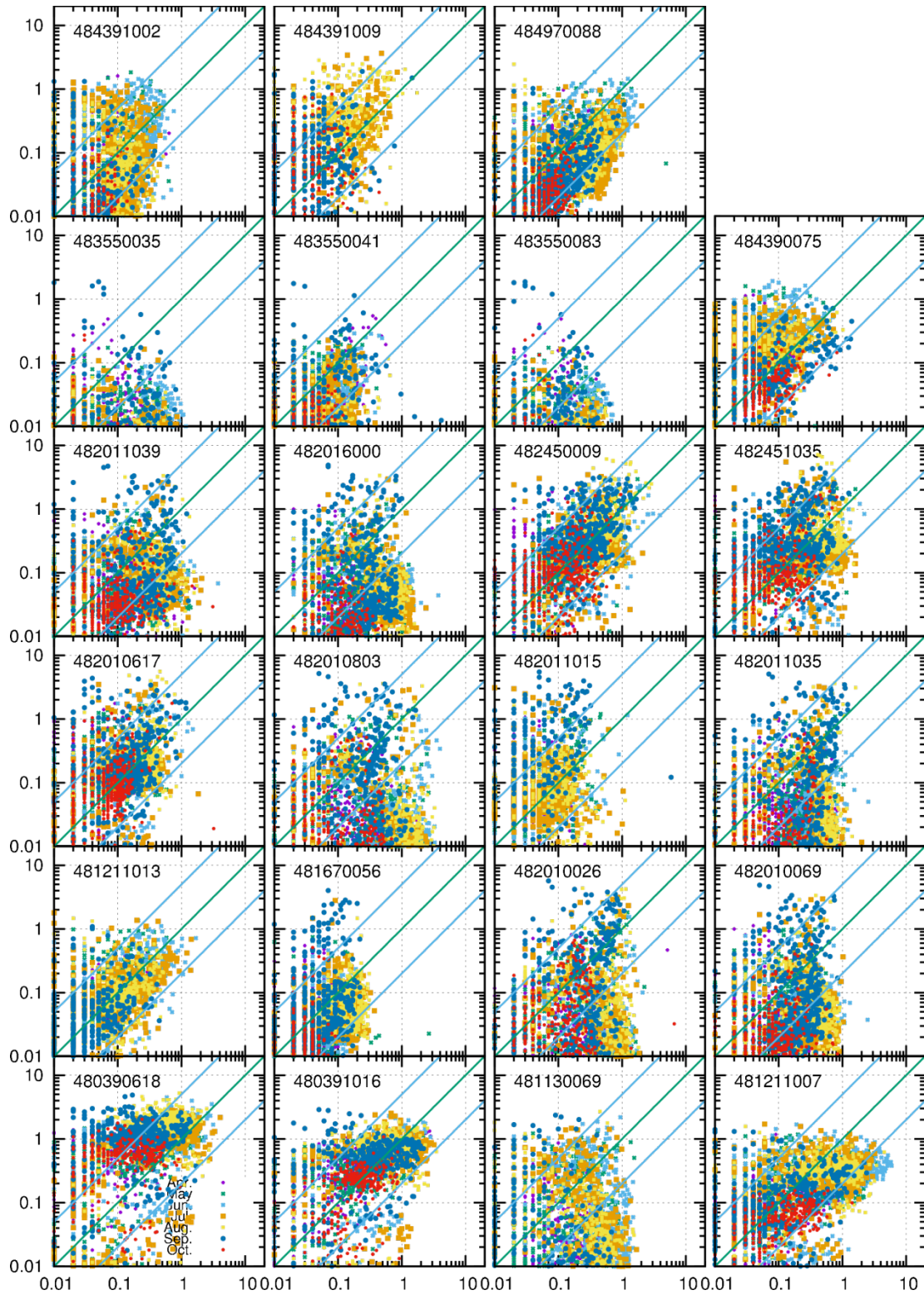
Figure 23 Predicted (4-km) vs. observed hourly average isoprene at all Texas Auto-GC sites with valid measurements in April to October 2011. (Units are ppb). The green lines are 1:1, 1:5 and 5:1 ratios.
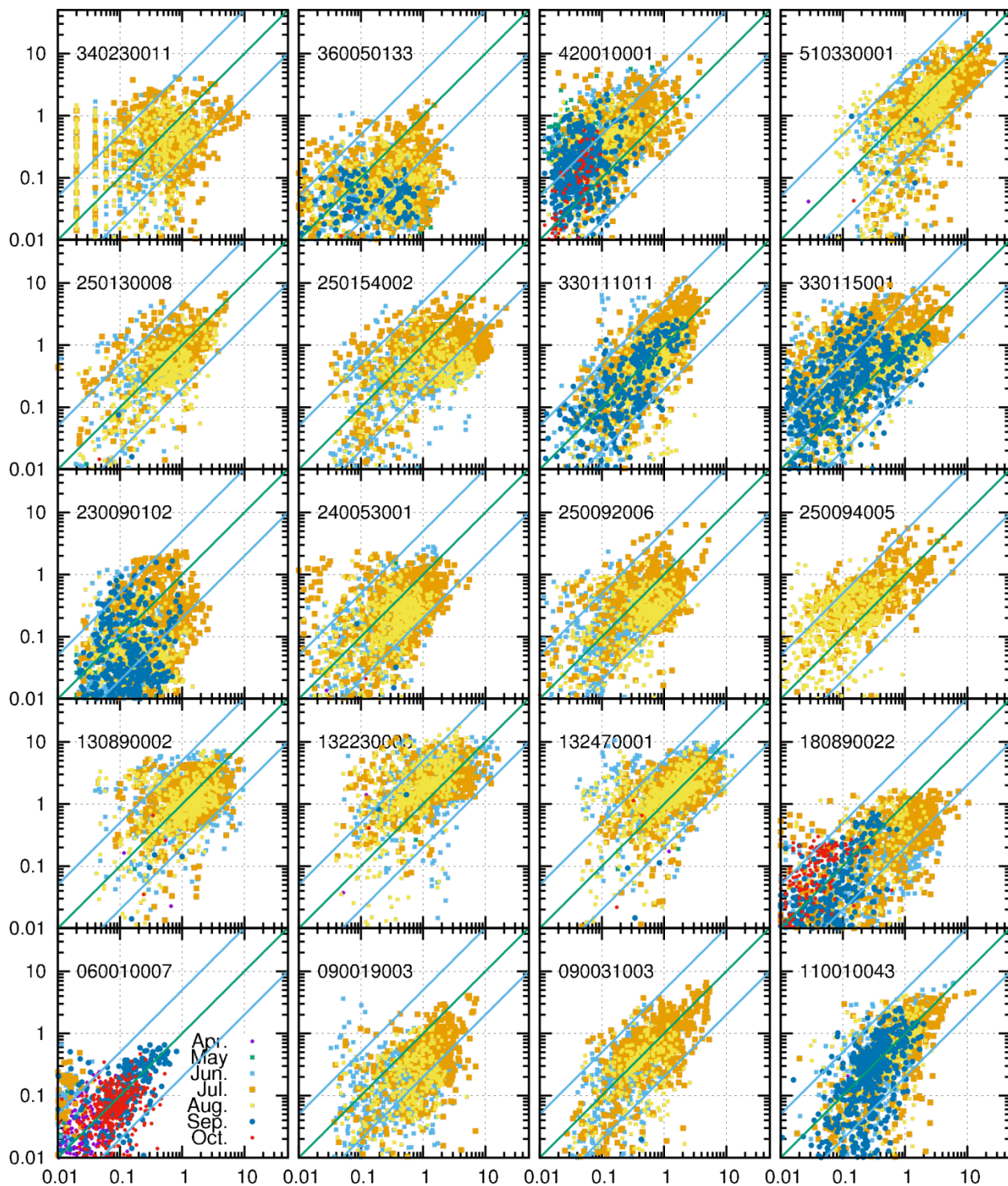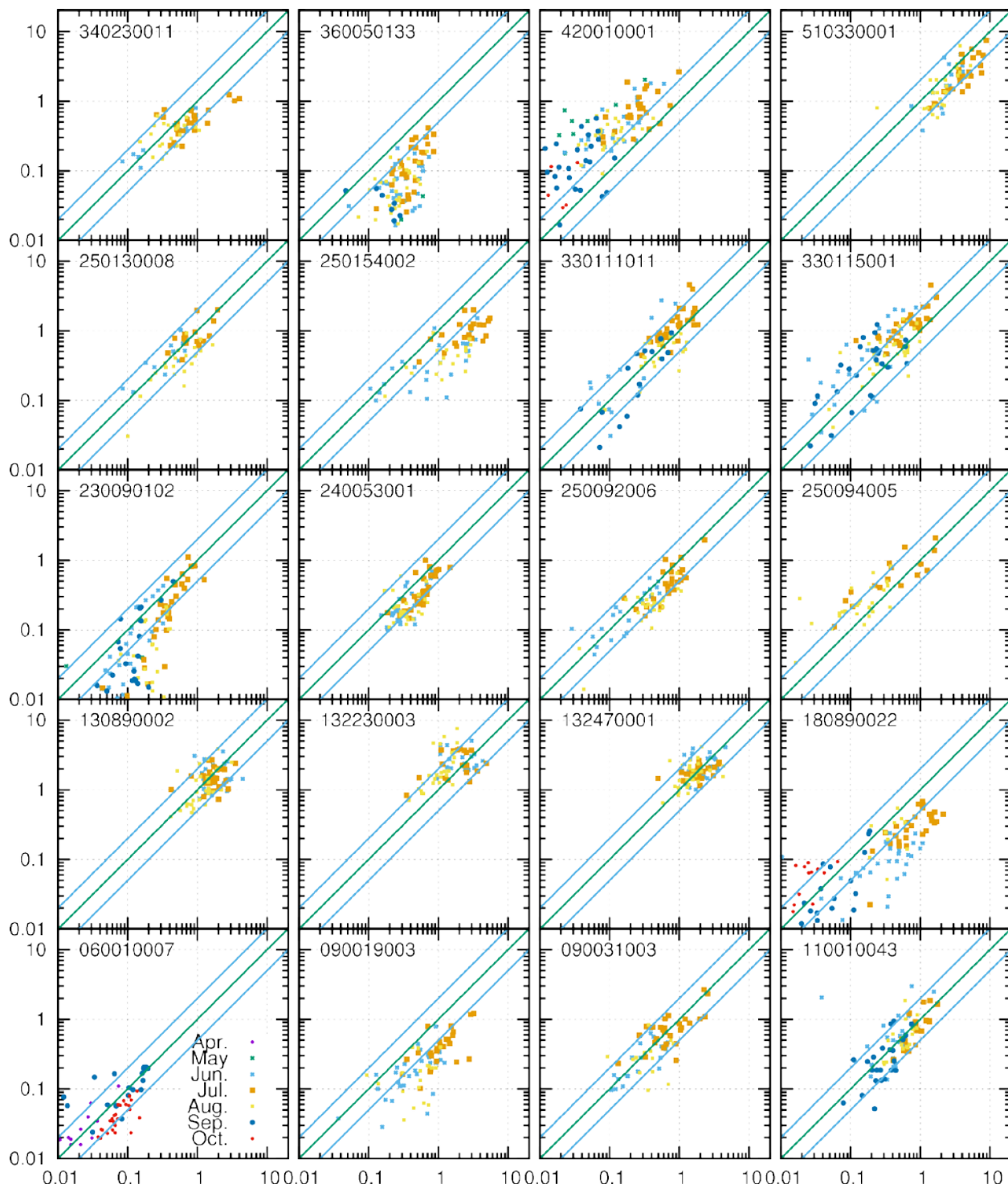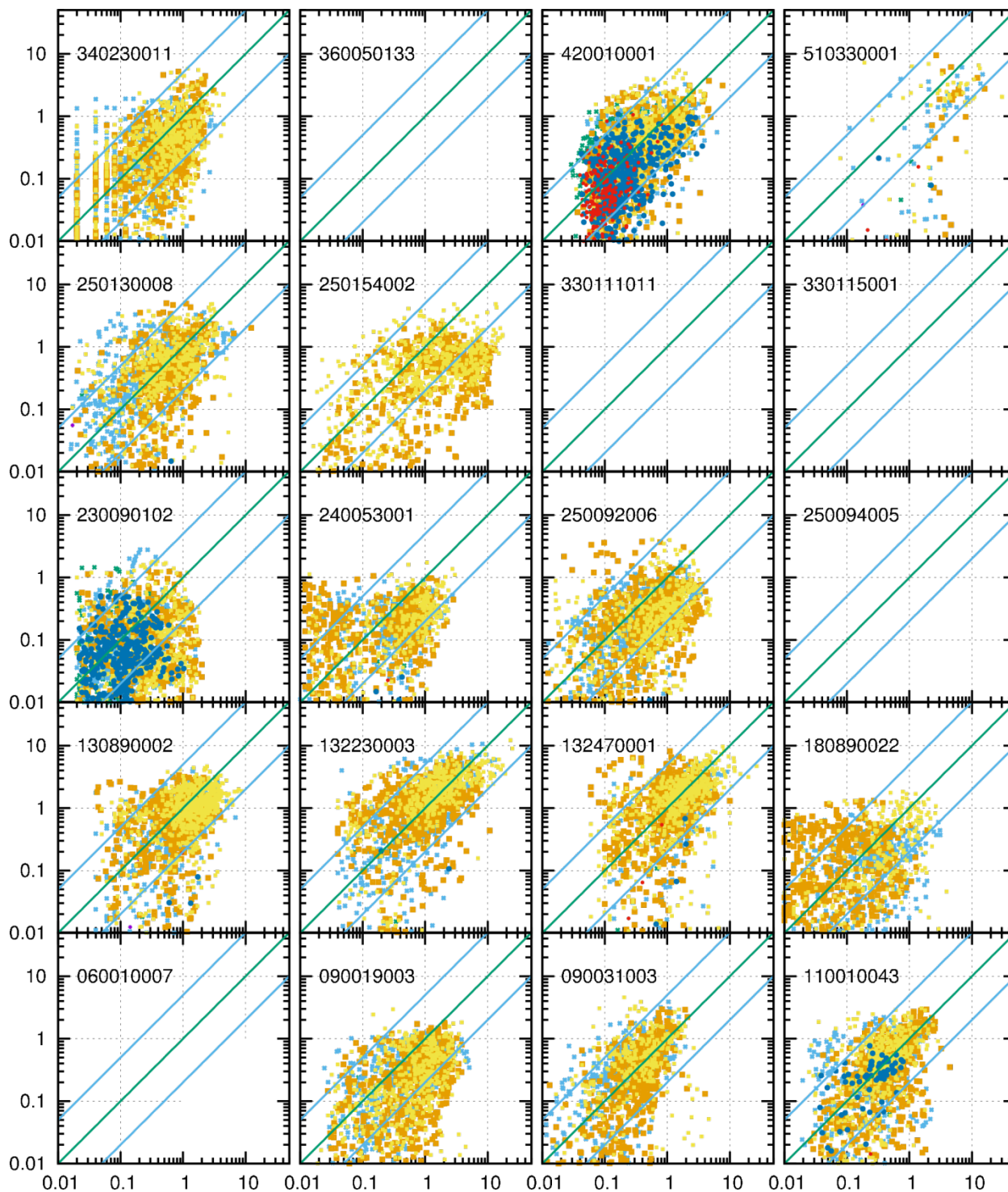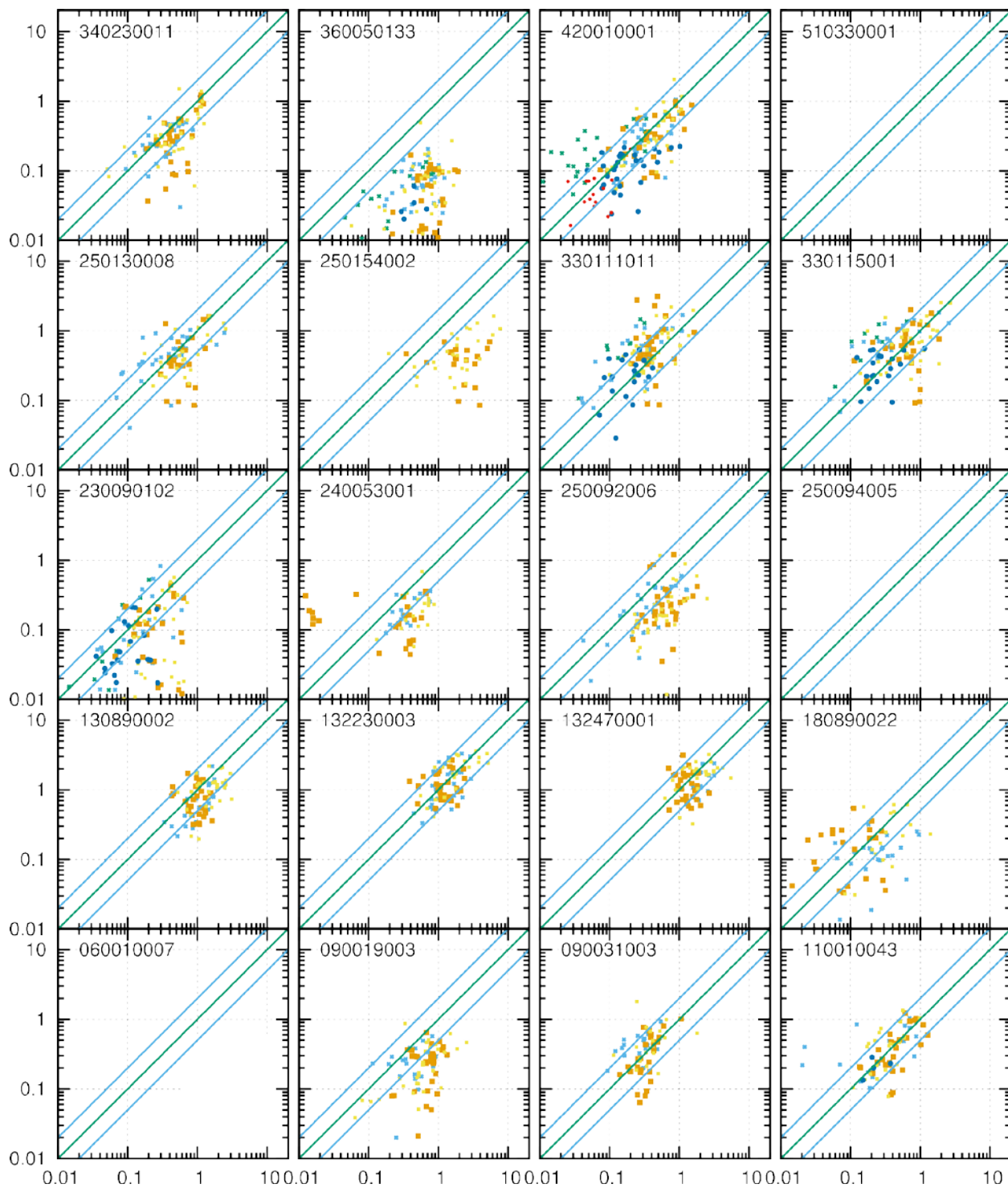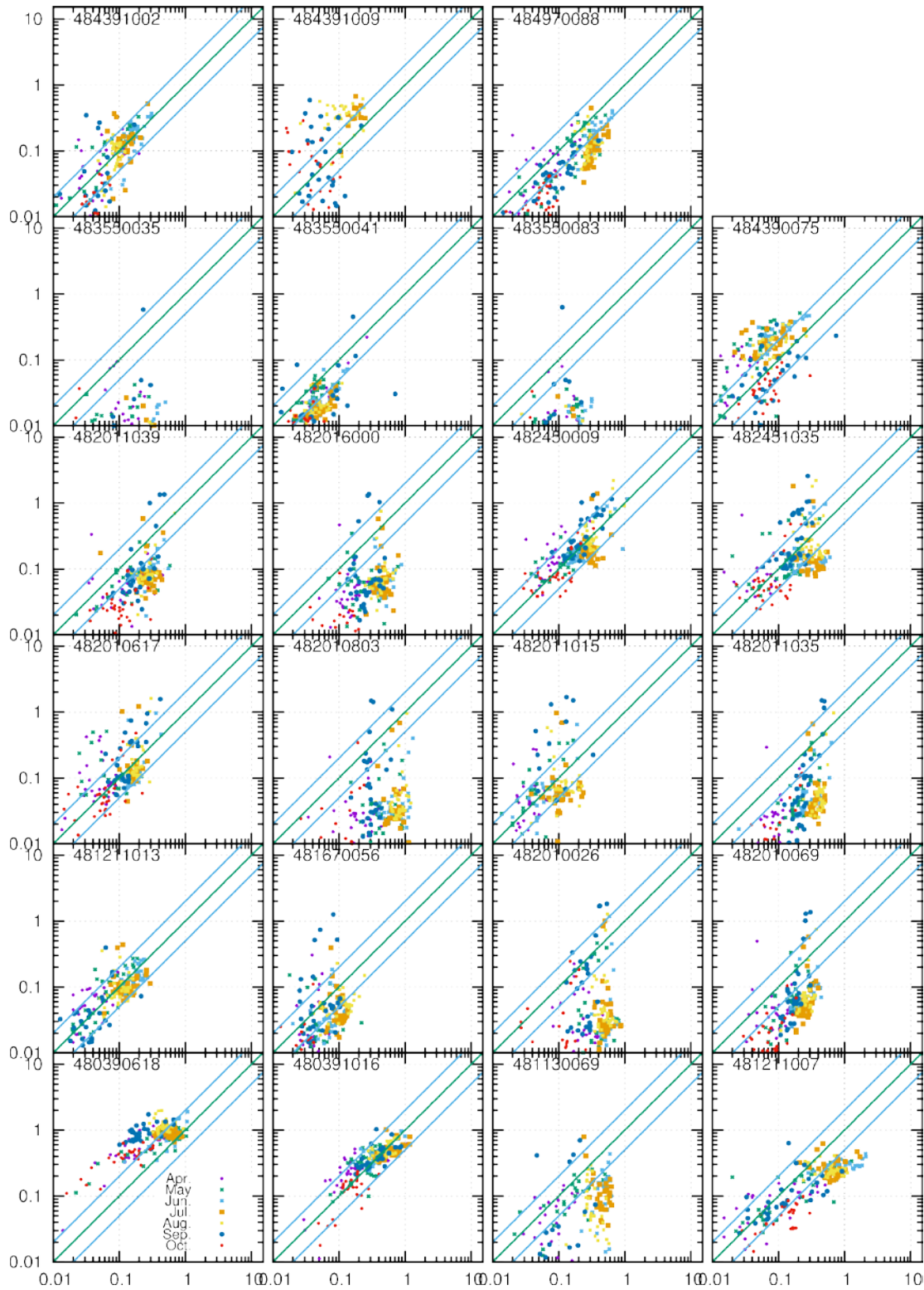
Figure 24 Predicted (4-km) vs. observed daily average isoprene at all Texas Auto-GC sites with valid measurements in April to October 2011. (Units are ppb). The green lines are 1:1, 1:5 and 5:1 ratios.

2.6.3 Evaluation of ozone concentrations

Time series of ozone at all monitor sites in 2011 and 2007 can be found in Appendix B and C, respectively. In this section, the capability of the model in reproducing the observed ozone concentrations in the 4-km Texas domain are shown in Figure 25 using mean normalized bias (MNB) and mean normalized error (MNE) for each modeled month in 2007 and 2011. In both years, ozone concentrations are under-predicted, except for July when ozone concentrations are slightly over-predicted. Overall the ozone performance is better in 2011 than that in 2007. Daily peak ozone concentrations in 2011 are generally well predicted. Although the accuracy of paired peak (APP) is slightly negative (Table 15), indicating under-prediction of peak ozone concentrations at the hour when the observation is at its peak, the accuracy of the unpaired peak is close to zero, especially in summer months. This suggests that the model is generally capable of predicting the peak ozone concentrations, although the timing of the peaks might be slightly off. AAP and AUP for 2007 are also worse than those in 2011 (Table 16). This further confirms the more severe problem of ozone under-predictions in 2007. NO_2 and NOx concentrations at the monitoring sites generally agree with observations thus they are not the cause of ozone under-prediction. A sensitivity simulation was conducted to increase isoprene by a factor of 1.67 (which was chosen arbitrarily) in the 4-km domain for 2007. However, no significant increase in ozone concentrations was predicted. Additional analyses are needed to further understand the cause of the ozone under prediction problem in 2007.
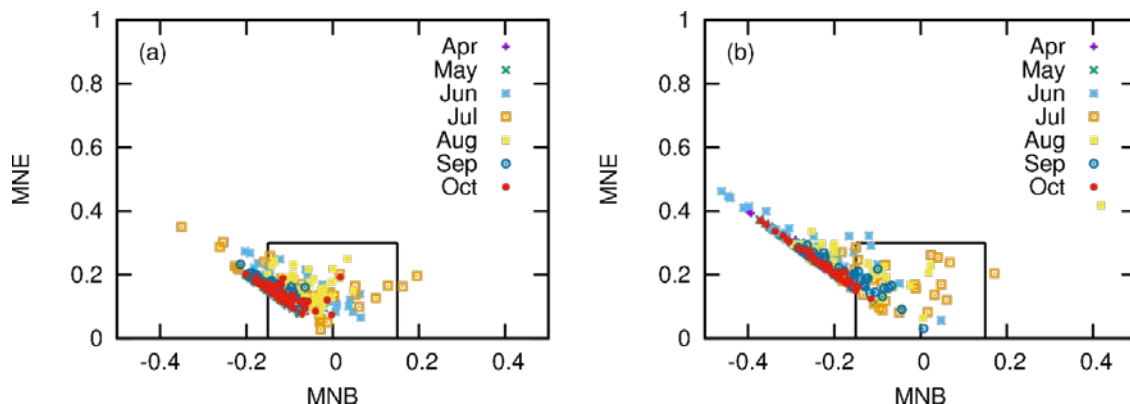
Figure 25 Mean normalized bias (MNB) and mean normalized error (MNE) for 1-hour ozone (>60 ppb) for each station in the 4-km domain in April to October (a) 2011 and (b) 2007. The inner boxes show the region of satisfactory model performance (MNB≤±0.15 and MNE≤0.3).

Table 15 Model performance of peak ozone for year 2011 (April to October) based on hourly 4-km results at all monitors in Texas in the 4-km domain.

	APP	AAPP	AUP	AAUP
April	-0.97	0.15	-0.09	0.12
May	-0.17	0.17	-0.12	0.13
June	-0.16	0.19	0.00	0.12
July	-0.11	0.39	-0.02	0.12
August	-0.10	0.17	0.01	0.17
September	-0.16	0.18	-0.10	0.15
October	-0.13	0.15	-0.07	0.12

Table 16 Model performance of peak ozone for year 2007 (April to October) based on hourly 4-km results at all monitors in Texas in the 4-km domain.

	APP	AAPP	AUP	AAUP
April	-0.30	0.30	-0.25	0.26
May	-0.30	0.30	-0.24	0.25
June	-0.24	0.29	-0.15	0.24
July	-0.19	0.23	-0.10	0.19
August	-0.19	0.26	-0.05	0.20
September	-0.21	0.23	-0.12	0.17
October	-0.24	0.24	-0.18	0.20

2.7 Impacts of drought on isoprene and ozone

2.7.1 Impact on isoprene emission and concentrations

As discussed in Section 2.3, MEGAN v2.10 considers the drought impacts on isoprene emissions from two perspectives. Firstly, the canopy model predicts a higher leaf temperature in general as a result of increased stomatal resistance thus affecting the energy balance calculation for the leaves. Higher leaf temperature leads to higher isoprene emissions. Since drought index (DI) is used to parametrize this effect on stomatal resistance, the emissions generated considering this effect is termed the DI emissions for simplicity of discussion in the following. Secondly, isoprene emission reduction due to reduced photosynthesis under drought is parameterized as a function of soil moisture and wilting point. The emissions generated considered this effect is termed the DP emissions for simplicity. In the following, we consider three different sets of isoprene emissions: 1) base case emissions without DI and DP, 2) emissions considered DI effect only and 3) emissions consider both DI and DP effects (DIDP case).

Figure 26 compares the three sets of emissions for July 2011. Figure 26(b) shows that considering the DI effect alone leads to increases in the isoprene emissions in southeast US, mostly significantly in regions where the DI index indicates severe drought (see Figure 5) by more than 3 moles s^{-1} per 36x36 km^2 grid cell. Figure 26(c) shows that MEGAN v2.10 predicts a reduction in isoprene emissions in regions where the soil moisture are low, especially in some regions in east Texas, where the reductions predicted to be more than 3 moles s^{-1} per 36x36 km^2 grid cell. In some regions (e.g. in Florida and North and South Carolina), while the PDSI indicates severe drought condition, the soil moisture levels are still above the wilting point plus $\Delta\theta_1$ (see equation (1)) and no reduction of isoprene is predicted. Figure 26(d) shows that when the two effects are considered together, the overall emission increases only slightly in general.
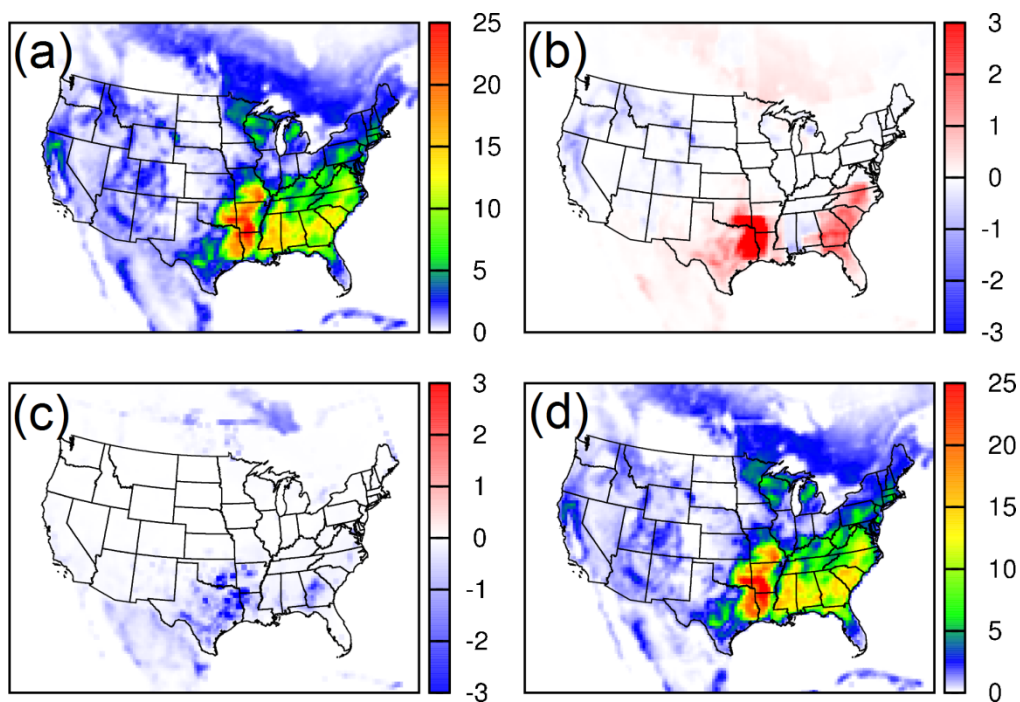
Figure 26 July 2011 monthly average emissions of isoprene generated (a) base case (DI=0 everywhere and no drought parameterization (DP), i.e. γsm=1), (b) difference in isoprene emissions based on gridded DI from NCAR but no DP (DI case – base case), (c) decrease of isoprene emissions due to DP (DPDI case – DI case), and (d) emissions considering both DI and DP (i.e. DIDP case). Units are mole/s.

Figure 27 shows the comparison of monthly average 1-hour isoprene concentrations of the base case and the drought case for June to September 2011. In general, the drought case predicts higher isoprene concentrations than the base case in the southeast US by approximately 0.5 to 1 ppb. As shown in Table 17, the higher isoprene predictions in the drought case slightly improve the MFB values at both non-Texas and Texas monitors but the MFE values remain unchanged. From Figure 28, it can be seen that the impact of drought on isoprene emissions in 2007 is less than that in 2011, with monthly average concentrations changes (both increase and decrease) less than 0.5 ppb. There is not obvious change in the model performance statistics either, as shown in Table 18.

In order to explore the drought impact on isoprene concentrations, monthly averaged diurnal variations for the base case and drought case are shown in Figure 29 for the stations outside Texas and in Figure 31 for Auto-GC stations in Texas. At the non-Texas sites, the predicted average diurnal variation agrees well with observations at most of the sites. The agreement at the Auto-GC sites are not as good, although this poorly agreement is due to the low concentrations of isoprene as discussed before. At the HRM#3 site (482010803) , which is an urban site, the isoprene concentrations are significantly under-predicted. At the Beaumont sites (482450009 and 482451013), isoprene concentrations are over-predicted in September and October 2011.The drought case predicts slightly higher concentrations at all locations but does not change the overall model performance. These results suggest that based on the current parametrizations of drought impacts in the MEGAN model, drought conditions experienced in both 2007 and 2011 did not greatly impact on isoprene emissions and their ambient concentrations.
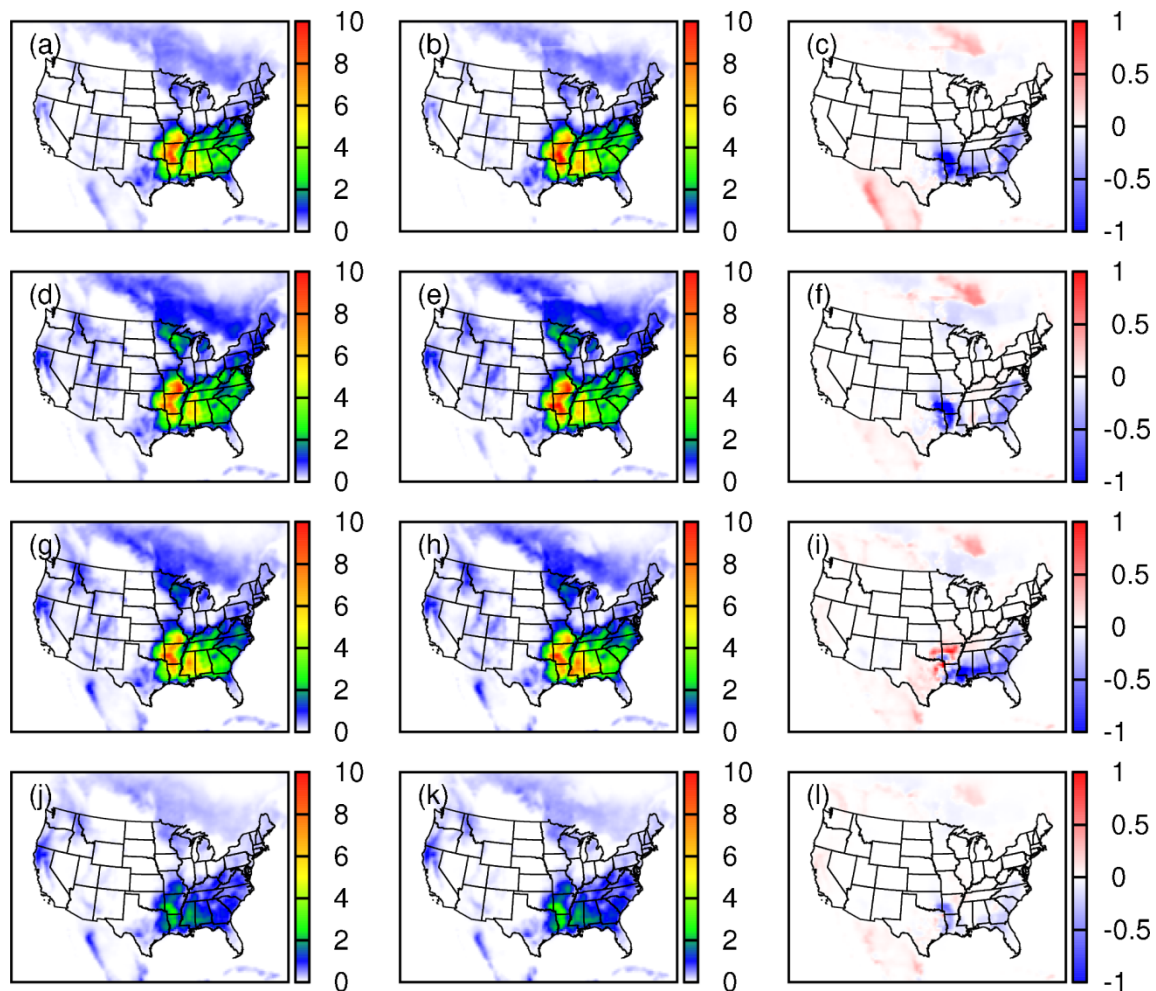
Figure 27 Monthly average isoprene concentrations of base case (a,d,g,j), drought (DI+DP) case (b,e,h,k) and their differences (base case – drought case, c,f,i,l) for June (a-c), July (d-f) and August (g-i) and September (j-l) 2011. Units are ppb.

Table 17 Comparison of model performance of hourly isoprene predictions base case (Base) vs. drought case (DIDP) for 2011

	Non-Texas MFB		Non-Texas MFE		Texas MFB		Texas MFE	
	Base	DIDP	Base	DIDP	Base	DIDP	Base	DIDP
April	-0.37	-0.36	0.90	0.90	-0.41	-0.37	1.02	1.02
May	-0.31	-0.30	1.52	1.53	-0.38	-0.33	0.99	0.99
June	-0.29	-0.25	0.87	0.86	-0.51	-0.46	1.07	1.07
July	-0.31	-0.31	0.86	0.86	-0.49	-0.48	1.07	1.08
August	-0.31	-0.29	0.89	0.89	-0.47	-0.65	1.12	1.24
September	-0.50	-0.50	1.10	1.10	-0.38	-0.36	1.10	1.11
October	-0.53	-0.53	1.14	1.14	-0.71	-0.68	1.09	1.09
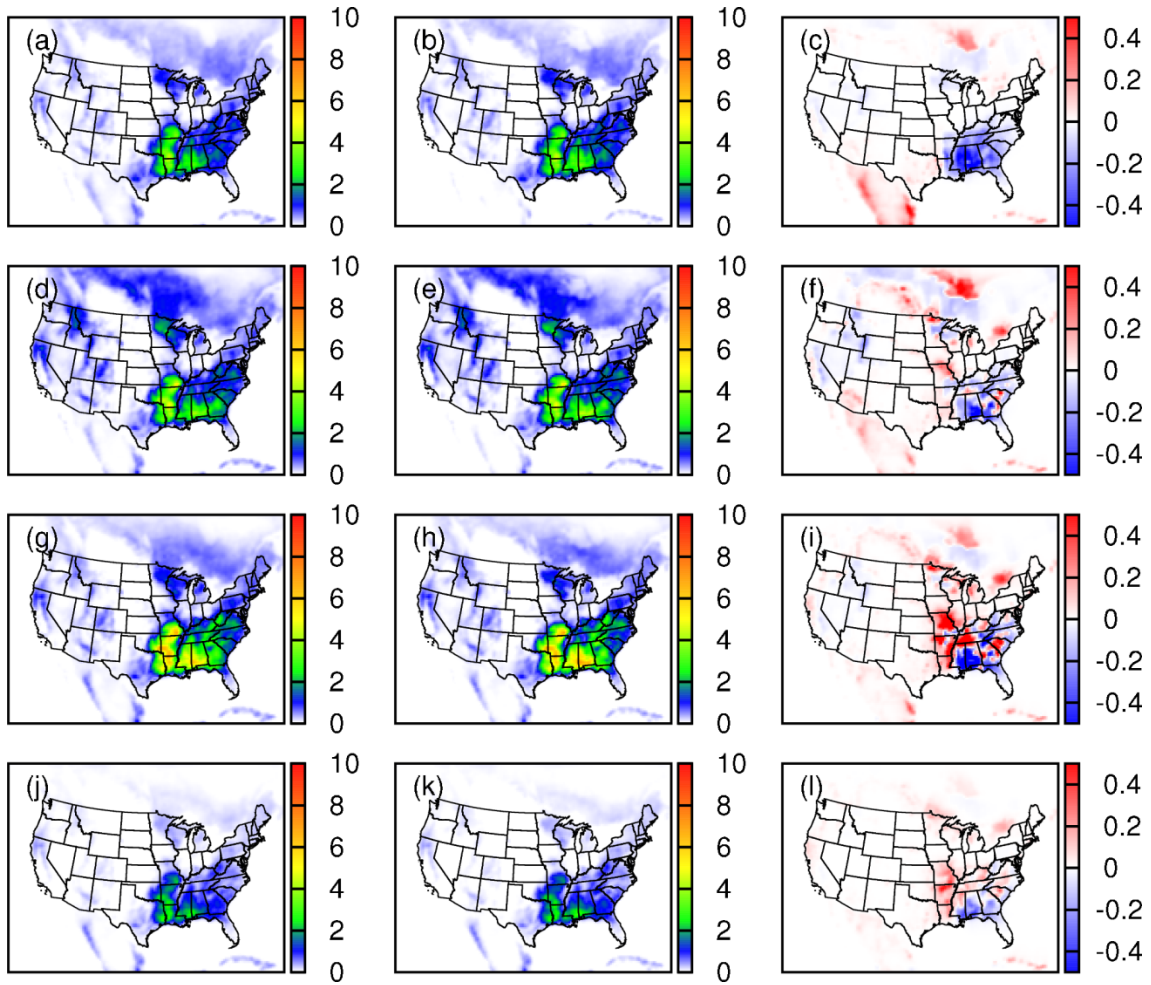
Figure 28 Monthly average isoprene concentrations of base case (a,d,g,j), drought (DI+DP) case (b,e,h,k) and their differences (base case – drought case, c,f,i,l) for June (a-c), July (d-f) and August (g-i) and September (j-l) 2007. Units are ppb.

Table 18 Comparison of model performance of hourly isoprene predictions base case (Base) vs. drought case (DIDP) for 2007

	Non-Texas MFB		Non-Texas MFE		Texas MFB		Texas MFE	
	Base	DIDP	Base	DIDP	Base	DIDP	Base	DIDP
April	-1.37	-1.35	1.59	1.58	-0.43	-0.44	1.04	1.04
May	-0.04	-0.03	1.01	1.01	-0.46	-0.47	1.00	1.00
June	-0.35	-0.31	0.86	0.85	-0.41	-0.43	1.03	1.03
July	-0.52	-0.52	0.98	0.98	-0.48	-0.49	0.97	0.97
August	-0.53	-0.55	0.99	0.99	-0.47	-0.48	1.02	1.03
September	-0.76	-0.75	1.05	1.05	-0.37	-0.39	1.08	1.08
October	-1.23	-1.25	1.37	1.40	-1.05	-1.05	1.35	1.36
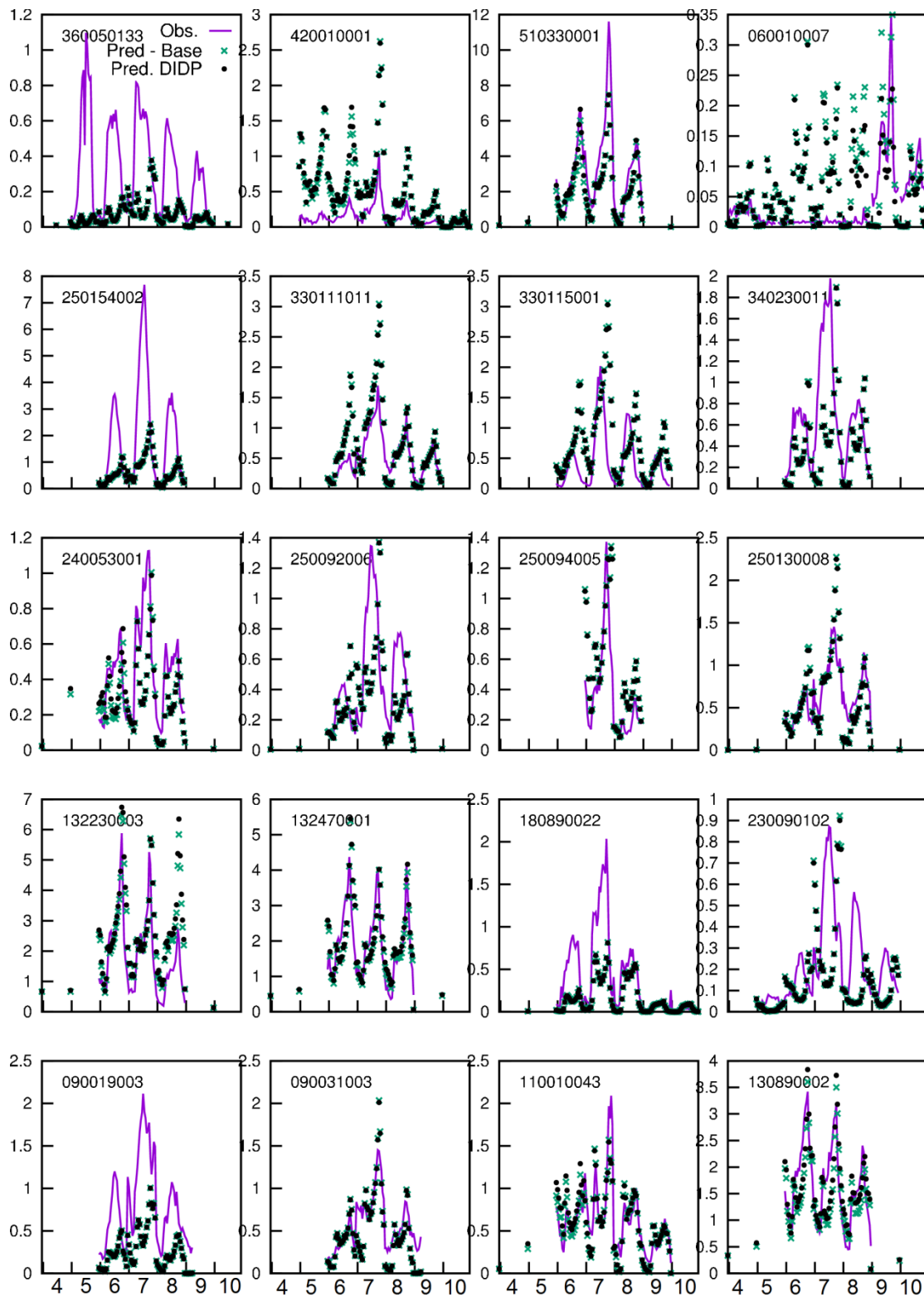
Figure 29 Monthly averaged diurnal variation of isoprene at non-Texas sites. Predictions of base case and drought case (DIDP) are from the 36-km domain.

49
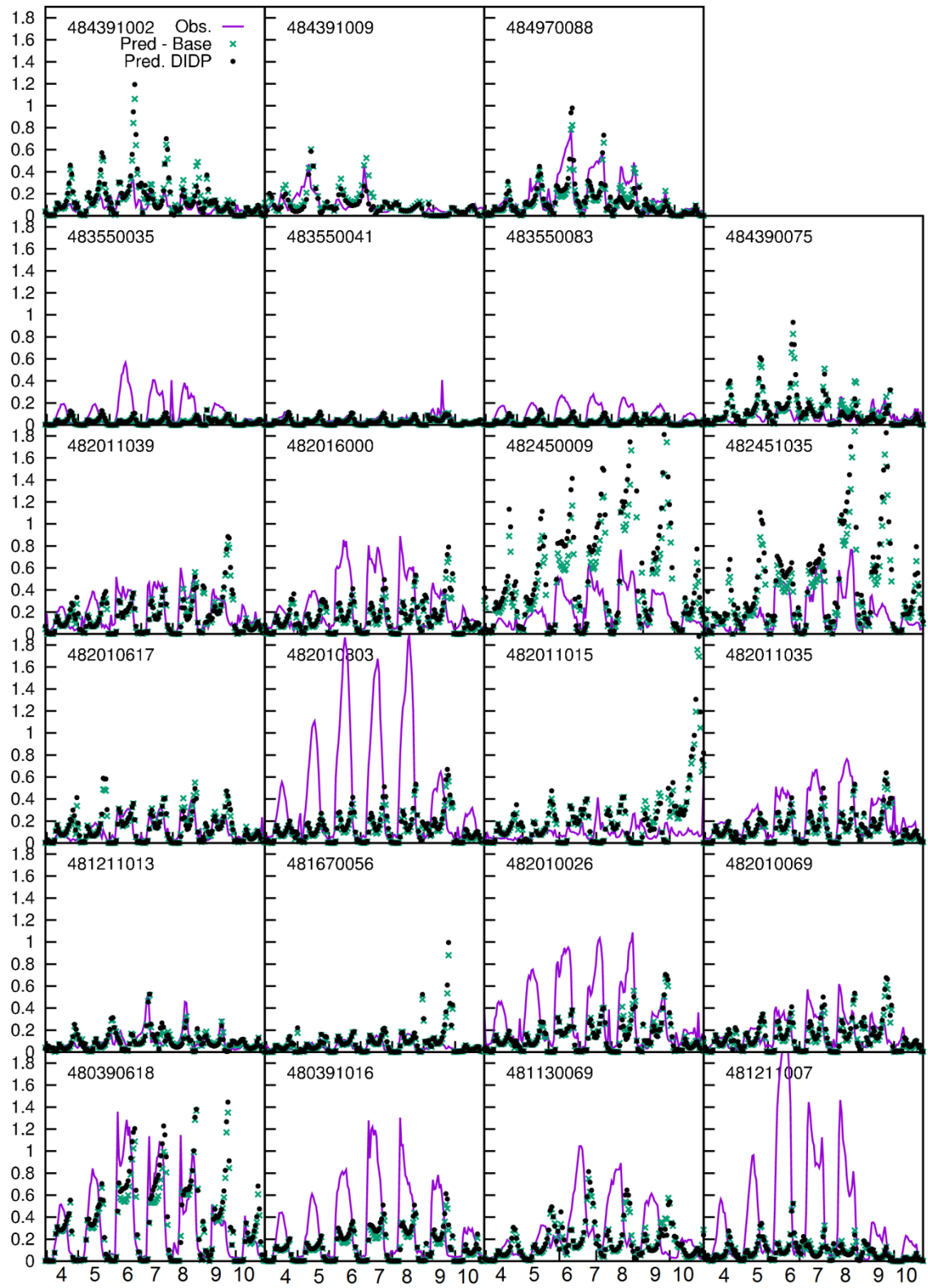
Figure 30 Monthly averaged diurnal variation of isoprene at AutoGC sites. Predictions of base case and drought case (DIDP) are from the 36-km domain.

2.5.3 Impact on ozone concentrations

Figure 31 shows that changes in the isoprene emissions lead to slight decrease in the monthly average peak hour (CST 1400) ozone concentrations in June and July 2011 by less than 0.5 ppb in most areas. However, higher isoprene emissions under drought in August 2011 lead to higher ozone concentrations of approximately 0.5-1 ppb in wide areas throughout the south and southeast US. As the isoprene emission changes are smaller in 2007, changes in peak ozone concentrations are also small (less than 0.5 ppb in most places), as shown in Figure 32.
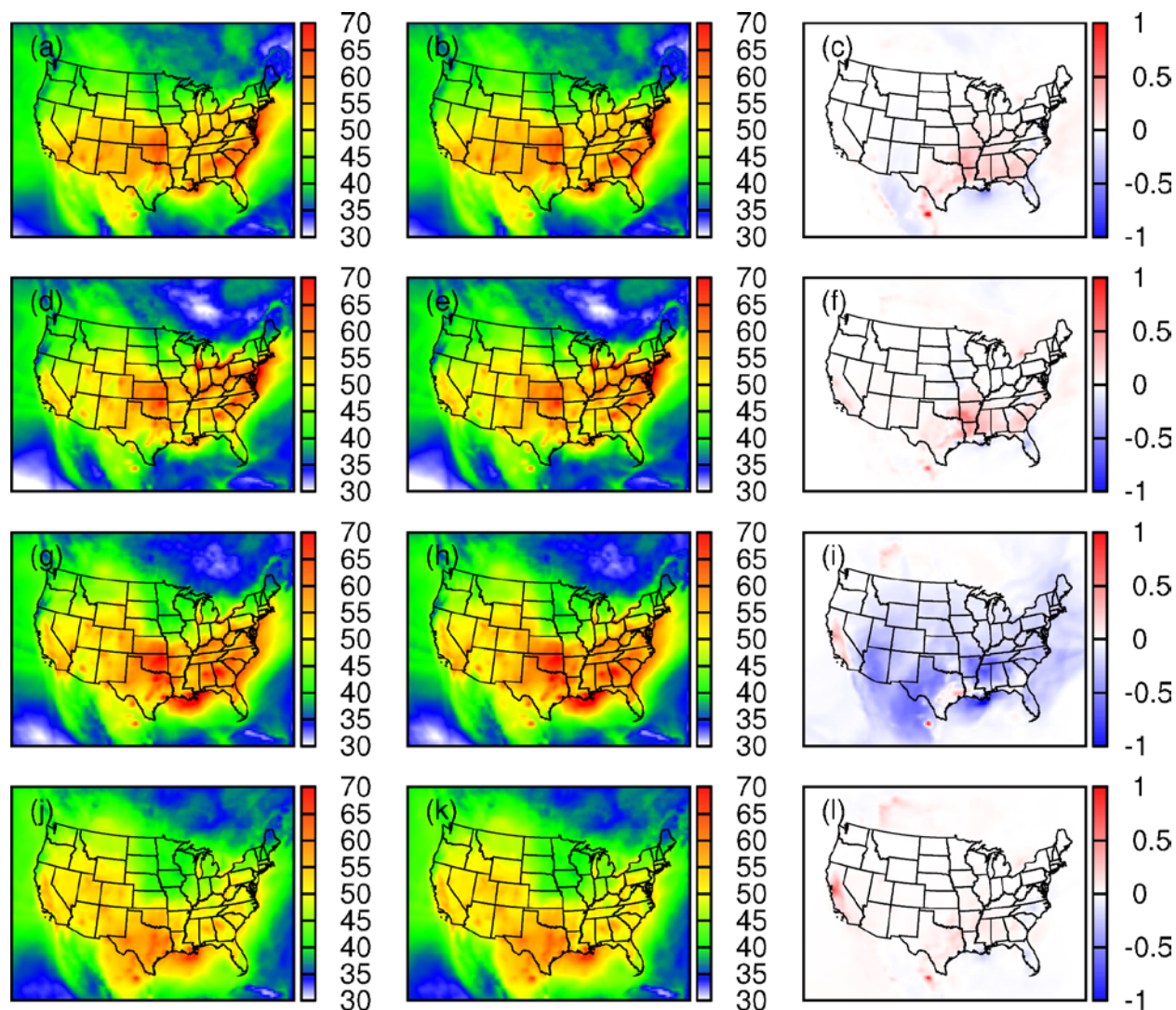
Figure 31 Monthly average 1-h (1400 CST) ozone concentrations of base case (a,d,g,j), drought (DI+DP) case (b,e,h,k) and their differences (base case – drought case, c,f,i,l) for June (a-c), July (d-f) and August (g-i) and September (j-l) 2011. Units are ppb.
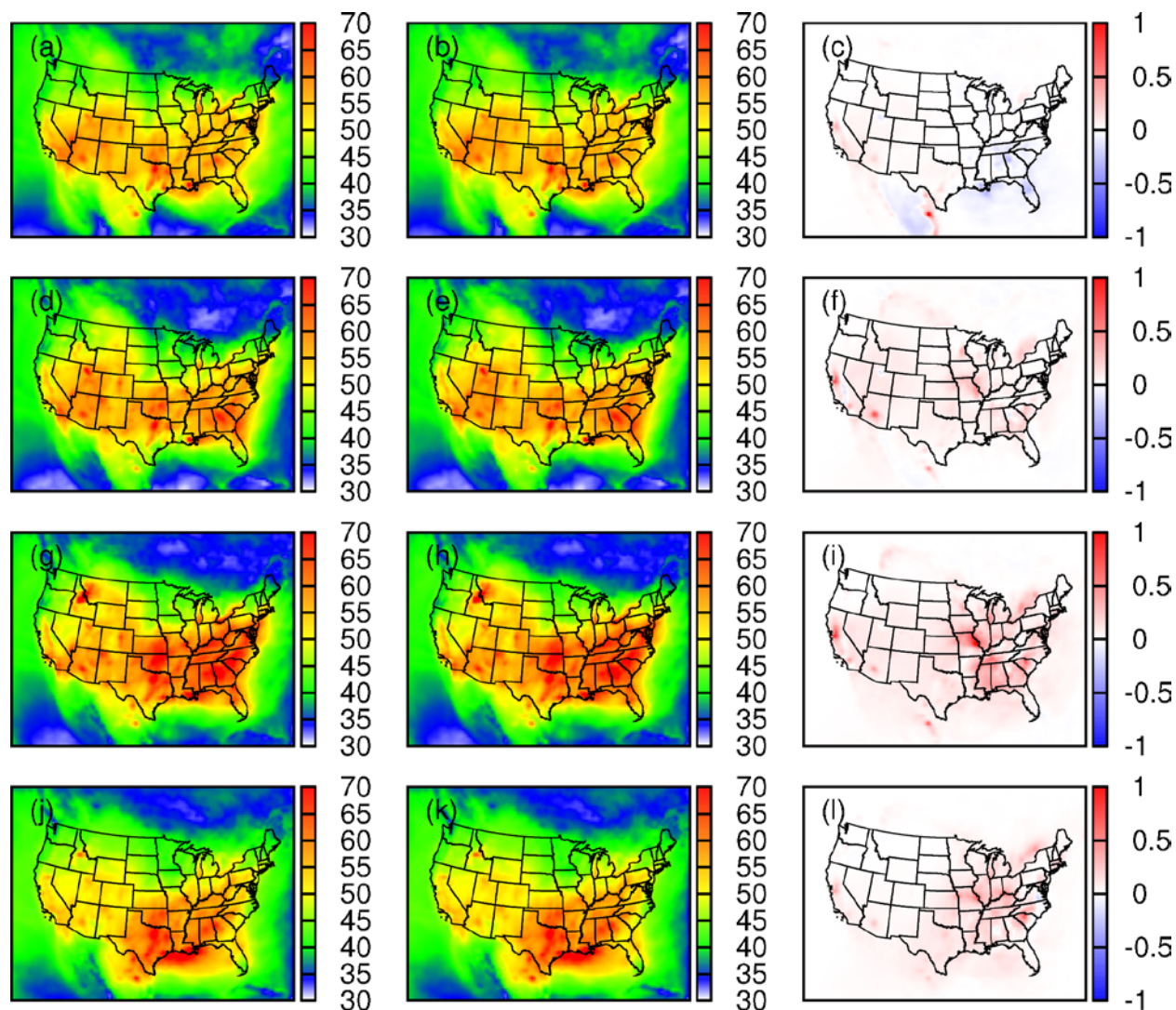
Figure 32 Monthly average 1-h (1400 CST) ozone concentrations of base case (a,d,g,j), drought (DI+DP) case (b,e,h,k) and their differences (base case – drought case, c,f,i,l) for June (a-c), July (d-f) and August (g-i) and September (j-l) 2007. Units are ppb.

Ozone model performance statistics for the DIDP case based on the 4-km domain are essentially the same as those from the base case simulation. The APP and AAPP for July 2011 improve slightly from -0.11 and 0.17 to -0.09 and 0.16, respectively. The MNB and MNE values also improve slightly, from -0.07 and 0.16 to -0.06 and 0.15, respectively. As the Texas region is wet in 2007, we didn't perform a drought simulation for the 4-km domain.

2.8 *Summary*

The original MEGAN v2.10 model was updated in this study to include a parameterization of the soil moisture activity factor γ_{SM} following the equation in Guenther et al.[9] to better predict isoprene emissions under drought conditions. The updated MEGAN model calculates the weighted activity factor in each grid cell using soil-texture based wilting point and root zone distribution in four soil layers as a function of plant functional type (PFT). In addition, a bug in

the original MEGAN v2.10 model was fixed to correctly read a gridded Palmer Drought Severity Index (PDSI) field for the canopy model to estimate leaf surface temperature under drought conditions, which could also affect isoprene emissions. The regional soil moisture field needed for the MEGAN model was estimated using the WRF model with the Noah land surface scheme initialized with the soil moisture field from NLDAS-2 with Noah-2.8. Wilting point data needed for the drought parametrization were estimated using the Penn State CONUS-SOIL database and the soil-related hydraulic parameters from Table 2 of Chen and Dudhia [1]. The predicted soil moisture generally agrees with observations.

The MEGAN model with its own isoprene emission factor (EF) field severely over-predicts isoprene concentrations. Alternative EF fields generated from two different versions of the BEIS models (v3.14 and v3.61) and their accompanying land use data bases (BELD3 and BELD4, respectively) were applied in the updated MEGAN model. Comparison of predicted hourly and daily averaged isoprene concentrations at all isoprene monitors in and out of Texas in a total of 14 months in 2007 and 2011 showed that the MEGAN model with EF fields from the new BEIS model (hereafter MEGAN-BEIS361) and its input data (BELD4) can significantly improve the model capability in reproducing the observed isoprene concentrations at all locations. While MEGAN-BEIS361 in general provides satisfactory isoprene predictions, under-estimation in the EF for urban land type (10 gC/km^2-hr) might have led to large under-predictions of isoprene at a number of urban sites in Houston and Dallas/Fort Worth areas in Texas.

Predicted isoprene emissions under drought condition considering the impact on leaf temperature alone leads to increase in isoprene emissions. The magnitude of emission increasing was reduced when soil moisture activity factor was also considered. When both factors were considered, the resulted isoprene and ozone concentrations in both 2007 and 2011 changed only slightly (less than 1 ppb for monthly average 1-hour isoprene at locations where drought was significant and less than 1 ppb for monthly average peak ozone concentrations).

2.9 Audits of Data Quality

All model input data (WRF, SMOKE, CMAQ) were prepared by PhD student Peng Wang . PI Qi Ying audited all the input data (100%) generated by the student through data visualization software. The validity of the model outputs (WRF and CMAQ) were extensively evaluated using model performance statistics, scatter plots and time series plots. All (100%) model performance statistics values generated by the student were examined by the PI. The validity of the input data, biogenic emissions and CMAQ results was further audited by the PI by independently running the biogenic emission model and CMAQ model with a different photochemical mechanism for one month (July 2011). The model performance statistics generated by the PI were compared with those generated by the student with the CB05 chemical mechanism and good agreement was found.

3. Comparing Isoprene Emission Field Measurements to Models

3.1 Field data

Field measurements of basal isoprene emissions were carried out during the 2011 drought season in east Texas along an urban-to-rural gradient (Barta et al., 2011). Samples were obtained and analyzed in the same fashion as described for the greenhouse measurements in this project. Calibrations were based on the same gas standard, which was confirmed against a new standard obtained for this project (comparative calibration curves are shown in Appendix G of this report).

Field data from 2011, an example shown in Figure 33 alongside the measured topsoil moisture at the site (see below), were normalized to the maximum seasonal flux in order to evaluate the seasonal drop in emissions, which we assumed to have been strongly driven by the drop in soil moistures throughout the development of the severe 2011 drought in east Texas.
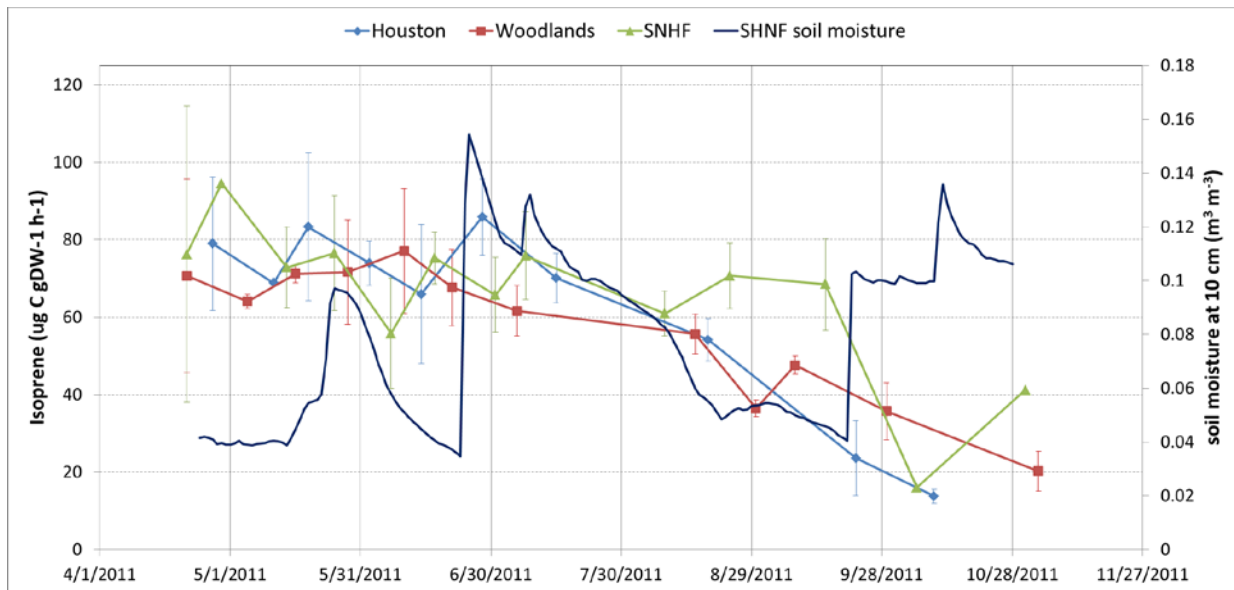
Figure 33 Basal isoprene emissions from post oak leaves during 2011 (field days showing averages ±1 sd, connected by lines) alongside measured (average daily) topsoil moisture at the Sam Houston National Forest field site (continuous measurement at nearby weather station).

3.2 Soil moisture estimates

Soil moisture in the root zone, θ [m^3 m^{-3}], was derived using a simple soil moisture model developed by Manfreda et al. [38] that is based on input from a measurement located in the topsoil alongside knowledge of the soil's wilting point, θ_w, and field capacity, θ_c . Soil relative saturation (aka θ/n) at time t_j in the soil layer below the topsoil, θ_2/n_2, is constantly updated from knowledge of wilting point, $\theta_{w,2}$, and topsoil field capacity, $\theta_{c,1}$, following

$$\theta_2(t_j)/n_2 = 1/n_2 \times (\theta_{w,2} + (\theta_2(t_{j-1}) - \theta_{w,2}) \exp(-a \Delta t) + (1 - \theta_{w,2}) b\, y(t_j) \Delta t) \qquad (5)$$

with

$n_{1,2}$ = soil porosity (based on texture)

$y(t_j) = \theta_1(t_j)/n_1 - \theta_{c,1}/n_1$, fraction of excess water in topsoil infiltrating lower layer
$a = ET_2 / ((1 - \theta_{w,2}) n_2 z_2)$, ET_2 = (evapotransporational) water loss from lower layer
$b = n_1 z_1 / ((1 - \theta_{w,2}) n_2 z_2)$
$z_{1,2}$ = soil depths of topsoil and lower layer
$\Delta t = t_j - t_{j-1}$, model time step (here: 15 min)

The model was designed mainly for semi-arid environments, aka topsoil runoff is presumed negligible, and so is percolation to layers below the chosen depth of the "lower" layer, z_2. The model calculates a single average soil moisture for a root-zone layer below the topsoil (0-0.1 m) that extends to a predefined depth, which should be chosen based on the prevalent vegetation rooting depth (here: 0.1-1 m or 0.1-2 m). Wilting points and field capacities were derived from knowledge of the local soil textures (from topsoil collected in 2012 and analyzed by the Texas A&M *Soil, Water, and Forage Testing Laboratory, Department of Soil and Crop Sciences*, http://soiltesting.tamu.edu, alongside the USGS web soil survey, WSS, data base [39]), and an analysis of the actual soil moisture measurements (model EC5 soil moisture sensor from Decagon Devices, Inc., Pullman, WA, installed between 5 and 10 cm soil depth). For instance, seasonal field capacity was derived from a close look at the locally measured topsoil moisture during and after large rain events, and identified as the first plateau after rapid drainage. Local soil texture measurements and tabulated data used in the land surface model that feeds soil moistures into MEGAN (Noah) matched within 1-2% volumetric soil moistures (Table 9). Local field capacity is important because the model uses measured exceedances of field capacity (parameter y) to move soil moisture into the lower layer (infiltration). The remaining input factors to the model are daily water losses to evapotranspiration, *ET*, runoff and drainage/percolation, and soil depth of the root zone.

Table 19 Soil moisture model input data (in soil moisture fraction, i.e. m^3/m^3)

sites	wilting point	field capacity	wilting points (Noah)
Sam Houston NF	0.05	0.14	0.06 (0.1 m) to 0.12 (2 m)
The Woodlands	0.05	0.15	0.05 (0.1 m) to 0.06 (2 m)
Houston, JDHS	0.1	0.23	0.08 (0.1 m) to 0.11 (2 m)

We assumed drainage to be negligible during the growing season in 2011. *ET* was calculated for each site using the Penman equation in the format suggested by Shuttleworth (2007), equation 1, which allowed using locally measured meteorological data as input values instead of modeled values. Daily *ET* varied from less than 1 to 7 mm.

$$ET = (m\, R_n + \gamma\, (6.43 \times (1+0.536 \times U) \times \delta e)) / (\lambda_v\, (m + \gamma)) \qquad (6)$$
where
ET = Evaporation rate [mm day^{-1}]
m = Slope of the saturation vapor pressure curve [kPa K^{-1}]
R_n = Net irradiance [MJ m^{-2} day^{-1}] (calculated from measured PAR, albedo, and surface T)
γ = psychrometric constant = $0.0016286 \times P(kPa)/ \lambda_v$ [kPa K^{-1}]
U = wind speed [m s^{-1}]
δe = vapor pressure deficit [kPa]
λ_v = latent heat of vaporization of water [MJ kg^{-1})]

Ambiguity arises first as a result of root-zone depth not being known for the oak species investigated for this study. Typically, soil moisture down to one meter depth is used but up to depths of two meters is presumed to be accessible, and here we calculated two scenarios: one with a root zone depth to 1 m and one with a root zone depth to 2 m. The latter leads to an average higher soil moisture in this simple model as daily losses to *ET* occur from a larger volume.

We first compared calculated soil moistures to the output data from the Noah model currently used to feed MEGAN. Figure 34 shows the best and worst comparisons between the data-driven simple model and the depth-averaged Noah model results. In the case of urban Houston, the Noah model output is unrealistically high; in the case of Sam Houston National Forest, the Noah model shows larger fluctuations, possibly as a result of the slower updating procedure and higher soil layer resolution (the model assumes three layers, 0.1-0.4 m, 0.4-1.0 m, and 1-2 m depths, where the simple model assumes only one root-zone layer). Overall, the two models compared slightly better when a layer depth of only one meter was assumed rather than two meters.
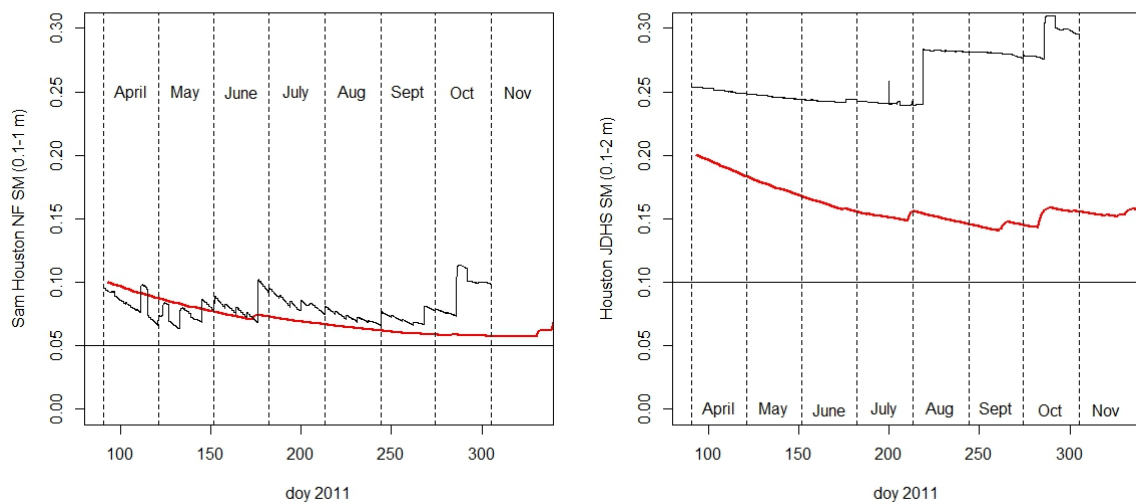
Figure 34 Soil moisture comparisons between the local, simple model (updated every 15 min) based on continuous onsite topsoil measurements (thick red lines) and the equivalent, depth-averaged soil moisture output from the Noah model (updated daily and weekly) for the grid cell that incorporates the measurement site (thin, black lines); the horizontal line marks the wilting point. The left panel shows a good, the right panel a poor correspondence.

3.3 Comparisons to the soil moisture activity factor

Using the current MEGAN parametrization for soil moisture, we calculated the soil moisture activity factor, γ_{SM}, following equation 2 (Guenther et al., 2012), and presumed it to be directly comparable to observed relative basal isoprene emissions. This is approximately correct considering that long-term temperature and light effects on basal isoprene emissions are typically very small compared to their instantaneous effects and/or soil moisture, θ. Once the latter drops

below the wilting point, θ_w, plus the empirical "buffer" value (here: $\Delta\theta_1$=0.04), θ_1, basal isoprene emissions are expected to drop linearly with soil moisture presuming the model correctly reflects the average physiological plant response affecting isoprene production.

$$\begin{aligned} \gamma_{SM} &= 1 & &\text{for } \theta > \theta_1 \\ \gamma_{SM} &= (\theta - \theta_w)/\Delta\theta_1 & &\text{for } \theta_w < \theta < \theta_1 \;,\; \theta_1 = \Delta\theta_1 + \theta_w \qquad\qquad (7) \\ \gamma_{SM} &= 0 & &\text{for } \theta \leq \theta_w \end{aligned}$$

In Figure 35, we depict observed relative isoprene emissions rates in comparison to the simple model 1-m and 2-m soil moisture γ_{SM} factors, as well as one 1-m γ_{SM} factor for the Woodlands site (30.157 N, 95.496 W). While almost all data fall between the local model γ_{SM} factors, the Noah grid cell soil moisture γ_{SM} factor may have dramatically overestimated the isoprene reduction response during spring and summer in this case. Note that the studied water oak in the Woodlands grew close to a drainage ditch and may thus have had access to higher soil moistures on average. It tended to respond rapidly to limited local rainfalls that wetted only the topsoil layer and had reduced isoprene emissions earlier in the season (May and June) than post oak. Figure 36 shows the same comparison for the Sam Houston NF site. Again, the data fall close to or between the local soil moisture derived gamma-factors, and the fluctuations in gamma factors are much larger for the underlying land surface model derived 1-m soil moisture.
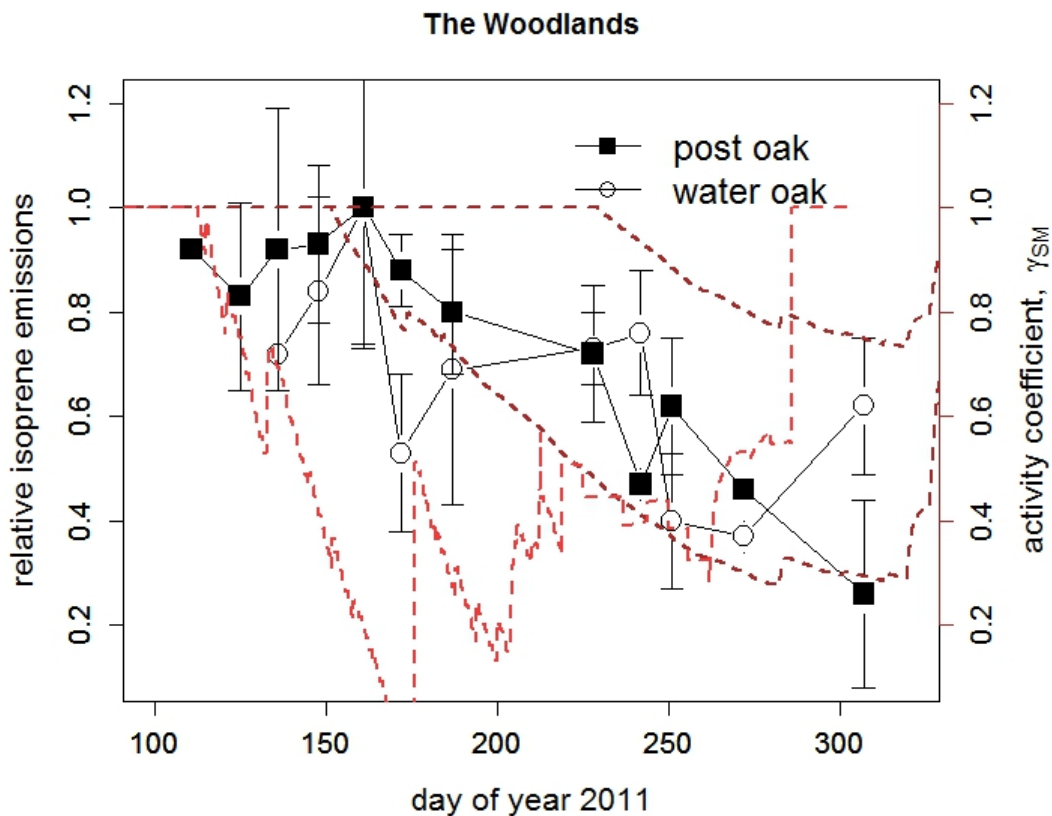
The Woodlands

Figure 35 Relative basal isoprene emissions (±1 sd) from post oak and water oak trees in The Woodlands during 2011 as compared to calculated soil moisture activity factors. The two dark dashed brown lines reflect the simple model for a 1-m (lower) and 2-m (upper) root-zone depth,

while the light brown curve reflects the Noah land surface model average grid-cell 1-m average soil moisture calculation.

In the second case, the forested landscape, the higher activity factor fluctuations appear to be reflected in the water oak measurements, which maximized in late June when soil moistures from the land surface model led to gamma factors of one. Overall, it appears as if the water oak data is better reflected by the 1-m root-zone depth soil moisture, while the post oak results show a mixture that may indicate that post oak trees have access to water deeper in the soil, potentially up to two meters. This is an expected result reflecting the lower drought resistance and general occurrence of water oak in lowlands, as compared to a geographically wider post oak distribution based on a strong central tap-root and low water flow resistance that improves the species' drought hardiness [40, 41].

Improvements in the model-to-measurement comparison can be achieved through either improved knowledge of root-zone depth or adjustment of the drought response parameterization, such as via a larger or smaller "buffer" factor ($\Delta\theta_1 = 0.04$ in MEGAN). For example, an improved match between γ_{SM} (1-m) and relative post oak basal isoprene emissions in Figure 35 would be achieved choosing $\Delta\theta_1 = 0.03$, but an improved match between water oak relative basal emissions and γ_{SM} (1-m) would rather be achieved by selecting a smaller root-zone depth, e.g. 0.5 m, while keeping track of lower layers.
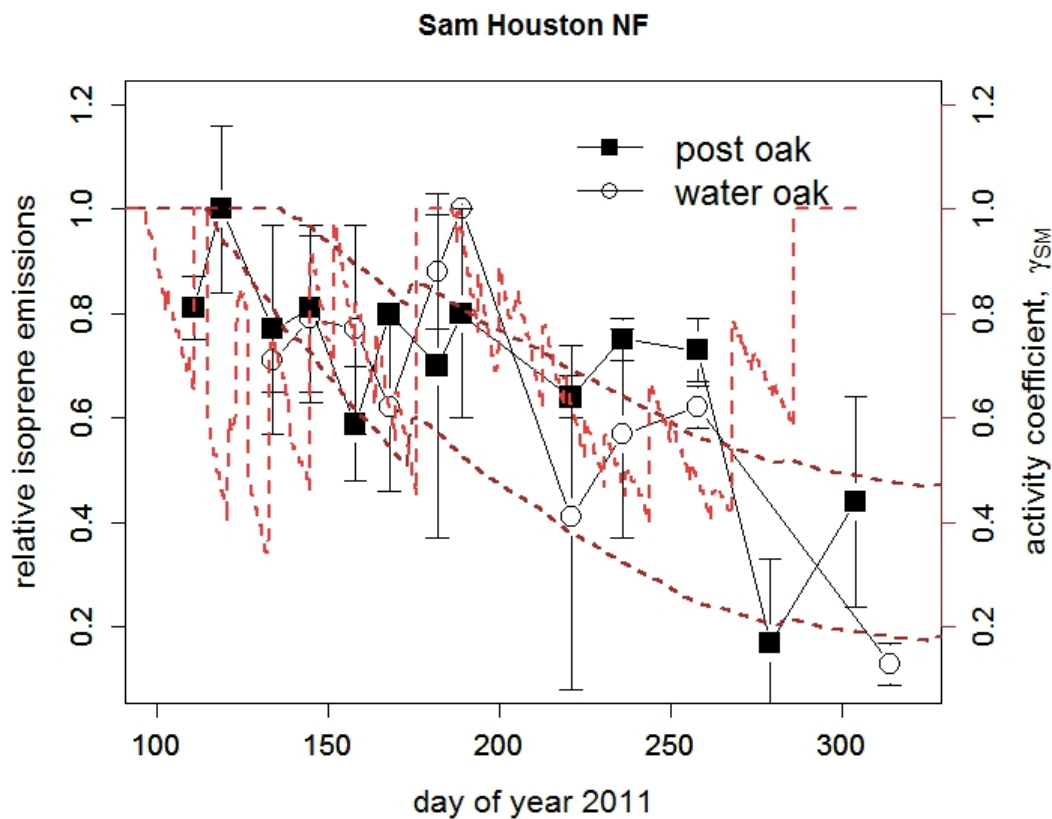
Figure 36 Sam as Figure 35 but for the Sam Houston National Forest site during 2011 as compared to calculated soil moisture activity factors.

3.4 Conclusions

These results cannot alleviate the ambiguity of the drought response of isoprene emitting oaks that results from (i) the root-zone soil depth of the species, and (ii) the drought response parametrization. Instead, they demonstrate that a uniform root-zone depth selection and a uniform drought response parametrization may lead to regionally paradoxical results. In regions dominated by more drought resistant oak species such as *Quercus stellata* a deeper root zone may have to be considered alongside a narrower range of soil moistures that affect isoprene emissions, while the opposite should be considered in regions dominated by less drought resistant species such as *Quercus nigra*. Since such adjustments to the emission model require more detailed land model inputs rather than model parameter changes, we recommend a focus on improving land surface information, particularly rooting depth and soil moisture estimates. However, the results from this study should be interpreted with care due to limited number of measurements.

4. Comparing Isoprene Emission Measurements on Greenhouse Grown Texas Oak Species to the current Model

Two-year old (in 2014) Post Oak (*Quercus stellata*) and Water Oak (*Quercus nigra*) seedlings were grown in a well-characterized sandy loam soil mix (Appendix E2; fertilized after analysis) in pots under greenhouse conditions on the College Station campus. Leaf physiology and isoprene emissions measurements were performed regularly on both well-watered and droughted specimen in fall 2014 and spring 2015. A CIRAS-2 (PPSystems, Amesbury, MA) leaf level photosynthesis analyzer was used to evaluate leaf physiology, and Tenax as well as activated carbon adsorption cartridges were used to sample isoprene via a bypass during the measurements. Cartridges were analyzed via a standard TD-GC-FID analysis procedure (section 4.1) with a precision of better than 5% and an accuracy of better than 10%. All experiments were performed at standard temperature and light level settings (30 °C and 1000 µmol m^{-2} s^{-1} PAR), giving the so-called *basal emissions*.

Experiments in fall 2014 were inconclusive with respect to the effect of drought since plants had been stressed by various factors including pests as a result of moving and greenhouse management. Here, we include the results from spring 2015 measurements on sets of newly developed leaves. While these experiments were more successful than the fall 2014 measurements, we caution that the results are specific to young, potentially immature leaves, as evident from comparatively low photosynthesis rates.

4.1 VOC analysis

Cartridges with biogenic VOCs (BVOCs) were analyzed using a thermal desorption (TD) gas chromatography (GC) flame ionization detection (FID) technique. The TD instrument used is a Perkin-Elmer ATD400 thermal desorber; the GC-FID instrument is an HP5890 series II with electronic pressure control (EPC) board.

The system was operated with hydrogen as carrier and FID fuel gas, coming from a Matheson TriGas Chrysalis II model 250 HPNM hydrogen generator. The hydrogen is of 99.9999% purity and flowing through an additional indicating moisture trap for quality control. Pressure-controlled carrier gas flow is routed through the GC's injector toward the ATD400.

4.1.1 VOC sampling

VOCs were sampled via adsorption onto standard prefilled ¼" OD, 0.15" ID, 3.5" long glass cartridges designed for use with thermal desorption instruments. We use both commercially obtained (Perkin-Elmer) and some "homemade" glass cartridges. Either were filled with Tenax (see below) a combination of activated carbon adsorbents held in place by glass wool plugs. We use a packing of 125 mg Carbopack B and 55 mg Carbopack X of 60/80 mesh size (Supelco, Bellefonte, PA), separated by a glass fiber disk.

For this project, an additional 24 cartridges filled with ~200 mg Tenax TA (Supelco, Bellefonte, PA) each as an alternative trapping material were obtained. Tenax cartridges were tested using different concentrations and volumes of isoprene to determine if this trapping material was the adequate for our experiment. It is often selected as the adsorbent of choice, however, after

completing a breakthrough curve and subsequently a calibration curve, it was concluded that we needed to keep using carbon adsorbent cartridges for the greenhouse study.

To sample VOCs emitted from a leaf inserted into the CIRAS-2 cuvette onto the adsorbent cartridges, the cuvette outflow was modified to allow parallel photosynthesis and emission sampling. The cuvette outflow (350 mL min^{-1}) line was substituted by a ¼" OD Teflon Y-tube in our system. One branch of the Y was routed to the system's internal pump at its rate of 100 mL min^{-1} for CO_2/H_2O gas exchange measurement, while the second branch was connected to an external sampling system. A 2-port Teflon, switch-activated 12 VDC solenoid valve (Biochem Fluidics, Boonton, NJ) installed into the second branch opens the flow of air from the cuvette to the trap at the beginning of sampling. An external 12 VDC pump operated by the same switch aspirates 200 mL min^{-1} as controlled by a precision mass flow controller (GFC-17, Aalborg, Orangeburg, NY) over the cartridge for a user-selected time period. A 0.5 L air sample was collected, i.e. the bypass was operated for 2.5 minutes. During this time, the excess cuvette flow drops to 100 mL min^{-1}, but leaf physiology is monitored at the same time to account for possible deviations as a result of this reduced excess cuvette flow.

Two kinds of blanks were regularly sampled for quality control: Empty cuvette blanks at experimental conditions (no leaf in cuvette) and cartridge blanks, to correct for variations in background VOC concentrations, and possible adsorption of ambient air onto sampling cartridges during handling and transportation, respectively. Between leaf sampling periods the cuvette is typically flushed with air for approximately 3 minutes to remove any residual VOCs. Empty cuvette blanks are sampled in the exact same manner as regular leaf emission samples, while cartridge blanks are only exposed to ambient air in a similar fashion as regular samples are during handling.

All sample cartridges were capped with standard Teflon caps equipped with o-rings (Perkin Elmer, Buckinghamshire, UK). The tubes are kept in glass containers whose lids are lined with Teflon caps to minimize volatile adsorption. Filled and fresh adsorption tubes are stored in separate glass containers, transported to and from the field on cold packs inside an insulated box (cooler) to minimize sample desorption and diffusion. All cartridges were desorbed and their contents analyzed within 72 hours of collection. All cartridges are additionally "cleaned" (desorbed without preconcentration and measurement) the night prior to next day's usage using a cleaning method programmed into the ATD400 automatic desorber. Cartridge cleanliness was assessed via the cartridge blanks each measurement day.

The analytical system had available 48 adsorption cartridges filled with the Carbopack B/Carbotrap X mixture. Cartridge types were tested for diffusive losses in the laboratory using two types of Teflon caps. All cartridges carried assigned, numbered caps, such as to be able to pinpoint a cartridge that fails quality assurance procedures. No other cartridge identification was set in place. All samples were in our direct custody between acquisition and processing. No gas sample cartridges were shipped or transported by any other means than inside their designated glass storage containers. Samples were identified by their numbered caps, with cap number, sampling time and person taking and handling the sample identified via field notebook entries.

4.1.2 ATD400

The ATD400 is an automated adsorption cartridge processing unit providing for
- sample tube leak testing,
- sample tube purge,
- sample tube desorption at preset interval length and desorption temperature,
- sample preconcentration and focusing, and
- sample injection.

Operating similar to an autosampler, its mechanics driven by compressed air, the ATD400 first selects a cartridge from its carousel, takes its caps off and brings it into the flow path. It then pressurizes the tube for leak testing, evaluated via a timed pressure drop as evaluated by an internal pressure sensor. If found non-leaking, the tube is first purged with carrier gas to remove air, particularly oxygen, then thermally desorbed (primary desorption) by clamping an oven of ¾ of the tube's length sideways onto the cartridge. After the preset desorption and preconcentration period (here: 10 min at 220°C), the oven is removed, the tube cooled, recapped, and placed back onto the carousel until the next cartridge is selected for analysis. The preconcentration and focusing trap is a narrow bore inert glass tube filled with a small Carbotrap X plug. It is cooled (-5°C) during the focusing step and rapidly heated (to 220°C for 5 min) to desorb all analytes (secondary desorption and injection) in a narrow band into the carrier gas stream. The desorbed sample is transferred via a heated capillary to the head of the chromatographic column and the ATD400 starts each chromatographic run automatically with secondary desorption. All transfer lines inside the ATD400 are made of glass-lined, inert SS tubing, and inert gas paths are routed using a central Valco valve, whose rotor was replaced in 2010. Turnaround time between cartridges was 45 minutes.

The ATD400 is programmed via its own access panel, independent of the GC software. For quality control, it stores several "methods" and reports deviations from the programmed protocol during and after a series of cartridges is completed.

In addition to the analysis method used to process "loaded" cartridges, we use a "cleaning method" to desorb all cartridges intended for use the following day during the night prior. Cleaning settings are similar to regular desorption setting instead for the fact that a cartridge's volatiles content is discarded instead of analyzed, and turn-around time per cartridge is thus reduced to approximately 15 minutes.

4.1.3 GC-FID system

We operated a HP5890 series II GC with Chemstation software. Analytes are separated on a 60-m $\times$ 0.25 mm MXT-624 Siltek® -treated stainless steel column (Restek Corporation, Bellefonte, PA) using a temperature program geared towards isoprene analysis. The oven/column temperature was initially held at 35°C for 4 min, than increased to 150°C at a rate of 10 °C min^{-1}. Then, temperature was increased to 220°C at 20°C min^{-1} heating rate and held for 11 min. The

carrier gas (H_2) flow rate is set to approximately 2 mL min^{-1} at 40 °C and controlled for constant flow. The FID is operated at 250 °C with a typical 10:1 ratio of zero air and hydrogen using nitrogen as make-up gas. Zero air is produced by a zero air generator in the laboratory (AADCO, FL, model 737, fed by de-oiled house compressed air).

The Chemstation software controls the GC temperatures and carrier gas flow rates, and records the FID signal. We program a set of cartridge measurements as a sequence using the same analysis method. Each cartridge in the sequence is uniquely identified by its cap number and the sample date in form of the file name as YYMMDD##. In addition, the sequence identifier includes leaf temperature, leaf external CO_2 mixing ratio during VOC sampling, sample size, and sample location/site.

The system is calibrated using a single ppm-level isoprene-containing calibration gas. The calibration gas is diluted into zero air at ratios between 1:100 to 1:5000 using two precision flow controllers, one 0-10 mL min^{-1} for the calibration gas, and one 0-5000 mL min^{-1} for zero air. A calibration curve (spanning low ppb to low hundreds of ppb) was generated on a regular basis (3-point for each measurement day, 6-8 point every 2-3 months) using the same cartridges used for field sampling. For each calibration sample, part of the zero air diluent flow is routed through a wash bottle filled with high purity water from an ion-exchange reversed osmosis system to create reproducible and representative humidity levels in order to simulate field sample conditions. Instrument precision is based on repeatability of calibration samples at different mixing ratios. Sensitivity and linearity is based on FID response as evaluated from peak areas determined by the Chemstation software and calculated mixing ratios using calibration gas dilution ratios. During each sampling day, a series of 3-4 calibration sample cartridges were produced in the morning, and these cartridges were transported, handled, and processed in the same manner as all other cartridges. Thus, field measurement precision was determined for each measurement day by the precision of the ad-hoc calibration curve obtained from the day's calibration samples.

4.1.4 Quality control (QC) measures

A series of quality control measures were implemented as part of the field sampling and chemical analysis routines (these apply to both the greenhouse measurements and the field measurements). They were

I.   regular zeroing and balancing of the NDIR analyzers as part of the CIRAS-2 system
II.   sample cartridge tracking for leakage and calibration gas repeatability
III.   "empty cuvette" blank sample collection for reference isoprene mixing ratio and cuvette system contamination tracking
IV.   blank cartridge samples (unloaded) for diffusive contamination tracking (e.g. leaks)
V.   duplicate sample taking to track leaf emission repeatability
VI.   calibration sample acquisition and handling alongside regular sample taking
VII.   detailed notebook entries on field activities accompanied by occasional photographs

Measure I was performed approximately hourly during instrument use. Measure II was performed as a spot check using random (instead of selected) cartridges to act as daily calibration samples cartridges. Measure III included samples taken from an empty, balanced cuvette

throughout a measurement day. Measure IV included additional cartridges per measurement day exposed to ambient air or laboratory air for an appropriate amount of time (1-3 min) reflecting regular sample handling. Measure V includes duplicate (replicate) samples taken immediately after a regular sample without changing any leaf conditions. Measure VI assured comparability from one sample day to another, including at least two, normally three to six calibration samples processed per measurement day. Finally, measure VII assured the identification of deviations from the norm, and the proper association of results with the respective leaves and field conditions.

In addition, a sample storage test was done to determine sample integrity over 72 hours. A total of 16 cartridges were filled (eight cartridges of each adsorbent) with a standard of a known concentration. These cartridges were stored in the laboratory during four consecutive days, resembling, but longer than storage of field samples. During those four consecutive days two cartridges from storage were analyzed in the GC together with another two cartridges (from each adsorbent) that were filled up on the same day of the analysis. A total of ten cartridges were analyzed every day, four cartridges from storage, four cartridges taken the same day, and two blanks. The results of this test showed that there was no VOC loss or gain during the storage process. Unless a day's of acquired samples are not processed due to analytical system failure, typical sample cartridge amounts of less than 40 guaranteed that there were no samples stored more than 48 hours before being processed by the ATD-GC-FID system.

4.2 Greenhouse experiments

4.2.1 Overview

The greenhouse experiment began in late summer of 2014, and two different drought experiments were performed during the funding period. The first experiment was performed during the fall of 2014, and the second experiment was implemented in spring 2015. The results presented here are from the experiments performed during May 2015; results from the inconclusive fall experiments can be found in Appendix H.

All potted plants were dormant (leafless) during the cooler season. Photosynthetic parameters and isoprene emissions were measured weekly as soon as new leaves expanded in spring 2015, and these measurements provided the necessary information for the experimental design. To select the start of the drought regime it was necessary to monitor the increase / start of photosynthetic activity and isoprene emissions linked to that activity, respectively. During leaf expansion, leaf chemistry is not completely developed, therefore there is a delay in isoprene production and emissions. In 2014, the different problems that the plants experienced due to a change in greenhouse location and insects outbreaks at the new greenhouse made the results from the first drought trial unreliable because it was not possible to determine if the changes in isoprene emissions were due to the stress from these setbacks, leaf senescence, or the implemented drought treatment.

In spring 2015, the experimental design plan was based on the results of the experiments done in 2014: from those experiments it was decided that five healthy plants of water oak and five healthy plants of post oak (3 plants under the drought treatment and 2 plants used as a control) were going to be measured over a period of 15 days. The number of plants to measure was decided based on a power analysis given the variability of the emissions, and the length of the

study was determined by the average number of days it took the potted plants to reach the soil's wilting point. There was no more than that number of healthy plants available in spring 2015. Since spring contains a significant development period for the plants/leaves before reaching (leaf) maturity, the choice was also based on reaching that maturity while considering that the project had to be finished by June. All plants in the greenhouse experienced the same physical environment (light, temperature, relative humidity). The control variable in the greenhouse was soil moisture as the driving force of drought stress. Thus, our experimental design is a 1-factor approach, in which everything else but soil moisture is "held constant" at greenhouse environmental conditions. Two sets of experimental drought were performed, one in May, one in June 2015.

Isoprene emissions, soil moisture, plant weight, and photosynthetic parameters were measured near daily in all the plants from May 11 to June 20 in the two separate experiments. During this period there were long episodes of heavy rain and cloudy skies, and it was therefore necessary to turn on the artificial lights in the greenhouse to support photosynthetic activity (Figure 13). Temperature and relative humidity in the greenhouse ranged between 25 to 33 °C, and 50 to >90%, respectively, due to limited ventilation of the greenhouse at that time of year.

4.2.2 Water regime

The project's first objective was to set up the experimental conditions and establish a baseline for the drought experiment. The plants had suffered different stresses that had previously made it impossible to determine a constant basal isoprene emission. It was necessary therefore to bring the plants to a healthy state, before applying the drought treatment.

The first step taken to decrease the mortality rate was to determine the amount of water that the plants needed. This was done by watering the plants once then repeatedly measuring photosynthesis rate while weighing the potted plants to determine their water use. This information was used to determine the proper amount of water to improve the viability of the plants; an example is shown in Figure 11 (note biological variability).

As a result of the analysis it was determined that plants had to be watered approximately 300 mL twice a week once leaves had fully expanded. The exact amount of water varied depending of the amount of biomass and plant species.
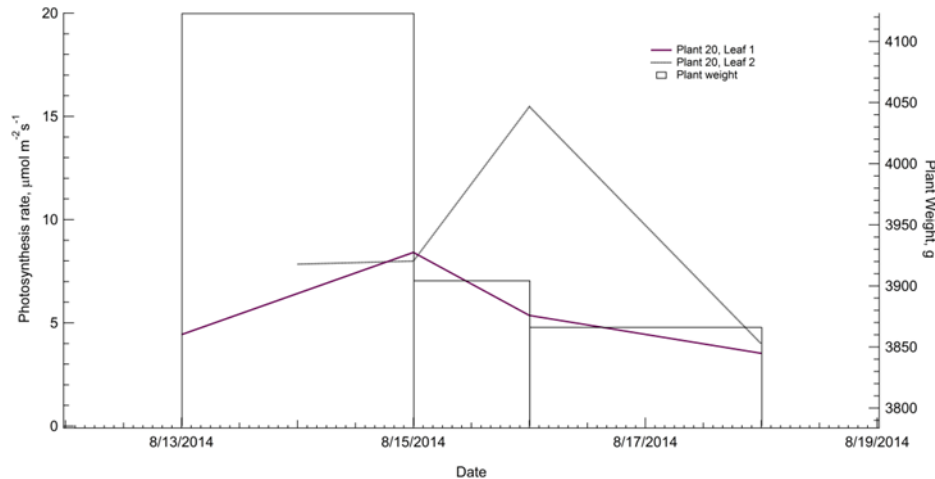
Figure 37. Photosynthesis rate and plant weight of a post-oak seedling.

4.2.3 Photosynthetic parameters

Plant physiological parameters (leaf temperature; CO_2 assimilation, Pn) and H_2O (transpiration) exchange rates, stomatal conductance (gs), and (calculated) leaf internal CO_2 concentration (Ci), and simultaneously emitted isoprene were measured at leaf-level.

Two leaves from the upper tier of the plants were selected in all the plants in the study (Figure 12). Leaves were marked and measured every day.

Figure 38. Marked leaves of post oak

The instrument employed was a 2010 model CIRAS-2 leaf level photosynthesis analyzer with a 2.5 cm^2 leaf area cuvette attachment, appropriate for the investigated species, with temperature control from 10 °C below to 10 °C above ambient, and light-level control from zero to above 2000 PAR (http://www.ppsystems.com/ciras2_portable_photosynthesis_system.htm). The system uses a pair of non-dispersive infrared (NDIR) analyzers to measure CO_2 and H_2O mixing ratios. The analyzers were regularly zeroed and balanced against each other for quality control.

The field data acquisition protocol was as follows:
   a) Turn on and equilibrate analyzer in the field;
         a. Assign file name for the experiment. Each file named contains the date (mm/dd/yy) and an extension "gh" for greenhouse.
         b. Measure air in empty cuvette, in order to obtain neutral "no-leaf" reading (zero fluxes) for quality control
         c. Standard conditions in the cuvette were set to a CO_2 concentration of 400 ppm. For standard conditions temperature and PAR were selected to be 30 °C and 1000 μmol photons m^{-2} s^{-1} respectively.
   b) Insert leaf in cuvette and wait for $[CO_2]$ set-point to be reached
   c) Wait for leaf to equilibrate to cuvette conditions
   d) Manually record equilibrium readings and sample volatiles. This was a cautionary practice as well as quality control procedure. These data would give the time at which the sampling started as well as the basal photosynthetic rates, which were later compared with the recorded data from the CIRAS instrument.
   e) Confirm leaf equilibrium after sampling for quality control. Repeat step 4 to have a duplicate if desired. Replicate samples were taken to confirm the emissions.
   f) Zero and balance the 2-channel NDIR analyzer regularly as required during field data acquisition (approximately hourly)
   g) Repeat b.-e. for the next leaf/plant.

All analyzer data was stored as ascii files on the analyzer's hard disk. Typical data density was 6 data points per minute. Upon return to the laboratory data was downloaded and backed up onto a PC and a portable hard disk backup device before further processing.

4.2.4 Environmental parameters

The greenhouse physical growth environment was monitored using a Campbell Scientific Inc. data logger (model CR1000). Temperature and relative humidity were monitored inside the greenhouse. Light (PAR) was monitored close to the "canopy". Soil moisture was monitored in all the pots (treatment and control). For quality control, all soil moisture sensors (Decagon model EC5) had been compared and calibrated in a single, wide diameter pot filled with the same soil mixture before deployment into the seedling pots.

Greenhouse environment data was downloaded once a week and processed to assure that watering schedules achieve the desired soil moisture levels per treatment (typically ≥ 0.15 cm^3 cm^{-3} or 15% volumetric soil moisture), with corrective action being taken if pots fell outside a 10% relative variability margin.
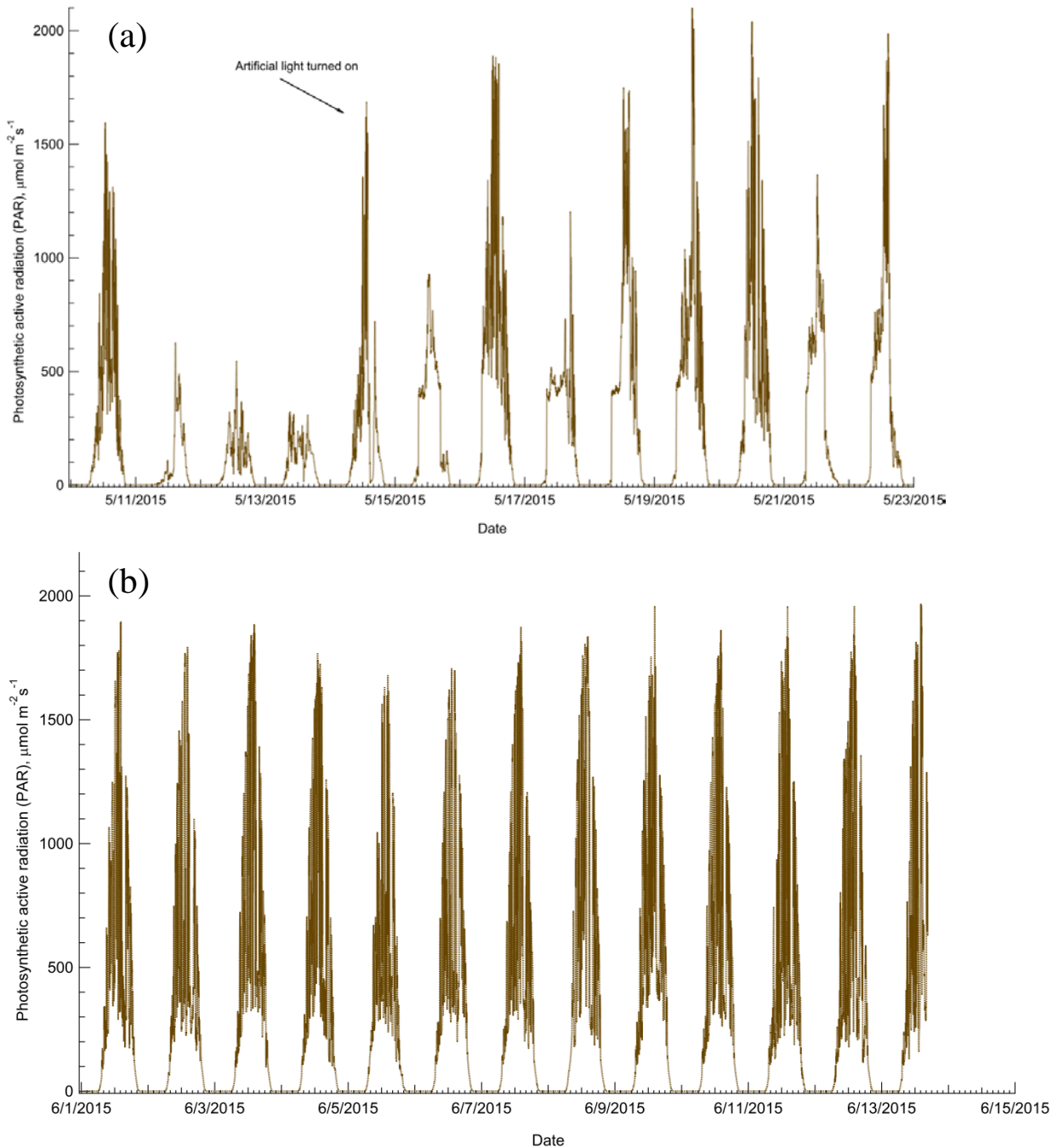
Figure 39 Photosynthetically active radiation during the length of the (a) 1st experiment in May, and (b) 2nd experiment in June, 2015.

Temperatures and relative humidity during the 2nd experiment fluctuated between 24 (night) to 33 °C (day) and 50 to 80%, respectively. There was thus high comparability between the two experimental periods.

4.2.5 Quality Assurance (QA) measures

Quality assurance measures for the CIRAS-2 data analysis included
   a) spot checking of data integrity (e.g. noise specifications/behavior), and data consistency (e.g. between field notes and data records)
   b) removal of outliers during averaging/processing
   c) span checks of the NDIR analyzers

Measure (a) occurred frequently during data processing when newly acquired data were processed for incorporation into a spreadsheet. Measure (b) occurred at the same time when records were averaged to reflect leaf physiology during the isoprene sampling period. Measure (c) was carried out to make sure the instrument does not show a significant drift over longer time periods.

Quality assurance measures for the cartridge sampling and isoprene measurements included
   a) successful demonstration of (i) a lack of sample loss during typical storage times; and (ii) a lack of breakthrough at a challenge mixing ratio of 100 ppb for the new Tenax cartridges
   b) checking of cartridge blanks for lack of unidentified VOC occurrences and lack of significance of known interferences, such as blank peaks
   c) subtracting empty cuvette blanks from leaf emission samples using an average of the nearest samples in time
   d) comparing measurement day calibration samples from one day to the next to ensure FID stability, and spot check individual cartridge integrity
   e) comparing measurement day calibration samples to the extended calibration curve

4.3 Physiology and isoprene emissions of post oak

Isoprene emissions from post oak in the control group were constant during the experiment (Figure 14, May experiment). As expected the photosynthesis rate and isoprene emissions decreased in the drought treatment specimens (Figure 15).

The results during the 2nd experiment in June were similar to the 1st. Reference plants showed only small day-to-day fluctuations of photosynthesis rates and correlated isoprene emissions.
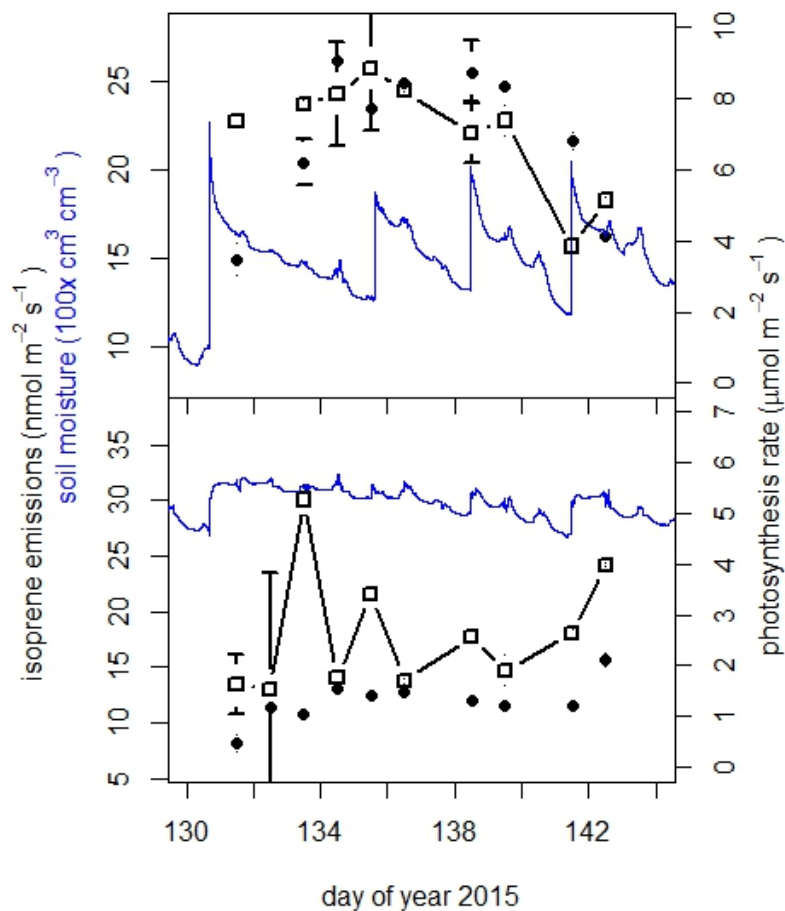
Figure 40 Post Oak control plant photosynthesis rate (open squares) and isoprene emissions (filled circles), alongside measured pot soil moisture (blue lines). Errors bars are 1 sd, with most not bigger than the symbol. Top and bottom panels show individual plants with measurements on multiple leaves.

In contrast to the control plants, drought-stressed post oak showed the expected drop in photosynthesis rates and isoprene emissions as soil moisture approached the wilting point (Figure 15). However, large variability remained a feature of our data, with typically low and fluctuating day-to-day photosynthesis rates, especially as soil moisture approached the wilting point. We attribute this to likely not uniformly distributed soil moisture in the pot alongside an also not likely uniformly distributed root network.
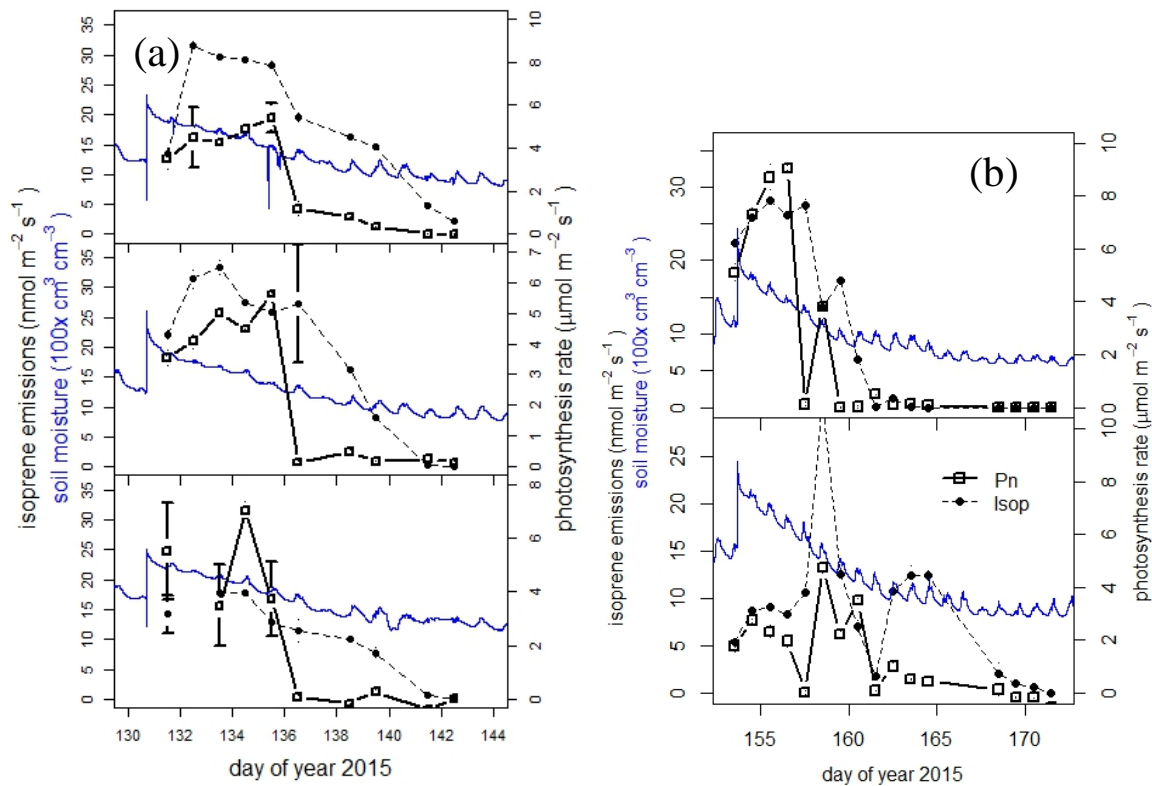
Figure 41 (a) Same as Figure 14, but for three drought stressed post oak plants. The permanent wilting point for the post oaks in these pots is 0.1 cm^3 cm^{-3} (10%) but photosynthesis dropped much earlier to near zero for two out of the three plants, likely because the soil moisture sensor did not capture the "correct" soil moisture where most roots were located in the pot. (b) Same as Figure 15a, but for two drought stressed post oak plants during the 2nd experiment in June.

4.4 Physiology and isoprene emissions of water oak

Isoprene emissions of water oak showed virtually the same behavior as compared to the post oak plants. Isoprene emissions remained near constant in the control treatments (Figure 16, May experiment) but decreased in the drought treatment plants (Figure 17). One plant, not shown here, did not display such a decrease in either photosynthesis or isoprene emissions.

The results for the 2nd water oak experiment in June were also similar to the 1st. Reference plants showed day-to-day fluctuations of isoprene emissions typically correlating with photosynthesis rates, while drought-stressed water oak showed a sensitive response of photosynthesis rates and isoprene emissions as soil moisture approached the wilting point (Figure 17b).

71
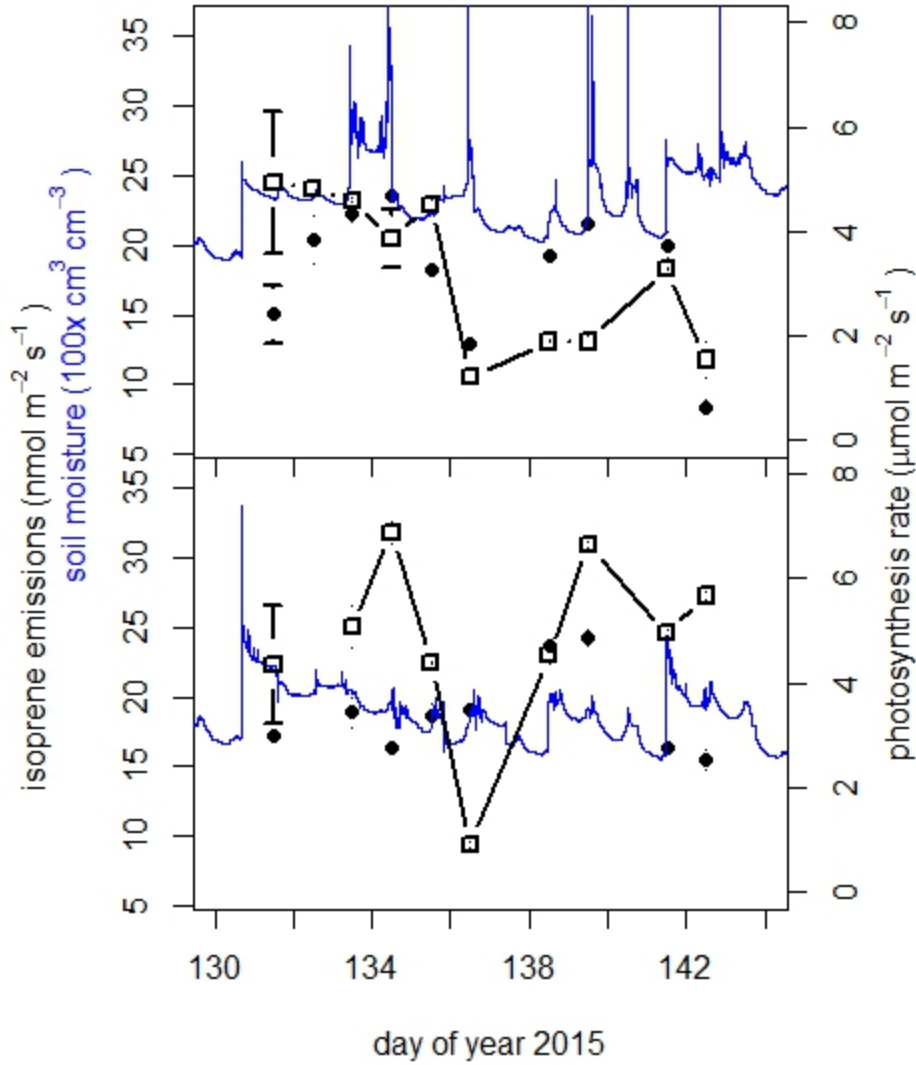
Figure 42 Water Oak control plant photosynthesis rate (Pn, open squares) and isoprene emissions (Isop, filled circles), alongside measured pot soil moisture (blue lines). Errors bars are 1 sd, with most not bigger than the symbol. Top and bottom panels show individual plants with measurements on multiple leaves.
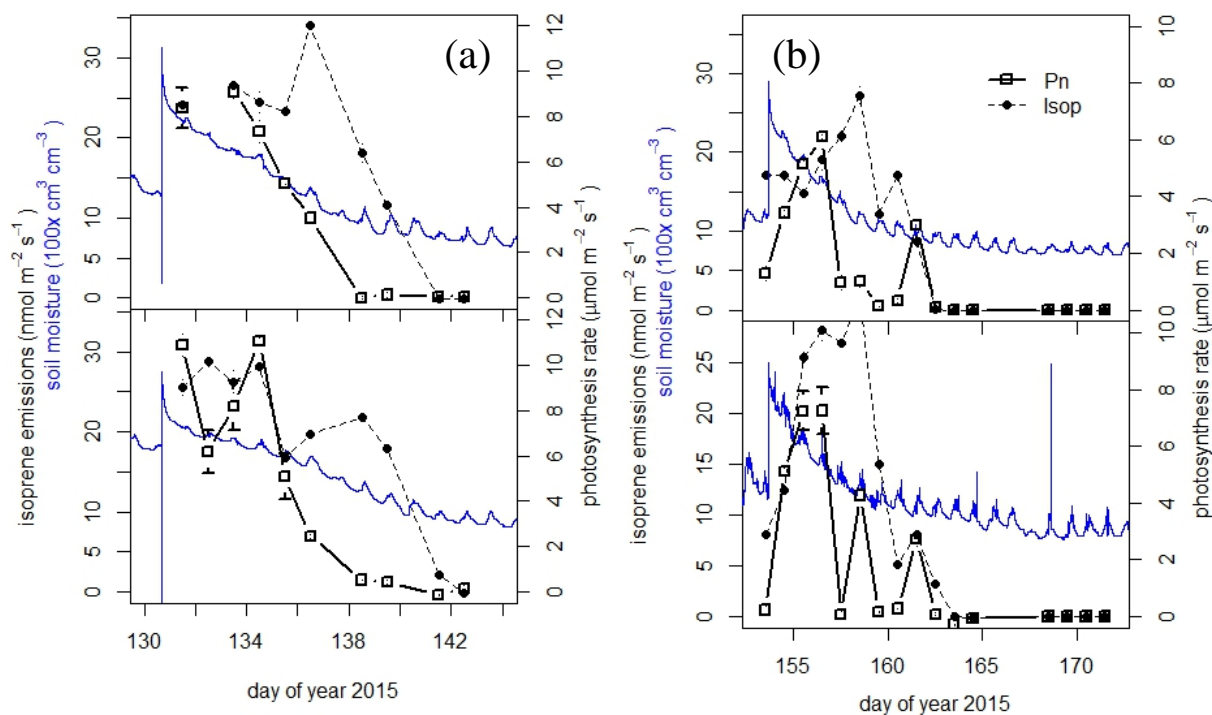
Figure 43 Same as Figure 16, but for two drought stressed water oak plants. The permanent wilting point for the water oaks in these pots is 0.1 cm^3 cm^{-3} (10%) and photosynthesis dropped to near zero right around that value for both plants, in May during day 138 (top) and day 140/41 (bottom).

4.5 Distinguishing drought stress via the isoprene emission to Pn ratio

High variability in isoprene emissions (Isop) and photosynthesis rates (Pn) tend to mask the drought effects on either flux. Thus, we also present the Isop:Pn ratio to highlight the differences between the control and drought-stressed specimens. Figure 18 depicts results for five post oak specimens and four water oak specimens during the June experiment.

73
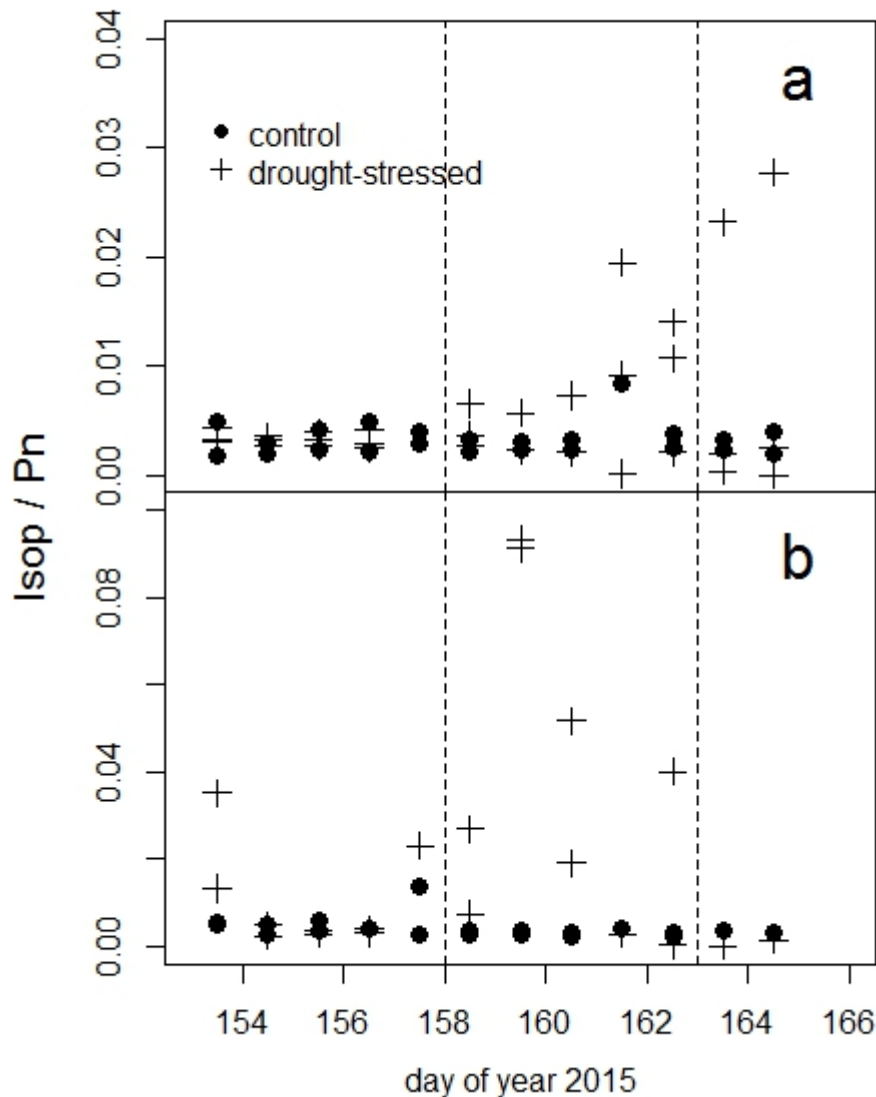
Figure 44 Relative isoprene emissions (Isop) per photosynthesis rate (Pn) for control and drought stressed plants during the 2nd experiment, (a, top) showing post oak, (b, bottom) showing water oak. The vertical dashed lines mark the approximate period during which soil moistures in the pots dropped from $\theta_w + \Delta\theta_1$ to θ_w.

Before soil moisture was dropping into the critical range, the isoprene emission to Pn ratio remained similar between control and drought-stressed plants, but increased strongly for the stressed plants as Pn decreased. When the wilting point was reached all but one specimen dropped back closer to the control range because of near zero Pn and/or Isop. Note that the post oak ratios changed less than the water oak ratios, and water oak showed higher variability.

4.6 Comparison to the current MEGAN model implementation

For the purposes of this comparison we averaged the available data. Since the data set is comparatively small, no error bars are included since their size may be misleading. The average

soil moisture was used to compute the γ_{SM} factor, and the average isoprene emission of the first four days was used as reference value for normalization.

Figure 19a shows the average post oak results, Figure 19b those for the water oak from the 1st (May) experiment, and Figures 20a and 20b the results from the 2nd (June) experiment. The soil moisture response factor was smoothed in both cases from the raw data to dampen the diurnal cycle typically observed due to each plant's hydraulic recovery at night.

The surprisingly close agreement with the model, particularly for the May experiment, suggests that (i) the drought treatment was successful, (ii) the current model implementation is adequate, and (iii) it is not significantly different between these two species. While the water oak appeared to deal with the drought slightly better than the post oak during the 1st experiment, the situation was reversed during the 2nd. While we at first surmised that this could have been driven by the difference in rooting structure between these oak species, a closer look at the root system after the drought-stressed specimens perished revealed no significant differences with the exception of a slightly thicker main (tap-) root of the post oak.
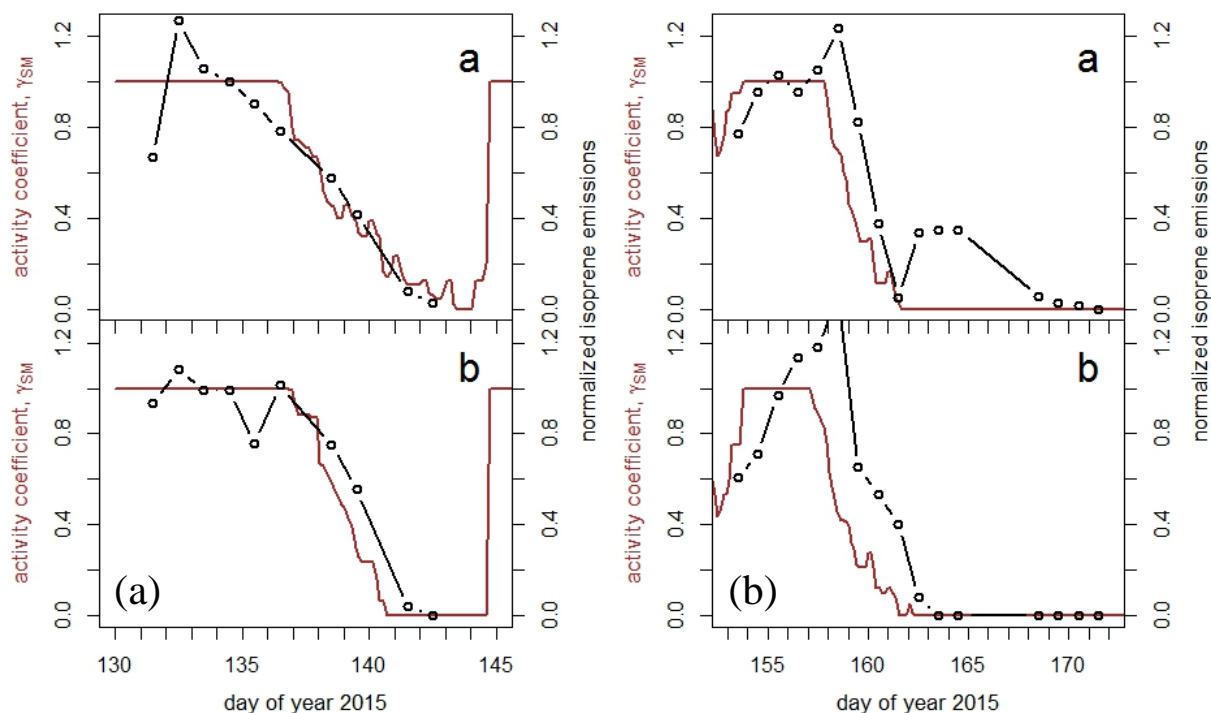
Figure 45 (a) Soil moisture activity factor as compared to normalized isoprene emissions from 3-year old potted post oak in the greenhouse (3-specimen average). (b) Same as Figure 19a (a: post oak; b: water oak) but for the June experiment (2-specimen average in both cases, outlier removed)

4.7 Conclusions

Our greenhouse experiments suggest that the current MEGAN isoprene emission model drought stress implementation is adequate for two common oak species in Texas, *Quercus stellata* and *Quercus nigra*. In combination with our field work shown in section 3, we conclude that a more

narrow range of $\Delta\theta_1$, such as 0.03 or 0.05 instead of 0.04, may not be the right choice to improve the model for field data since we found no significant physiological difference between the oak species in the greenhouse. Since this addresses some of the ambiguity described in section 3, we can thus further conclude that, under field conditions, it will be critical to assess the "correct" depth of the root zone. Since the potted specimen in the greenhouse cannot develop roots as they would under the field conditions, it will remain important to assess field grown trees under drought conditions to evaluate species differences. However, our work suggests that these differences are not based upon leaf physiology but more likely upon root physiology, requiring a comparative assessment of rooting structure and depth in order to improve isoprene emission model performance. In addition, since the soil moisture activity factor is sensitive to changes within $\theta+\Delta\theta_1$, smoothing of the soil moisture input values is recommended along with improved models and model-measurement comparisons of soil moisture.

Note that the representativeness of our study with respect to soil properties in Texas was addressed indirectly by comparing results from a field and a greenhouse study. Since the isoprene emission model parameter, γ_{SM}, evaluated here is based upon soil wilting point, which in turn is based upon soil texture, in principle, accurate soil texture, not soil type, maps are the most important input parameter alongside the soil moisture model. A well-drained, sandy soil of low wilting point was used in the greenhouse study for practical purposes since it dries out more rapidly than more clayey soils. However, higher wilting points due to higher soil clay contents at our field sites produced similar drought responses as compared to the greenhouse results, and thus we have no reason to assume that soil type or soil texture variability across Texas plays a significant role in the investigated responses. We have, however, demonstrated a potential lack of representativeness of large-scale soil moisture models (section 3), leading to potentially large differences between modeled and measured isoprene emissions due to the large sensitivity of the model parameter when soil moisture is close to the soil wilting point. As a result, isoprene emission model estimates may not be incongruent with measurements due to an incorrect model parameterization, but rather due to incorrect input data to the model.

4.8 Audits of Data Quality

10% of the calculations assembled in the Excel data sheets that contain all greenhouse measurements and the field measurements at the Freeman Ranch near San Marcos and other sites were randomly audited. All spreadsheets have been assembled by postdoctoral researcher Dr. Monica Madronich, and the audit was performed by Co-PI Dr. Gunnar Schade.

5. Conclusions

In Section 2 of the report, the original MEGAN v2.10 model was updated to include a parameterization of the soil moisture activity factor γ_{SM} following the equation in Guenther et al.[9] to better predict isoprene emissions under drought conditions. The updated MEGAN model calculates the weighted activity factor in each grid cell using soil-texture based wilting point and root zone distribution in four soil layers as a function of plant functional type (PFT). In addition, a bug in the original MEGAN v2.10 model was fixed to correctly read a gridded Palmer Drought Severity Index (PDSI) field for the canopy model to estimate leaf surface temperature under drought conditions, which could also affect isoprene emissions. The regional soil moisture field needed for the MEGAN model was estimated using the WRF model with the Noah land surface scheme initialized with the soil moisture field from NLDAS-2 with Noah-2.8. Wilting point data needed for the drought parametrization were estimated using the Penn State CONUS-SOIL database and the soil-related hydraulic parameters from Table 2 of Chen and Dudhia [1]. The predicted soil moisture generally agrees with observations.

The MEGAN model with its own isoprene emission factor (EF) field severely over-predicts isoprene concentrations. Alternative EF fields generated from two different versions of the BEIS models (v3.14 and v3.61) and their accompanying land use data bases (BELD3 and BELD4, respectively) were applied in the updated MEGAN model. Comparison of predicted hourly and daily averaged isoprene concentrations at all isoprene monitors in and out of Texas in a total of 14 months in 2007 and 2011 showed that the MEGAN model with EF fields from the new BEIS model (hereafter MEGAN-BEIS361) and its input data (BELD4) can significantly improve the model capability in reproducing the observed isoprene concentrations at all locations. While MEGAN-BEIS361 in general provides satisfactory isoprene predictions, under-estimation in the EF for urban land type (10 gC/km^2-hr) might have led to large under-predictions of isoprene at a number of urban sites in Houston and Dallas/Fort Worth areas in Texas.

Predicted isoprene emissions under drought conditions considering the impact on leaf temperature alone leads to increase in isoprene emissions. The magnitude of emission increasing was reduced when soil moisture activity factor was also considered. When both factors were considered, the resulted isoprene and ozone concentrations in both 2007 and 2011 changed only slightly (less than 1 ppb for monthly average 1-hour isoprene at locations where drought was significant and less than 1 ppb for monthly average peak ozone concentrations).

The results described in Section 3 cannot alleviate the ambiguity of the drought response of isoprene emitting oaks that results from (i) the root-zone soil depth of the species, and (ii) the drought response parametrization. Instead, they demonstrate that a uniform root-zone depth selection and a uniform drought response parameterization may lead to regionally paradoxical results. In regions dominated by more drought resistant oak species such as *Quercus stellata* a deeper root zone may have to be considered alongside a narrower range of soil moistures that affect isoprene emissions, while the opposite should be considered in regions dominated by less drought resistant species such as *Quercus nigra*. Since such adjustments to the emission model require more detailed land model inputs rather than model parameter changes, we recommend a focus on improving land surface information, particularly rooting depth and soil moisture estimates.

The greenhouse experiments described in Section 4 suggest that the current MEGAN isoprene emission model drought stress implementation is adequate for two common oak species in Texas, *Quercus stellata* and *Quercus nigra*. In combination with the field work shown in section 3, it is concluded that a more narrow range of $\Delta\theta_1$, such as 0.03 or 0.05 instead of 0.04, may not be the right choice to improve the model for field data since we found no significant physiological difference between the oak species in the greenhouse. Since this addresses some of the ambiguity described in section 3, we can thus further conclude that, under field conditions, it will be critical to assess the "correct" depth of the root zone. Since the potted specimen in the greenhouse cannot develop roots as they would under the field conditions, it will remain important to assess field grown trees under drought conditions to evaluate species differences. However, our work suggests that these differences are not based upon leaf physiology but more likely upon root physiology, requiring a comparative assessment of rooting structure and depth in order to improve isoprene emission model performance. In addition, since the soil moisture activity factor is sensitive to changes within $\theta+\Delta\theta_1$, smoothing of the soil moisture input values is recommended along improved models and model-measurement comparisons of soil moisture.

Note that the representativeness of our study with respect to soil properties in Texas was addressed indirectly by comparing results from a field and a greenhouse study. Since the isoprene emission model parameter, γ_{SM}, evaluated here is based upon soil wilting point, which in turn is based upon soil texture, in principle, accurate soil texture, not soil type, maps are the most important input parameter alongside the soil moisture model. A well-drained, sandy soil of low wilting point was used in the greenhouse study for practical purposes since it dries out more rapidly than more clayey soils. However, higher wilting points due to higher soil clay contents at our field sites produced similar drought responses as compared to the greenhouse results, and thus we have no reason to assume that soil type or soil texture variability across Texas plays a significant role in the investigated responses. We have, however, demonstrated a potential lack of representativeness of large-scale soil moisture models (section 3), leading to potentially large differences between modeled and measured isoprene emissions due to the large sensitivity of the model parameter when soil moisture is close to the soil wilting point. As a result, isoprene emission model estimates may not be incongruent with measurements due to an incorrect model parameterization, but rather due to incorrect input data to the model.

References

1.   Chen, F.; Dudhia, J., Coupling an Advanced Land Surface–Hydrology Model with the Penn State–NCAR MM5 Modeling System. Part I: Model Implementation and Sensitivity. *Monthly Weather Review* **2001,** *129*, (4), 569-585.

2.   Li, G. H.; Zhang, R. Y.; Fan, J. W.; Tie, X. X., Impacts of biogenic emissions on photochemical ozone production in Houston, Texas. *Journal of Geophysical Research-Atmospheres* **2007,** *112*, (D10), D10309.

3.   Ying, Q.; Krishnan, A., Source contributions of volatile organic compounds to ozone formation in southeast Texas. *Journal of Geophysical Research-Atmospheres* **2010,** *115*, (D17), D17306.

4.   Zhang, H.; Ying, Q., Secondary Organic Aerosol Formation and Source Apportionment in Southeast Texas. *Atmos. Environ.* **2011,** *45*, (19), 3217-3227.

5.   Zhang, H.; Li, J.; Ying, Q.; Buzcu-Guven, B.; Olaguer, E. P., Source Apportionment of Primary and Secondary Formaldehyde during TexAQS 2006 using a Source-Oriented Chemical Transport Model. *Journal of geophysical research* **2012,** *doi: 10.1002/jgrd.50197*.

6.   Yarwood, G.; Wilson, G.; Emery, C.; Guenther, A. *Development of GloBEIS - A State of the Science Biogenic Emissions Modeling System. Final Report. Prepared for Texas Natural Resource Conservation Comission. December, 1999*; 1999.

7.   Vukovich, J. M.; Pierce, T. In *The Implementation of BEIS3 within the SMOKE modeling framework*, 2002; MCNC-Environmental Modeling Center, Research Triangle Park and National Oceanic and Atmospheric Administration: 2002.

8.   Guenther, A.; Karl, T.; Harley, P.; Wiedinmyer, C.; Palmer, P. I.; Geron, C., Estimates of global terrestrial isoprene emissions using MEGAN (Model of Emissions of Gases and Aerosols from Nature). *Atmospheric Chemistry and Physics* **2006,** *6*, 3181-3210.

9.   Guenther, A. B.; Jiang, X.; Heald, C. L.; Sakulyanontvittaya, T.; Duhl, T.; Emmons, L. K.; Wang, X., The Model of Emissions of Gases and Aerosols from Nature version 2.1 (MEGAN2.1): an extended and updated framework for modeling biogenic emissions. *Geosci. Model Dev.* **2012,** *5*, (6), 1471-1492.

10.   Brilli, F.; Barta, C.; Fortunati, A.; Lerdau, M.; Loreto, F.; Centritto, M., Response of isoprene emission and carbon metabolism to drought in white poplar (Populus alba) saplings. *New Phytologist* **2007,** *175*, (2), 244-254.

11.   Centritto, M.; Brilli, F.; Fodale, R.; Loreto, F., Different sensitivity of isoprene emission, respiration and photosynthesis to high growth temperature coupled with drought stress in black poplar (Populus nigra) saplings. *Tree Physiology* **2011,** *31*, (3), 275-286.

12.   Fares, S.; Mahmood, T.; Liu, S. R.; Loreto, F.; Centritto, M., Influence of growth temperature and measuring temperature on isoprene emission, diffusive limitations of photosynthesis and respiration in hybrid poplars. *Atmospheric Environment* **2011,** *45*, (1), 155-161.

13.   Fortunati, A.; Barta, C.; Brilli, F.; Centritto, M.; Zimmer, I.; Schnitzler, J. P.; Loreto, F., Isoprene emission is not temperature-dependent during and after severe drought-stress: a physiological and biochemical analysis. *Plant Journal* **2008,** *55*, (4), 687-697.

14.   Funk, J. L.; Jones, C. G.; Gray, D. W.; Throop, H. L.; Hyatt, L. A.; Lerdau, M. T., Variation in isoprene emission from Quercus rubra: Sources, causes, and consequences for estimating fluxes. *Journal of Geophysical Research-Atmospheres* **2005,** *110*, (D4).

15.   Gray, D. W.; Lerdau, M. T.; Goldstein, A. H., Influences of temperature history, water stress, and needle age on methylbutenol emissions. *Ecology* **2003,** *84*, (3), 765-776.

16.   Guidolotti, G.; Calfapietra, C.; Loreto, F., The relationship between isoprene emission, CO2 assimilation and water use efficiency across a range of poplar genotypes. *Physiologia Plantarum* **2011,** *142*, (3), 297-304.

17.   Llusia, J.; Llorens, L.; Bernal, M.; Verdaguer, D.; Penuelas, J., Effects of UV radiation and water limitation on the volatile terpene emission rates, photosynthesis rates, and stomatal conductance in four Mediterranean species. *Acta Physiologiae Plantarum* **2012,** *34*, (2), 757-769.

18.   Llusia, J.; Penuelas, J.; Prieto, P.; Estiarte, M., Net ecosystem exchange and whole plant isoprenoid emissions by a mediterranean shrubland exposed to experimental climate change. *Russian Journal of Plant Physiology* **2009,** *56*, (1), 29-37.

19.   Loreto, F.; Fischbach, R. J.; Schnitzler, J. P.; Ciccioli, P.; Brancaleoni, E.; Calfapietra, C.; Seufert, G., Monoterpene emission and monoterpene synthase activities in the Mediterranean evergreen oak Quercus ilex L. grown at elevated CO2 concentrations. *Global Change Biology* **2001,** *7*, (6), 709-717.

20.   Ormeno, E.; Mevy, J. P.; Vila, B.; Bousquet-Melou, A.; Greff, S.; Bonin, G.; Fernandez, C., Water deficit stress induces different monoterpene and sesquiterpene emission changes in Mediterranean species. Relationship between terpene emissions and plant water potential. *Chemosphere* **2007,** *67*, (2), 276-284.

21.   Pegoraro, E.; Abrell, L.; Van Haren, J.; Barron-Gafford, G.; Grieve, K. A.; Malhi, Y.; Murthy, R.; Lin, G. H., The effect of elevated atmospheric CO2 and drought on sources and sinks of isoprene in a temperate and tropical rainforest mesocosm. *Global Change Biology* **2005,** *11*, (8), 1234-1246.

22.   Pegoraro, E.; Rey, A.; Greenberg, J.; Harley, P.; Grace, J.; Malhi, Y.; Guenther, A., Effect of drought on isoprene emission rates from leaves of Quercus virginiana Mill. *Atmos. Environ.* **2004,** *38*, (36), 6149-6156.

23.   Penuelas, J.; Filella, I.; Seco, R.; Llusia, J., Increase in isoprene and monoterpene emissions after re-watering of droughted Quercus ilex seedlings. *Biologia Plantarum* **2009,** *53*, (2), 351-354.

24.   Rennenberg, H.; Loreto, F.; Polle, A.; Brilli, F.; Fares, S.; Beniwal, R. S.; Gessler, A., Physiological responses of forest trees to heat and drought. *Plant Biology* **2006,** *8*, (5), 556-571.

25.   Rodriguez-Calcerrada, J.; Buatois, B.; Chiche, E.; Shahin, O.; Staudt, M., Leaf isoprene emission declines in Quercus pubescens seedlings experiencing drought - Any implication of soluble sugars and mitochondrial respiration? *Environmental and Experimental Botany* **2013,** *85*, 36-42.

26.   Simpraga, M.; Verbeeck, H.; Demarcke, M.; Joo, E.; Pokorska, O.; Amelynck, C.; Schoon, N.; Dewulf, J.; Van Langenhove, H.; Heinesch, B.; Aubinet, M.; Laffineur, Q.; Muller, J. F.; Steppe, K., Clear link between drought stress, photosynthesis and biogenic volatile organic compounds in Fagus sylvatica L. *Atmospheric Environment* **2011,** *45*, (30), 5254-5259.

27.   Shaw, W. J.; Allwine, K. J.; Fritz, B. G.; Rutz, F. C.; Rishel, J. P.; Chapman, E. G., Evaluation of the wind erosion module in DUSTRAN. *Atmos. Environ.* **2008,** *42*, (8), 1907-1921.

28.   Choi, Y. J.; Fernando, H. J. S., Implementation of a windblown dust parameterization into MODELS-3/CMAQ: Application to episodic PM events in the US/Mexico border. *Atmos. Environ.* **2008,** *42*, (24), 6039-6046.

29.   Ying, Q.; Wu, L.; Zhang, H., Local and inter-regional contributions to PM2.5 nitrate and sulfate in China. *Atmos. Environ.* **2014,** *94*, (0), 582-592.

30.   Zhang, H.; Li, J.; Ying, Q.; Yu, J. Z.; Wu, D.; Cheng, Y.; He, K.; Jiang, J., Source apportionment of PM2.5 nitrate and sulfate in China using a source-oriented chemical transport model. *Atmos. Environ.* **2012,** *62*, (0), 228-242.

31.   Zeng, X., Global Vegetation Root Distribution for Land Modeling. *Journal of Hydrometeorology* **2001,** *2*, (5), 525-530.

32.   Dai, A.; Trenberth, K. E.; Qian, T., A Global Dataset of Palmer Drought Severity Index for 1870 2002: Relationship with Soil Moisture and Effects of Surface Warming. *Journal of Hydrometeorology* **2004,** *5*, (6).

33.   Carlton, A. G.; Baker, K. R., Photochemical Modeling of the Ozark Isoprene Volcano: MEGAN, BEIS, and Their Impacts on Air Quality Predictions. *Environ. Sci. Technol.* **2011,** *45*, (10), 4438-4445.

34.   Warneke, C.; de Gouw, J. A.; Del Negro, L.; Brioude, J.; McKeen, S.; Stark, H.; Kuster, W. C.; Goldan, P. D.; Trainer, M.; Fehsenfeld, F. C.; Wiedinmyer, C.; Guenther, A. B.; Hansel, A.; Wisthaler, A.; Atlas, E.; Holloway, J. S.; Ryerson, T. B.; Peischl, J.; Huey, L. G.; Hanks, A. T. C., Biogenic emission measurement and inventories determination of biogenic emissions in the eastern United States and Texas and comparison with biogenic emission inventories. *Journal of Geophysical Research-Atmospheres* **2010,** *115*.

35.   Stavrakou, T.; Peeters, J.; Müller, J. F., Improved global modelling of HOx recycling in isoprene oxidation: evaluation against the GABRIEL and INTEX-A aircraft campaign measurements. *Atmos. Chem. Phys.* **2010,** *10*, (20), 9863-9878.

36.   Kota, S. H.; Schade, G. W.; Estes, M.; Boyer, D.; Ying, Q., Evaluation of MEGAN Predicted Biogenic Isoprene Emissions at Urban Locations using a Source-Oriented Community Multiscale Air Quality Model. *Atmos. Environ.* **2015,** *110*, 54-64.

37.   Park, C.; Schade, G. W.; Boedeker, I., Characteristics of the flux of isoprene and its oxidation products in an urban area. *Journal of Geophysical Research-Atmospheres* **2011,** *116*.

38.   Manfreda, S.; Brocca, L.; Moramarco, T.; Melone, F.; Sheffield, J., A physically based approach for the estimation of root-zone soil moisture from surface measurements. *Hydrol Earth Syst Sc* **2014,** *18*, (3), 1199-1212.

39.   Soil Survey Staff Web Soil Survey. http://websoilsurvey.nrcs.usda.gov/

40.   Ni, B. R.; Pallardy, S. G., Response of Liquid Flow Resistance to Soil Drying in Seedlings of 4 Deciduous Angiosperms. *Oecologia* **1990,** *84*, (2), 260-264.

41.   Pallardy, S. G.; Rhoads, J. L., Morphological Adaptations to Drought in Seedlings of Deciduous Angiosperms. *Can J Forest Res* **1993,** *23*, (9), 1766-1774.

Appendix A Discussion of treatment of drought impact on leaf temperature and isoprene emission in MEGAN v2.10

Summary: A bug in MEGANv2.1 is fixed. An additional input field, drought index (DI), is needed to fully address the effect of drought on isoprene emissions. It is programmed in the MEGAN code but never gets initialized. DI is a parameter used in the canopy model to calculate leaf temperature, which in turn affects isoprene emissions. The impact of the missing DI field is investigated. Using the DI field correctly leads to higher isoprene emissions, but the MEGAN drought parameterization (DP) leads to lower isoprene emissions. Considering the two effects leads to small changes in the isoprene emissions under drought condition, although including both DI and DP does lead to slightly better overall isoprene performance in the CMAQ model.

Detailed discussion:

MEGAN2.1 needs the Palmer Drought Severity Index (PDSI) in the canopy model to estimate γCE. This parameter is used in the EMPROC.F, around line 720:

```
                CALL GAMME_CE(IDATE,ITIME,LAT(I,J),LONG(I,J),
     &                  TEMP(I,J),D_TEMP(I,J), D_TEMP(I,J),
     &                  PPFD(I,J),D_PPFD(I,J), D_PPFD(I,J),
     &                  WIND(I,J),QV(I,J),
     &                  I_PFT,LAIc(i,j),PRES(I,J),DI(I,J),
     &                  NrCha,NrTyp,Canopychar, VNAME3D(s),
     &                  GAMMA_TD,GAMMA_TI)
```

Although the DI array is allocated (around line 457), it is never assigned values.

The GAMME_CE function is defined in canopy.f. Checking the source code, **DI** is used in calling the function DIstomata (around line 148):

```
    StomataDI  = DIstomata(DI )
```

The DIstimata function implements the following:

$$\text{DIstomata} = \begin{cases} 1 \text{ ,DI>DI}_{high} \\ 1-0.9\dfrac{\text{DI-DI}_{high}}{\text{DI}_{low}\text{-DI}_{high}} \text{ ,DI}_{low}\text{<DI} \le \text{DI}_{high} \\ 0 \text{ ,DI} \le \text{DI}_{low} \end{cases}$$

where DI_{high}=-0.5 and DI_{low}=-5. Thus, **StomataDI** varies from 1 (no drought) to 0 (extreme drought).

In the precompiled MEGAN code, it appears that an allocated array, although not initialized explicitly, is default to zero (this is not always the case, and FORTRAN standard does not

explicitly specify that uninitialized variable should be set to zero). This leads to **StomataDI=1** even under drought conditions.

The **StomataDI** variable is then passed into the subroutine CanopyEB (line 177). This is the canopy energy balance model to estimate leaf temperature. In the subroutine, **StomataDI** is further passed into the subroutine LeafEB, which does energy balance calculation for the leaf (lines 658 and 667).

In the LeafEB subroutine, **StomataDI** is finally passed into function ResSC to calculate stomatal resistence (line 720).

```
        StomRes  = ResSC(PPFD, stomataDI)
```

The **StomRes** variable is then passed to the function LeafLE to calculate the latent heat flux from the leaf.

And here is the ResSC function:
```
        FUNCTION ResSC(Par, StomataDI)
 !   Leaf stomatal cond. resistance s m-1
        IMPLICIT NONE
        INTEGER,PARAMETER :: real_x = SELECTED_REAL_KIND(p=14, r=30)
        REAL :: Par, StomataDI, SCadj, ResSC
 !--------------------------------------------------------------------
 --
        SCadj = StomataDI * ((0.0027 * 1.066 * Par) /
      &         ((1 + 0.0027 * 0.0027 * Par**2.)**0.5))

        IF (SCadj < 0.1) THEN
          ResSC = 2000
        ELSE
          ResSC = 200 / SCadj
        ENDIF

        END FUNCTION ResSC
```

The MEGAN code is not sufficiently well documented so the reference for this cannot be found at the moment. However, it is obvious that under extreme drought condition, **StomataDI** can be very small and even close to zero. This leads to large **RecSC** values and can reduce the latent heat flux from the leaf and thus lead to higher leaf temperature, and higher isoprene emissions under the right temperature range. In this study, we modified the MEGAN code to read a pre-calculated monthly DI field. The DI fields from 1850 to 2012 are downloaded from the NCAR website: http://www.cgd.ucar.edu/cas/catalog/climind/pdsi.html. A short program is used to re-project the 2.5x2.5 degree DI fields to the current model domains and converted the netCDF file into IOAPI format.

Appendix B Ozone time series for April to October 2011 at Selected Auto-GC sites
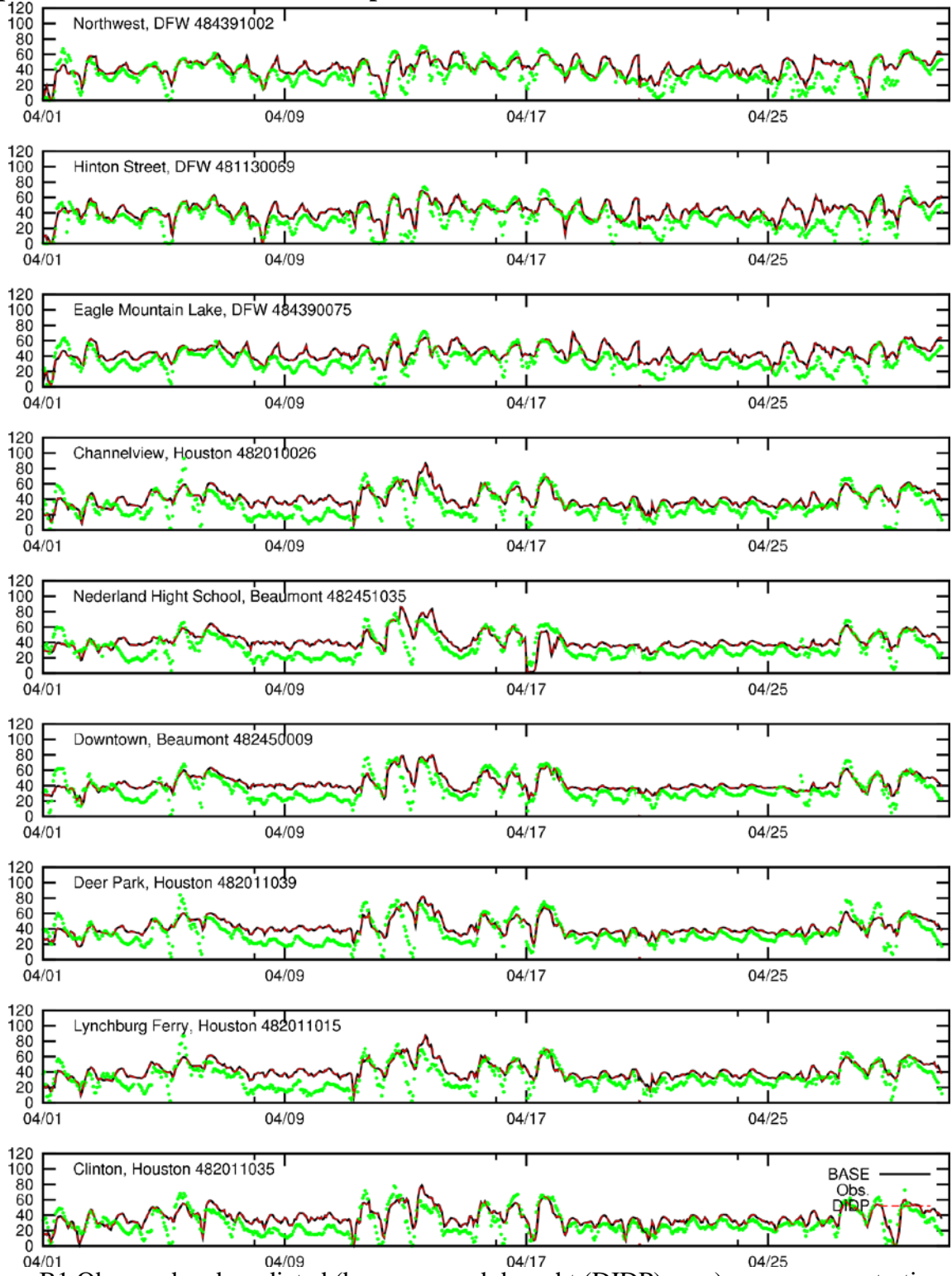
Figure B1 Observed and predicted (base case and drought (DIDP) case) ozone concentrations at Auto-GC sites for April 2011.
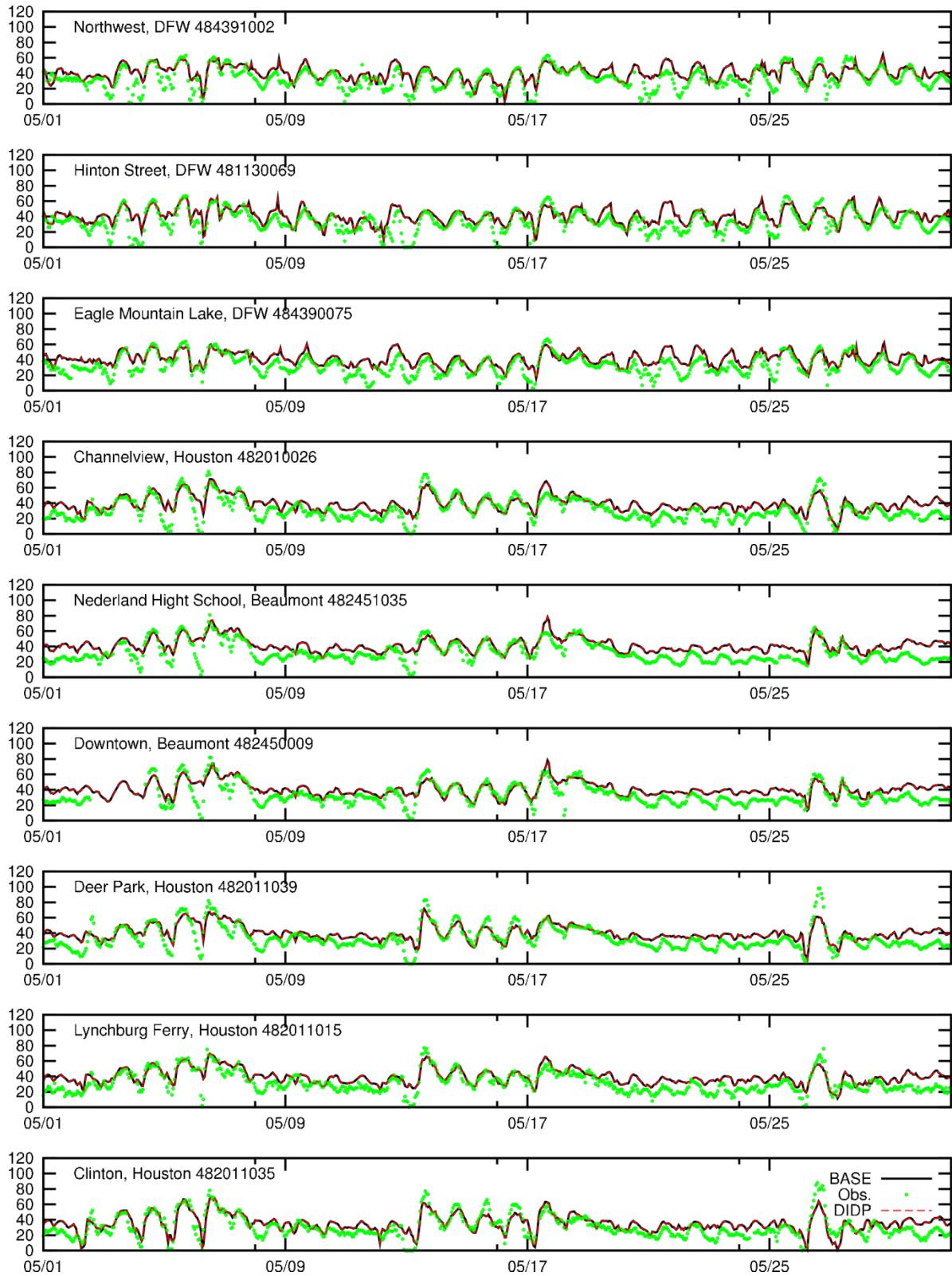
Figure B2 Observed and predicted (base case and drought (DIDP) case) ozone concentrations at Auto-GC sites for May 2011.
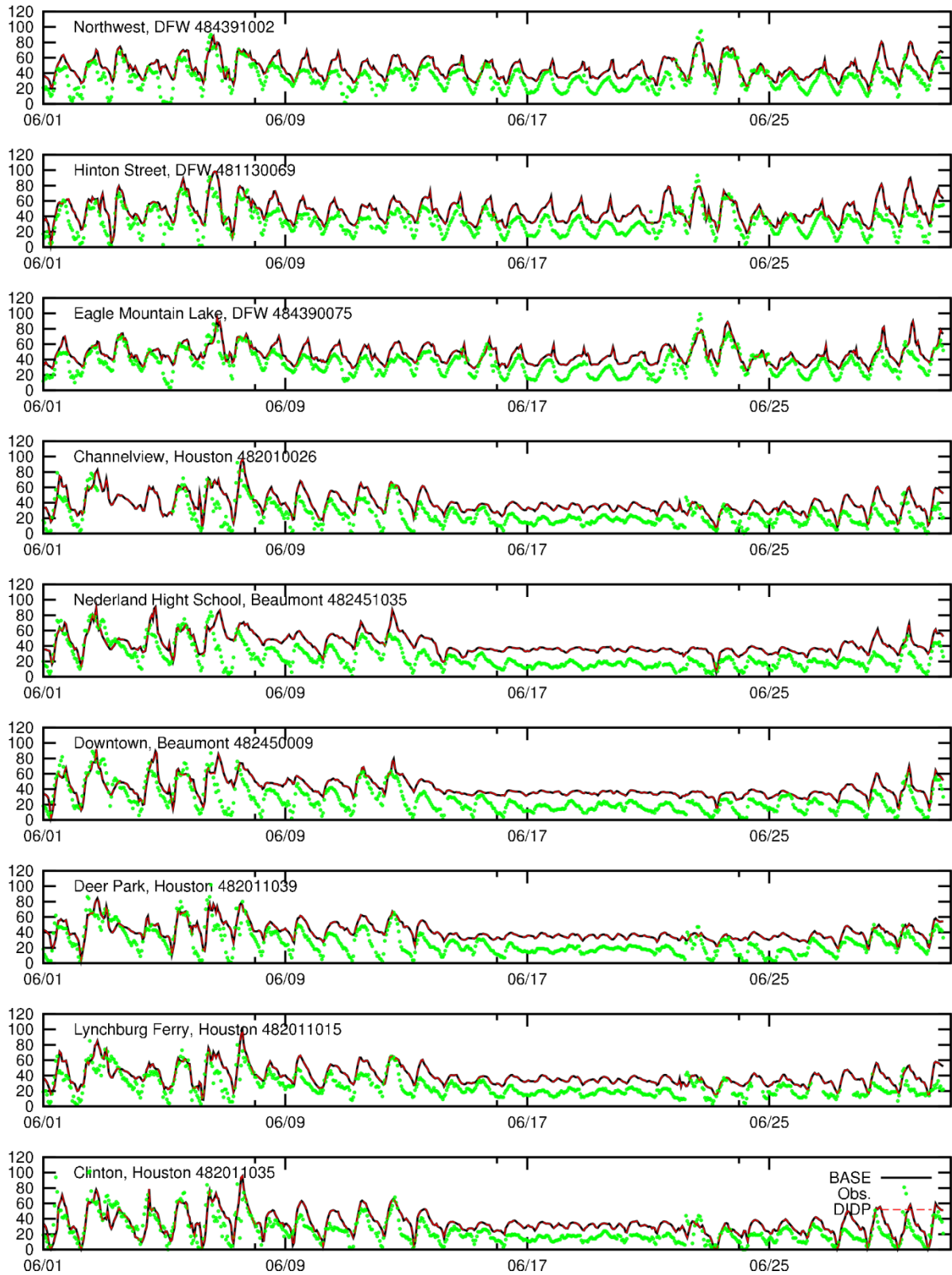
Figure B3 Observed and predicted (base case and drought (DIDP) case) ozone concentrations at Auto-GC sites for June 2011.
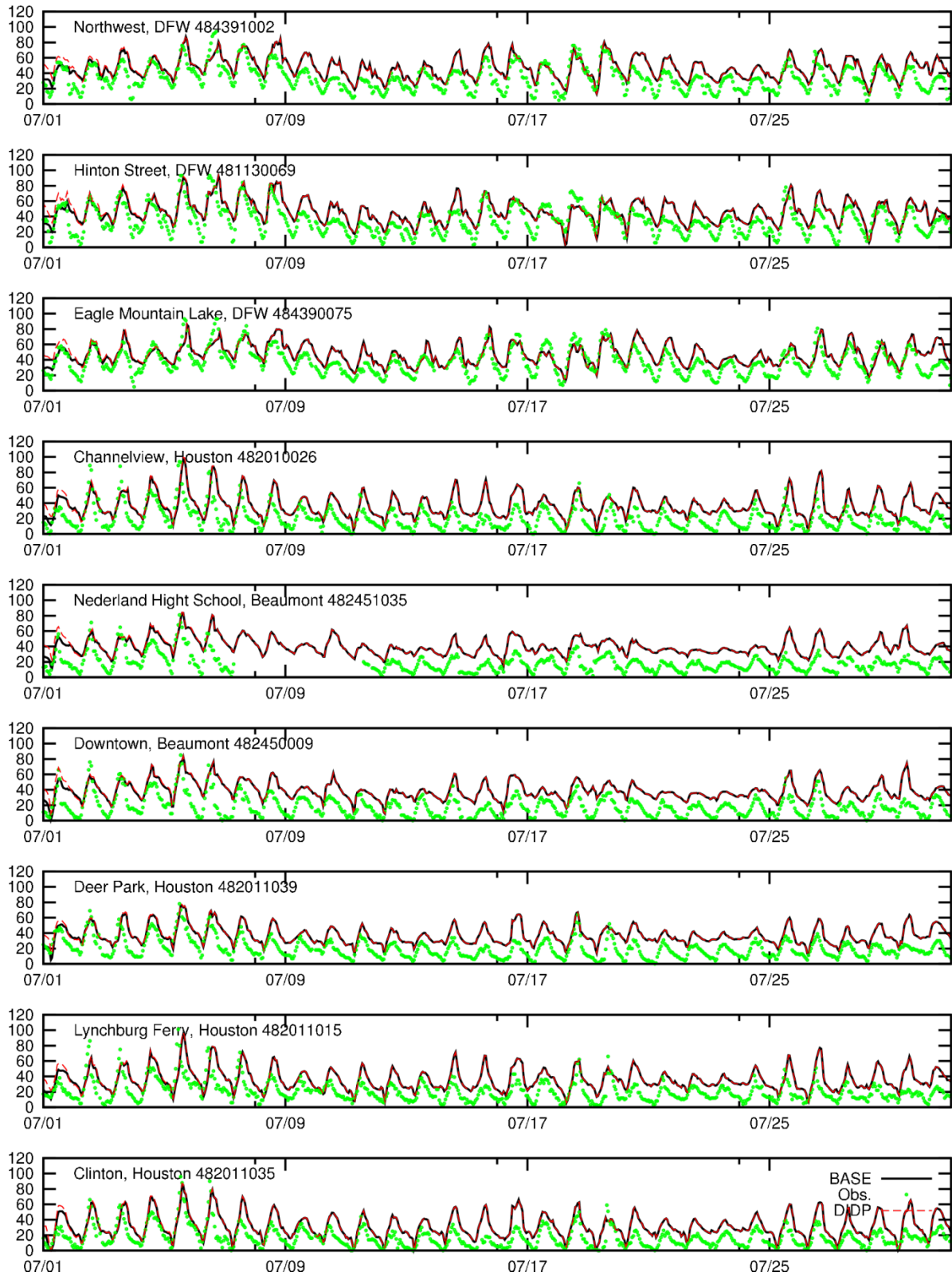
Figure B4 Observed and predicted (base case and drought (DIDP) case) ozone concentrations at
Auto-GC sites for July 2011.
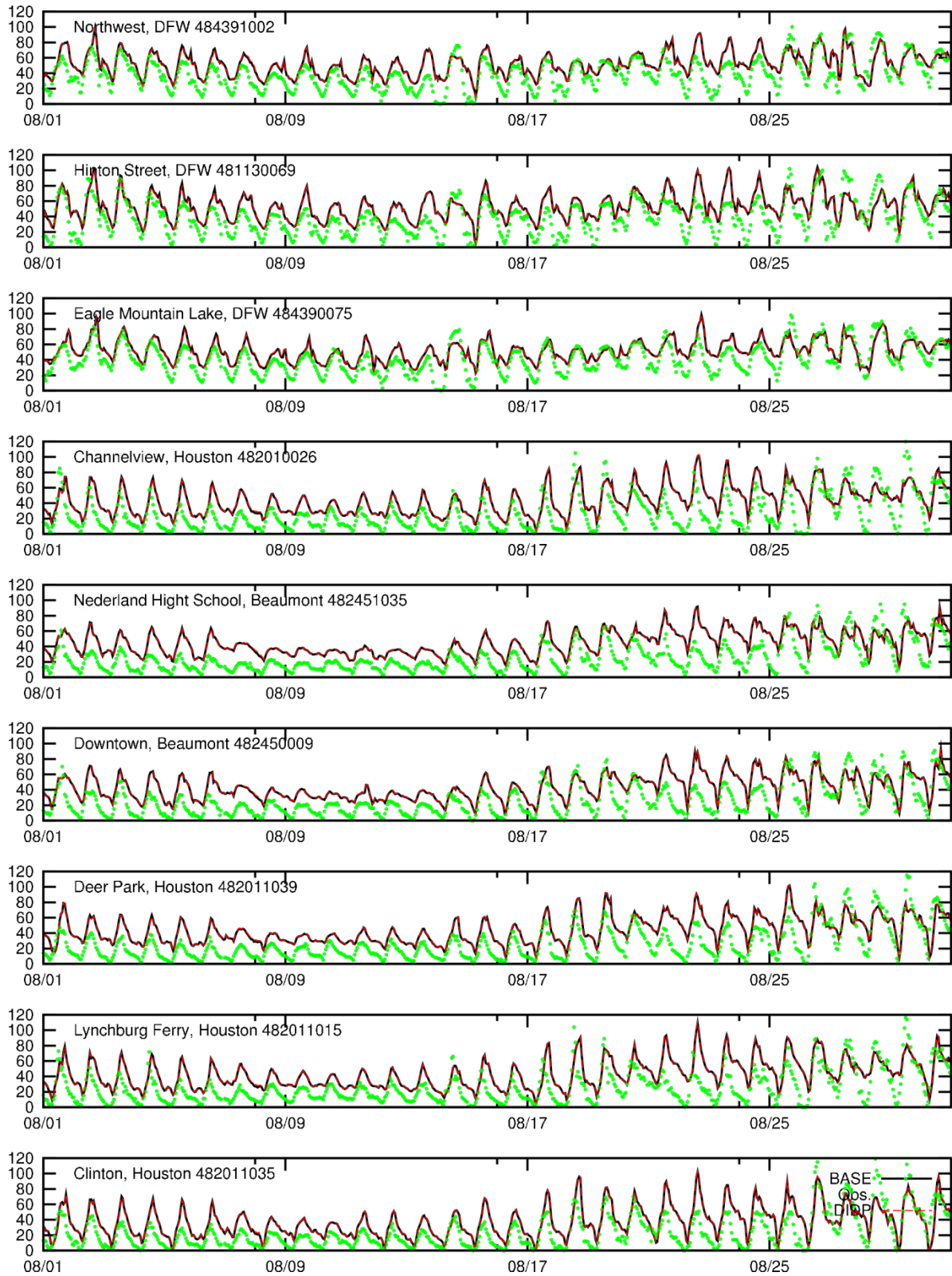
Figure B5 Observed and predicted (base case and drought (DIDP) case) ozone concentrations at Auto-GC sites for August 2011.
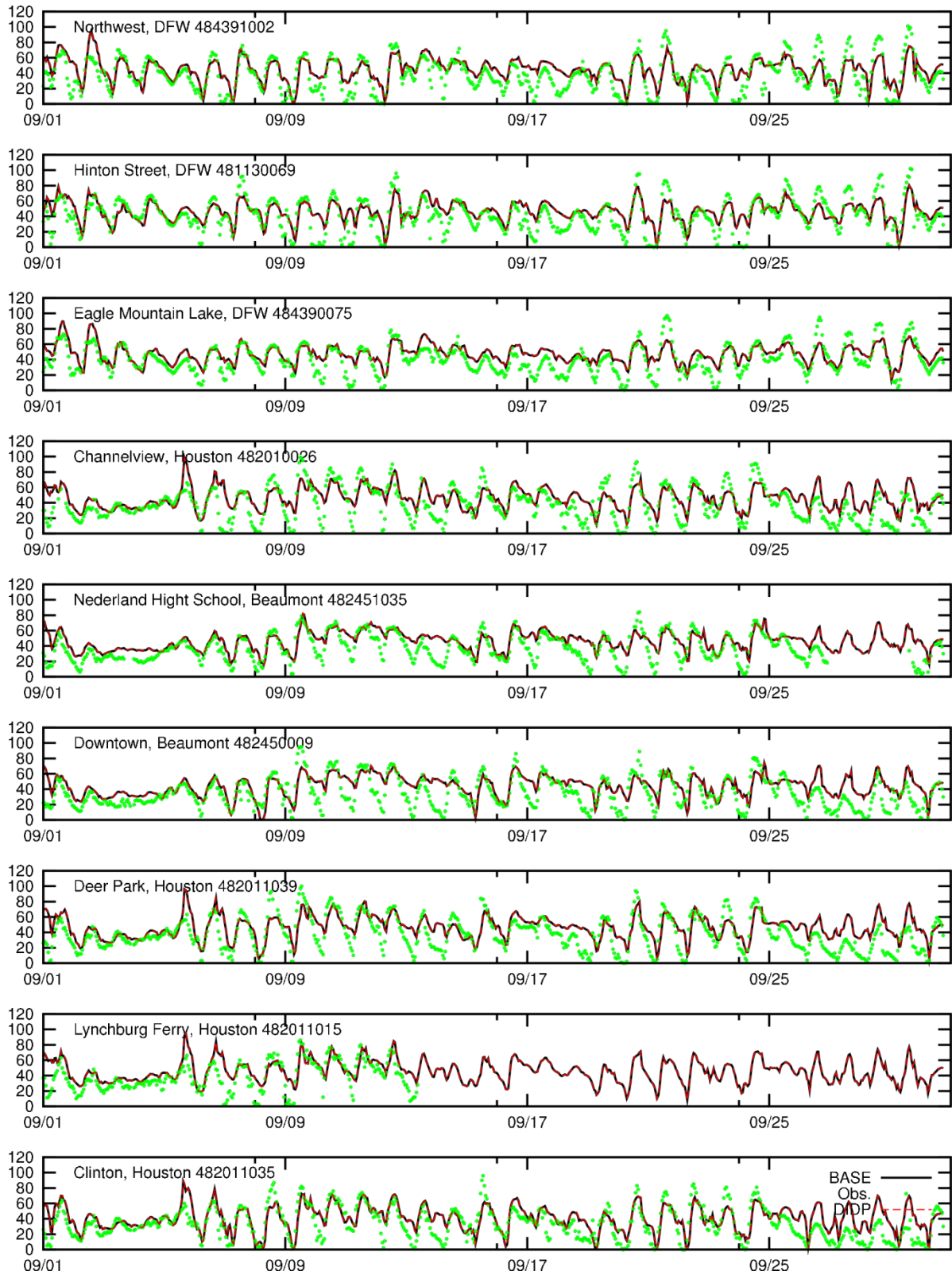
Figure B6 Observed and predicted (base case and drought (DIDP) case) ozone concentrations at Auto-GC sites for September 2011.
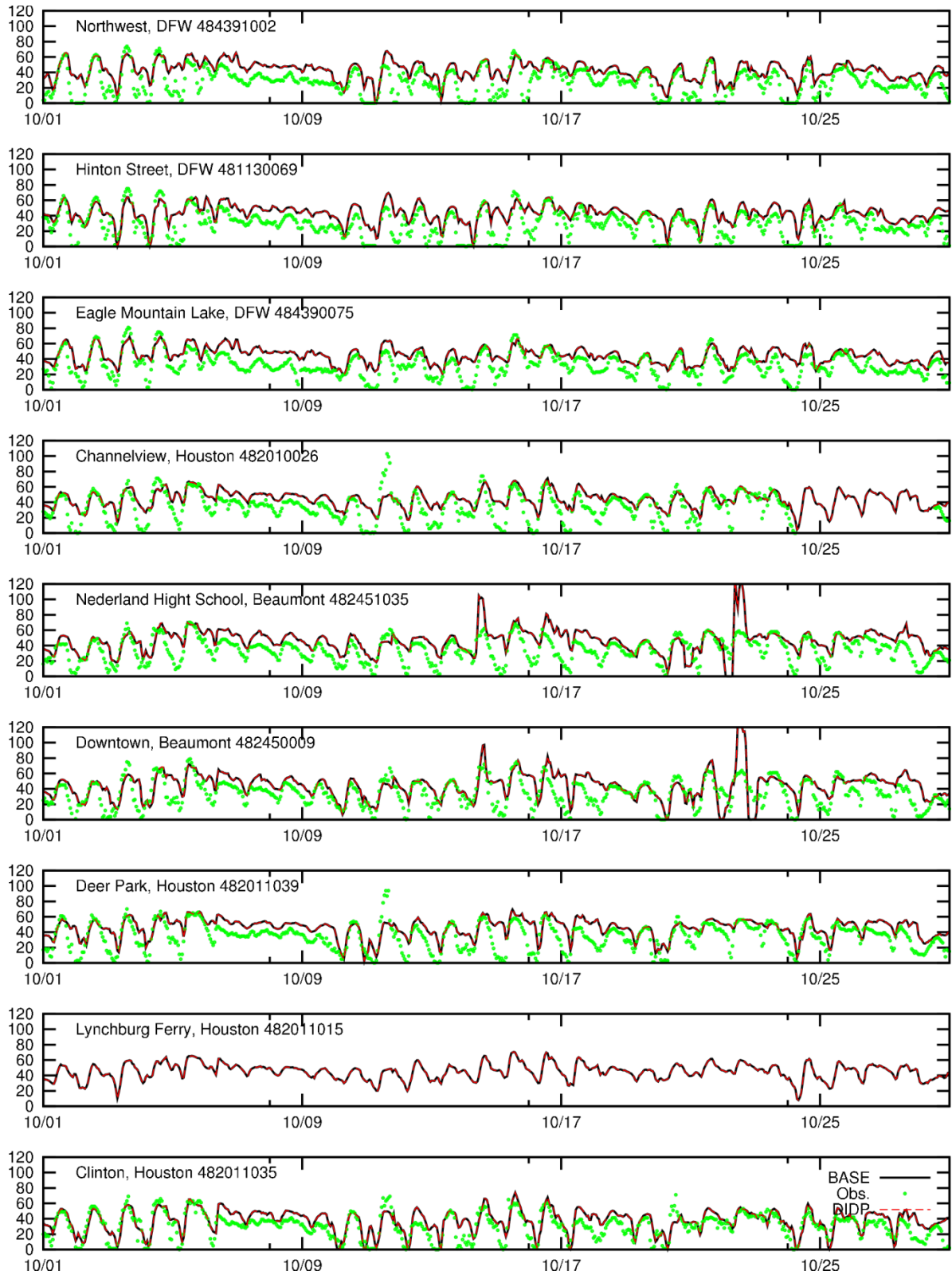
Figure B7 Observed and predicted (base case and drought (DIDP) case) ozone concentrations at Auto-GC sites for October 2011.

Appendix C Ozone time series for April to October 2007 at Selected Auto-GC sites
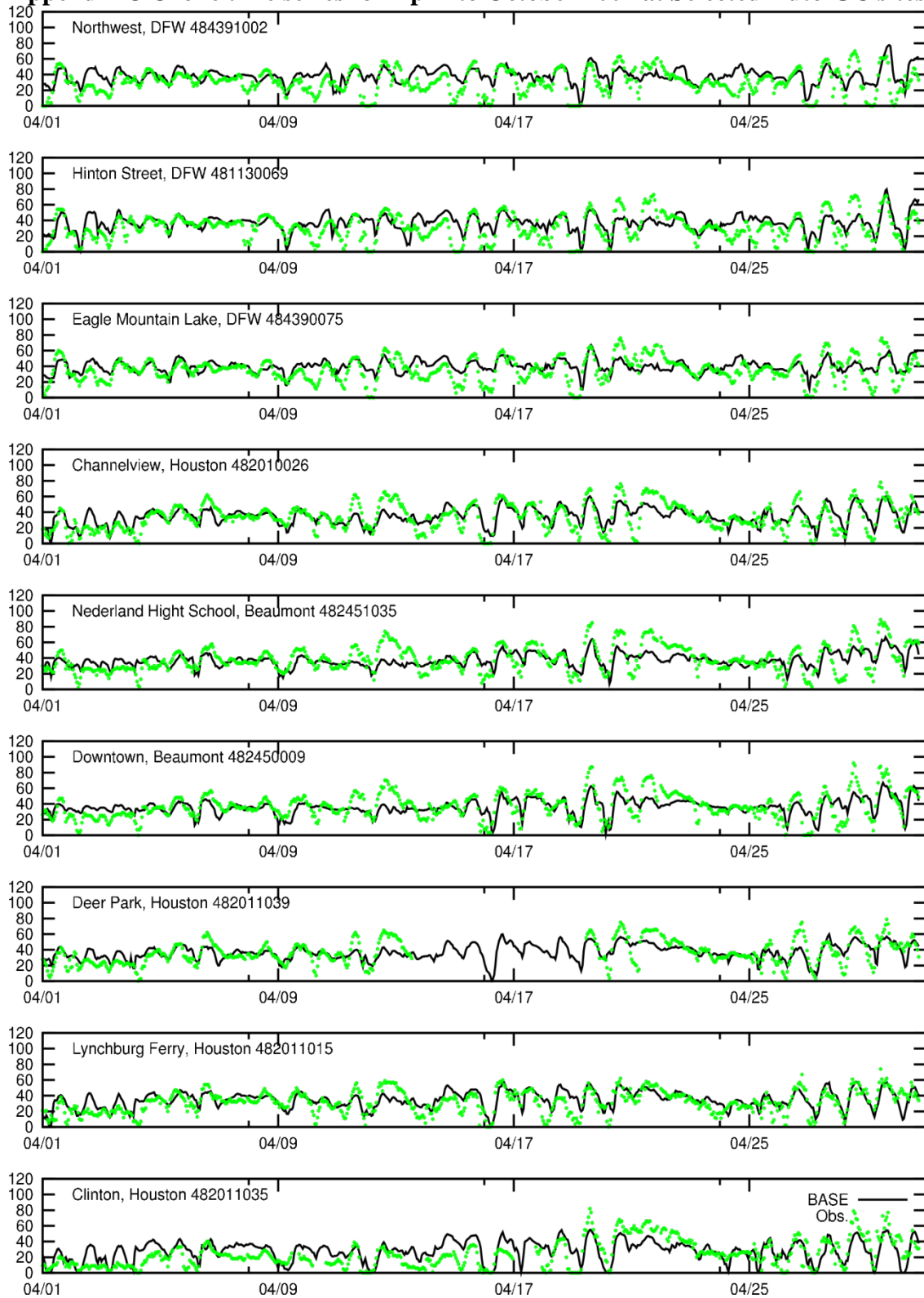
Figure C1 Observed and predicted ozone concentrations at Auto-GC sites for April 2007.
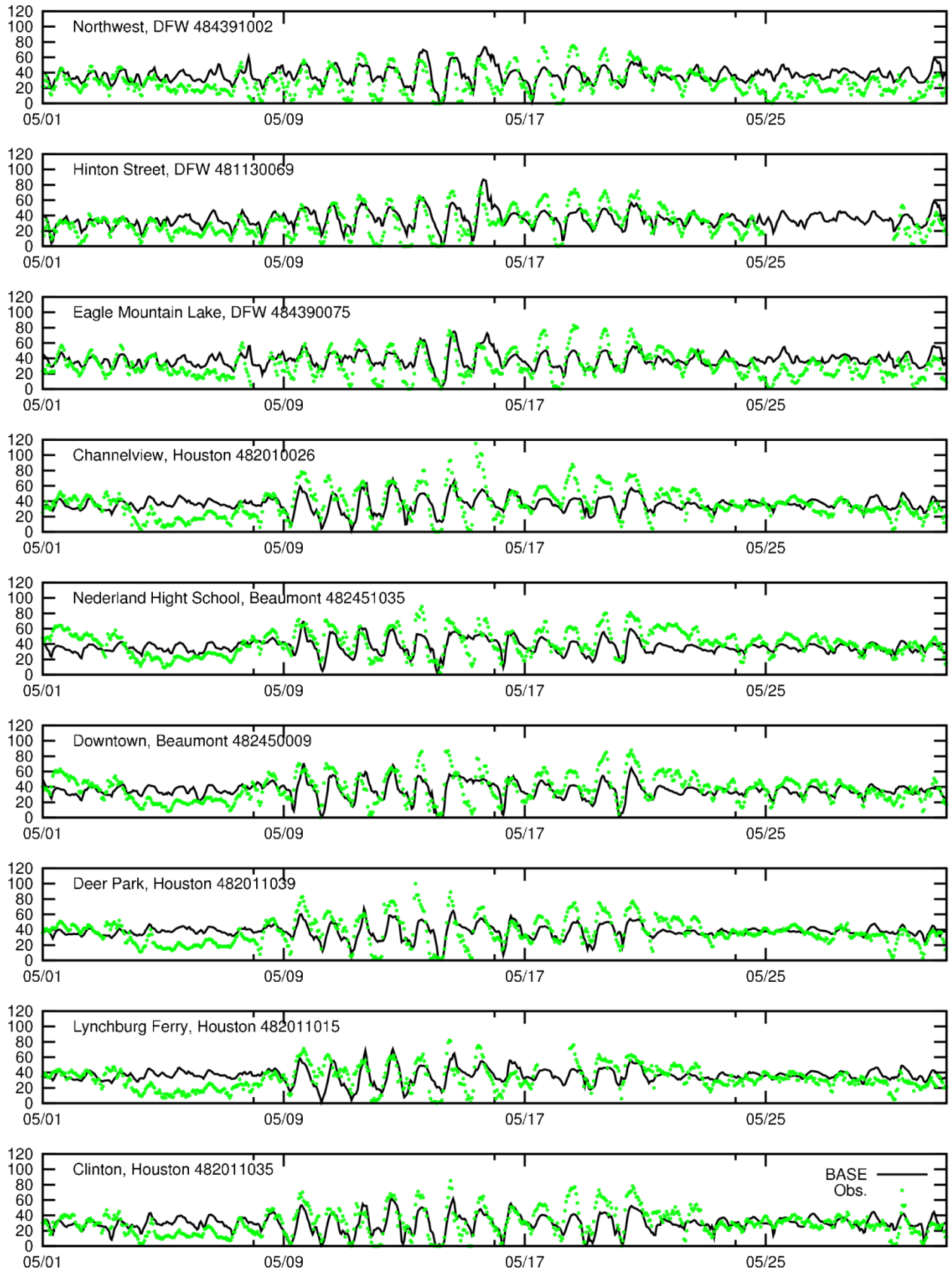
Figure C2 Observed and predicted ozone concentrations at Auto-GC sites for May 2007.
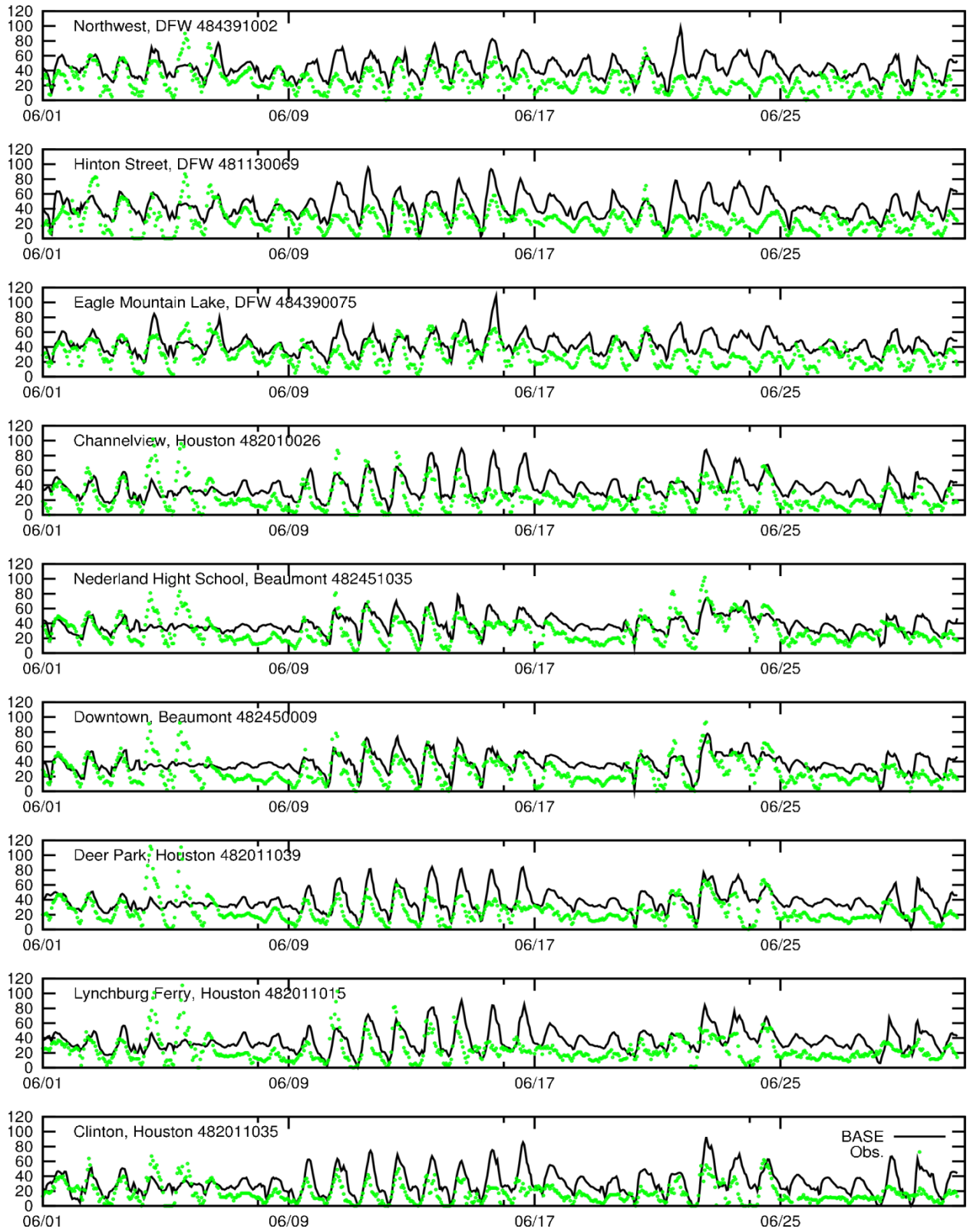
Figure C3 Observed and predicted ozone concentrations at Auto-GC sites for June 2007.
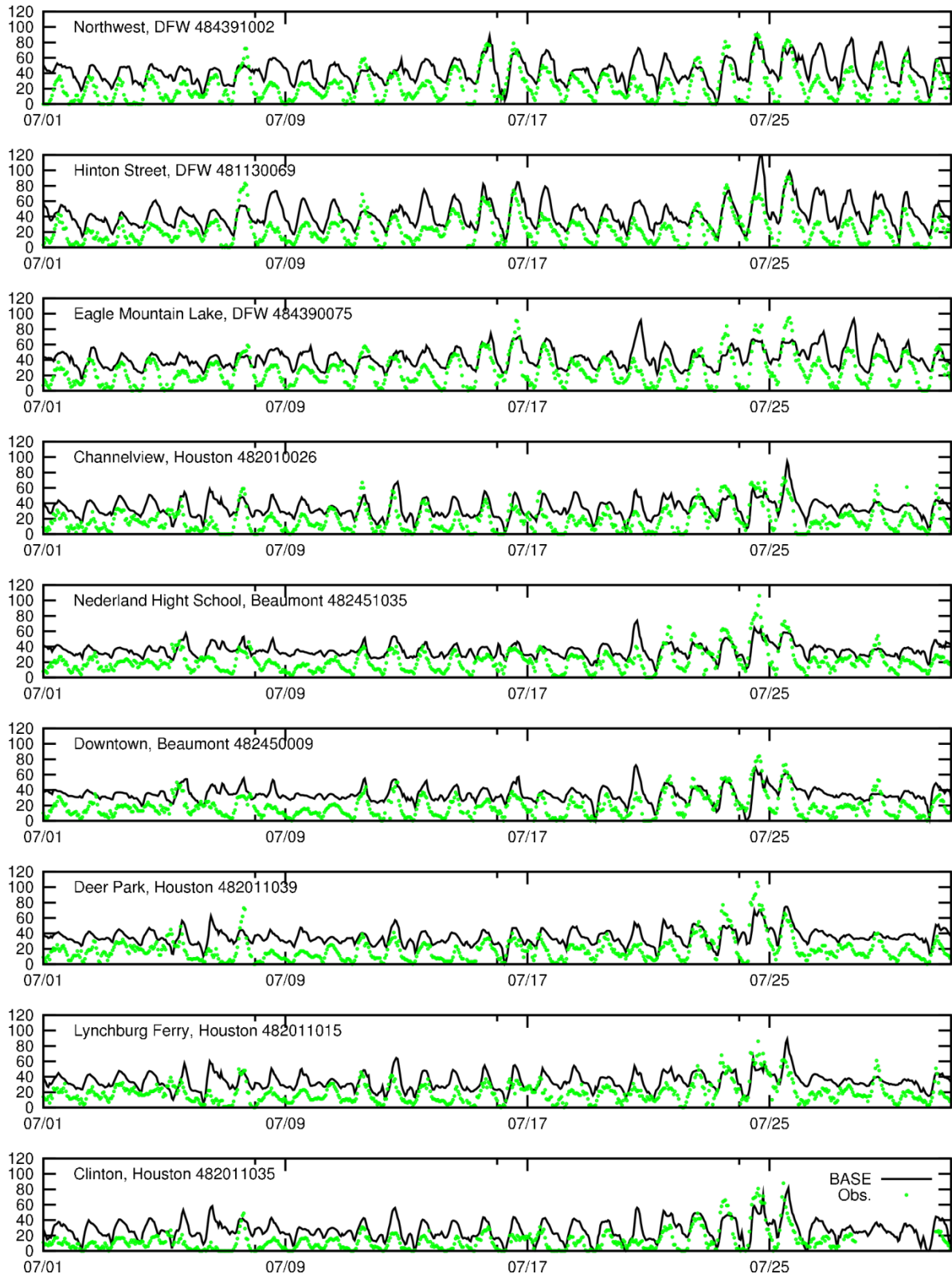
Figure C4 Observed and predicted ozone concentrations at Auto-GC sites for July 2007.
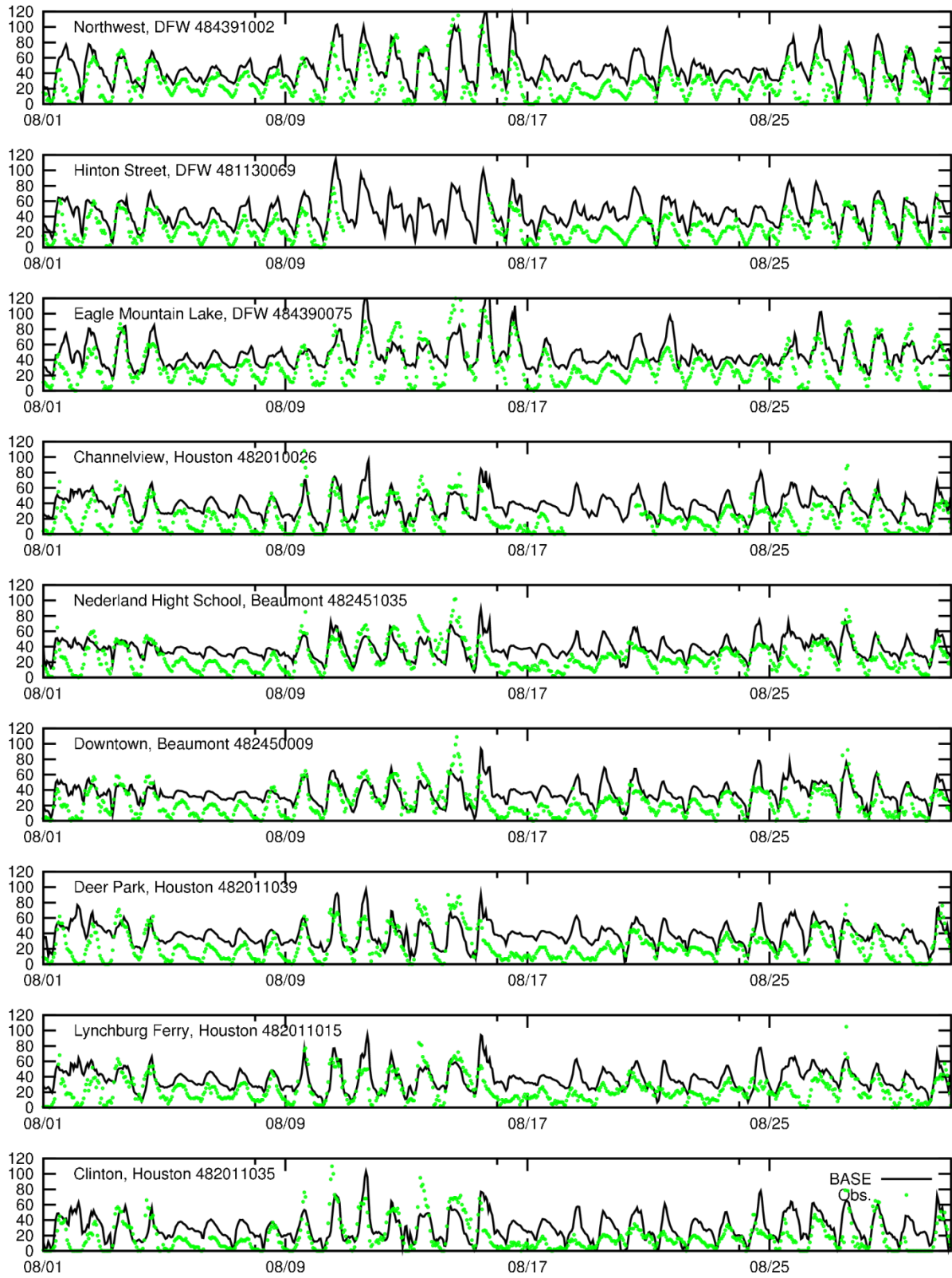
Figure C5 Observed and predicted ozone concentrations at Auto-GC sites for August 2007.
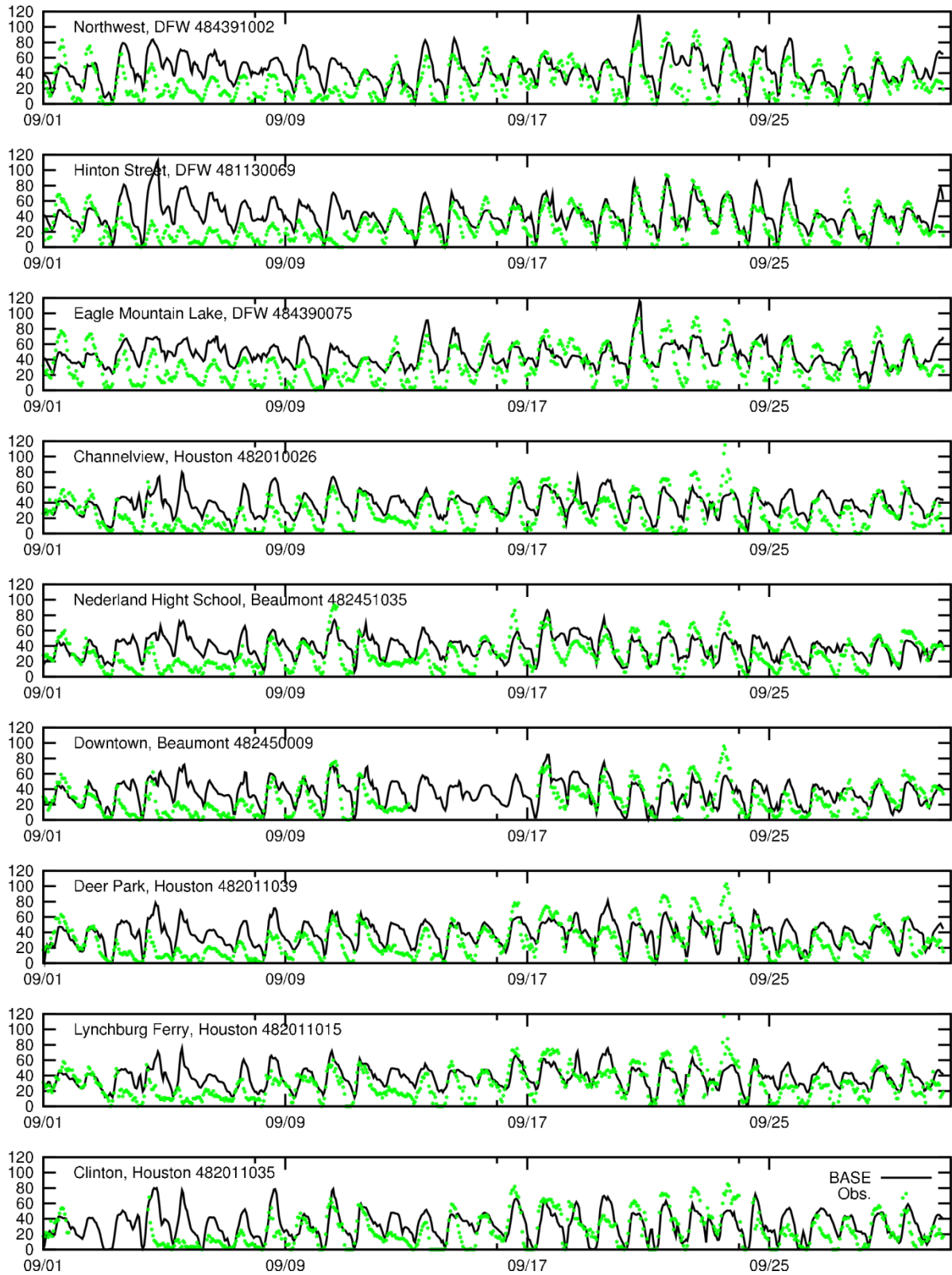
Figure C6 Observed and predicted ozone concentrations at Auto-GC sites for September 2007.
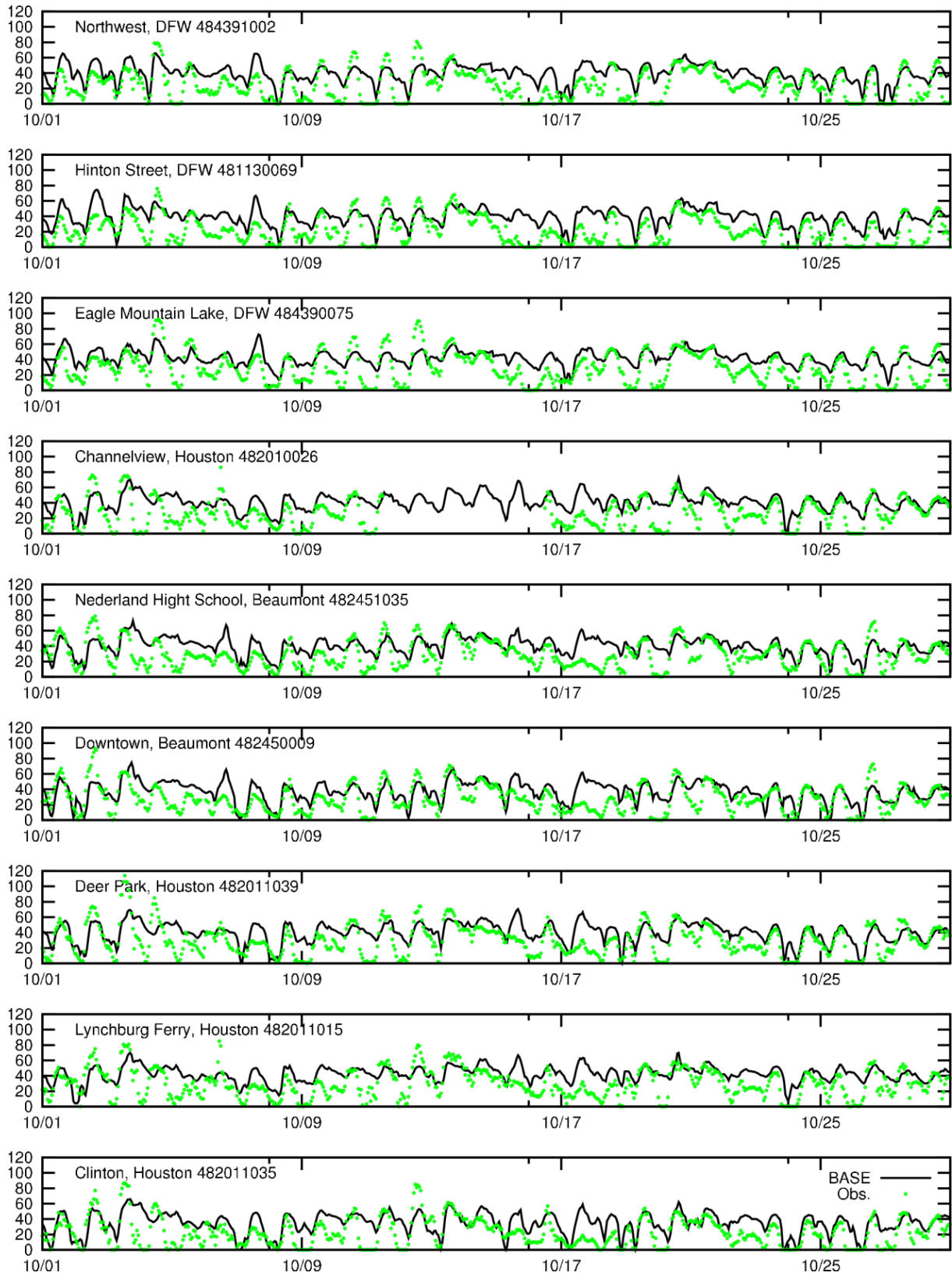
Figure C7 Observed and predicted ozone concentrations at Auto-GC sites for October 2007.

Appendix D Definition of Model Performance Statistical Measures

Statistical Measures	Definition
Mean bias	$\text{MB} = \dfrac{1}{N}\sum_{i=1}^{N}(C_{m,i} - C_{o,i})$
Gross error	$\text{GE} = \dfrac{1}{N}\sum_{i=1}^{N}\lvert C_{m,i} - C_{o,i} \rvert$
Root mean square error	$\text{RMSE} = \sqrt{\dfrac{1}{N}\sum_{i=1}^{N}(C_{m,i} - C_{o,i})^2}$
Normalized mean bias	$\text{NMB} = \dfrac{\sum_{i=1}^{N} C_{m,i} - C_{o,i}}{\sum_{i=1}^{N} C_{o,i}}$
Normalized mean error	$\text{NME} = \dfrac{\sum_{i=1}^{N}\lvert C_{m,i} - C_{o,i}\rvert}{\sum_{i=1}^{N} C_{o,i}}$
Mean normalized bias	$\text{MNB} = \dfrac{1}{N}\sum_{i=1}^{N}\dfrac{C_{m,i} - C_{o,i}}{C_{o,i}}$
Normalized gross error	$\text{NGE} = \dfrac{1}{N}\sum_{i=1}^{N}\dfrac{\lvert C_{m,i} - C_{o,i}\rvert}{C_{o,i}}$
Mean fractional bias	$\text{MFB} = \dfrac{2}{N}\sum_{i=1}^{N}\dfrac{C_{m,i} - C_{o,i}}{C_{m,i} + C_{o,i}}$
Mean fractional error	$\text{MFE} = \dfrac{2}{N}\sum_{i=1}^{N}\dfrac{\lvert C_{m,i} - C_{o,i}\rvert}{C_{m,i} + C_{o,i}}$
Accuracy of paired peak	$\text{APP} = \dfrac{C_{p,opeak} - C_{o,opeak}}{C_{o,opeak}}$
Accuracy of unpaired peak	$\text{AUP} = \dfrac{C_{p,ppeak} - C_{o,opeak}}{C_{o,opeak}}$

Note: C_m is the model-predicted concentration i, C_o is the observed i, and N equals the number of prediction-observation pairs drawn from all monitoring stations. The subscripts ppeak and opeak are the hours when predicted and observed peak concentrations occur.

Appendix E1 Soil-related Parameters Used to Calculate Wilting Point

TABLE 2. Soil-related paramters in the LSM. The hydraulic properties are volumetric water content at saturation (Θ_s), saturation soil suction (Ψ_s), hydrualic conductivity at saturation (K_s), field capacity (Θ_{ref}), and wilting point (Θ_w). Here, b is an exponent in the function that relates soil water potential and water content.

Soil type	Θ_s (m³ m⁻³)	Ψ_s (m)	K_s (m s⁻¹)	b	Θ_{ref} (m³ m⁻³)	Θ_w (m³ m⁻³)
1) Sand	0.339	0.069	1.07E−6	2.79	0.236	0.01
2) Loamy sand	0.421	0.036	1.41E−5	4.26	0.283	0.028
3) Sandy loam	0.434	0.141	5.23E−6	4.74	0.312	0.047
4) Silt loam	0.476	0.759	2.81E−6	5.33	0.36	0.084
5) Silt	0.476	0.759	2.81E−6	5.33	0.36	0.084
6) Loam	0.439	0.355	3.38E−6	5.25	0.329	0.066
7) Sandy clay loam	0.404	0.135	4.45E−6	6.66	0.314	0.067
8) Silty clay loam	0.464	0.617	2.04E−6	8.72	0.387	0.12
9) Clay loam	0.465	0.263	2.45E−6	8.17	0.382	0.103
10) Sandy clay	0.406	0.098	7.22E−6	10.73	0.338	0.1
11) Silty clay	0.468	0.324	1.34E−6	10.39	0.404	0.126
12) Clay	0.468	0.468	9.74E−7	11.55	0.412	0.138
13) Organic material	0.439	0.355	3.38E−6	5.25	0.329	0.06
14) Water						
15) Bedrock	0.25	7.59	9.74E−8	11.55	0.233	0.094
16) Other (land–ice)	0.421	0.036	1.34E−6	11.55	0.283	0.028

Note: this table is extracted from Chen and Dudhia [1].

Appendix E2 Characterization of soil mixture used in the greenhouse experiments

TEXAS A&M AGRILIFE EXTENSION

Report generated for:
Gunnar Schade
Monica Madronich
1104 Eller O&M Building, TAMU
College Station, TX 77843

Other County
   Laboratory Number: 417174
   Customer Sample ID: 1
     Crop Grown: NO CROP GIVEN

Soil Analysis Report

Soil, Water and Forage Testing Laboratory
Department of Soil and Crop Sciences
2478 TAMU
College Station, TX 77843-2478
979-845-4816 (phone)
979-845-5958 (FAX)
Visit our website: http://soiltesting.tamu.edu

Sample received on: 7/30/2014
Printed on: 8/8/2014
Area Represented: not provided

Analysis	Results	CL*	Units	ExLow	VLow	Low	Mod	High	VHigh	Excess.
pH	7.9	(5.8)	-	Mod. Alkaline						
Conductivity	85	(-)	umho/cm	None			CL*			Fertilizer Recommended
Nitrate-N	1	(-)	ppm**							
Phosphorus	10	(0)	ppm							
Potassium	78	(0)	ppm							
Calcium	13,054	(180)	ppm							
Magnesium	174	(50)	ppm							
Sulfur	22	(13)	ppm							
Sodium	24	(-)	ppm							
Iron	7.04	(4.25)	ppm							
Zinc	0.40	(0.81)	ppm							
Manganese	2.02	(1.00)	ppm							
Copper	0.40	(0.16)	ppm							
Boron										
Limestone Requirement										

Textural Analysis Test (hydrometer)			Detailed Salinity Test (Saturated Paste Extract)			
Sand	71	%	pH	7.2		
Silt	14	%	Conductivity	0.50 mmhos/cm		
Clay	15	%	Sodium	72 ppm	3.124 meq/L	
Textural Class:	Sandy Loam		Potassium	11 ppm	0.276 meq/L	
			Calcium	47 ppm	2.330 meq/L	
Organic Matter	0.72	%	Magnesium	6 ppm	0.480 meq/L	
			SAR	2.64		
			SSP	50.31		

*CL=Critical level is the point which no additional nutrient (excluding nitrate-N, sodium and conductivity) is recommended. **ppm=mg/kg

Appendix F Model performance statistics of soil moisture

Year 2011

2011704

depth	0.05 m	0.10 m	0.20 m	0.25 m	0.50 m	0.60 m	1.00 m
avg_obs	0.15	0.11	0.13	0.30	0.19	0.28	0.23
avg_pre	0.14	0.13	0.13	0.21	0.13	0.19	0.16
MB	-0.01	0.02	0.00	-0.09	-0.06	-0.09	-0.06
RMSE	0.09	0.08	0.06	0.11	0.07	0.12	0.11
GE	0.07	0.07	0.06	0.09	0.06	0.09	0.10
MNB	0.18	0.08	0.17	-0.27	-0.32	-0.26	-0.06

201105

depth	0.05 m	0.10 m	0.20 m	0.25 m	0.50 m	0.60 m	1.00 m
avg_obs	0.17	0.12	0.13	0.32	0.17	0.28	0.21
avg_pre	0.16	0.13	0.12	0.24	0.12	0.22	0.15
MB	-0.01	0.01	-0.01	-0.07	-0.05	-0.06	-0.06
RMSE	0.09	0.08	0.08	0.09	0.07	0.08	0.11
GE	0.08	0.07	0.07	0.07	0.06	0.06	0.10
MNB	0.23	0.16	0.21	-0.21	-0.29	-0.18	-0.04

201106

depth	0.05 m	0.10 m	0.20 m	0.25 m	0.50 m	0.60 m	1.00 m
avg_obs	0.17	0.14	0.13	0.27	0.15	0.25	0.19
avg_pre	0.15	0.11	0.12	0.20	0.12	0.19	0.13
MB	-0.02	-0.04	-0.01	-0.07	-0.03	-0.06	-0.06
RMSE	0.05	0.08	0.07	0.08	0.06	0.07	0.12
GE	0.04	0.08	0.06	0.07	0.05	0.06	0.11
MNB	-0.06	-0.05	0.20	-0.25	-0.10	-0.20	-0.06

201107

depth	0.05 m	0.10 m	0.20 m	0.25 m	0.50 m	0.60 m	1.00 m
avg_obs	0.16	0.14	0.13	0.24	0.16	0.20	0.17
avg_pre	0.14	0.13	0.13	0.16	0.12	0.14	0.12
MB	-0.03	-0.01	-0.01	-0.09	-0.04	-0.06	-0.05
RMSE	0.05	0.05	0.06	0.09	0.06	0.06	0.10
GE	0.05	0.04	0.06	0.09	0.05	0.06	0.09
MNB	-0.10	0.09	0.24	-0.34	-0.22	-0.29	-0.08

201108

depth	0.05 m	0.10 m	0.20 m	0.25 m	0.50 m	0.60 m	1.00 m
avg_obs	0.20	0.13	0.13	0.32	0.17	0.28	0.21
avg_pre	0.19	0.13	0.12	0.24	0.13	0.22	0.14
MB	-0.01	0.01	-0.01	-0.07	-0.04	-0.06	-0.07
RMSE	0.06	0.06	0.09	0.09	0.06	0.08	0.12
GE	0.05	0.06	0.07	0.07	0.05	0.06	0.11
MNB	0.10	0.36	0.21	-0.21	-0.24	-0.18	-0.02

201109

depth	0.05M	0.10M	0.20M	0.25M	0.50M	0.60M	1.00M
avg_obs	0.11	0.08	0.10	0.24	0.13	0.20	0.13
avg_pre	0.13	0.13	0.13	0.13	0.12	0.13	0.15
MB	0.01	0.05	0.03	-0.11	-0.01	-0.06	0.02
RMSE	0.09	0.09	0.07	0.12	0.07	0.06	0.11
GE	0.08	0.07	0.06	0.11	0.05	0.06	0.10
MNB	0.35	0.20	0.15	-0.46	0.11	-0.33	0.08

201110

depth	0.05 m	0.10 m	0.20 m	0.25 m	0.50 m	0.60 m	1.00 m
avg_obs	0.14	0.11	0.13	0.25	0.14	0.20	0.13
avg_pre	0.16	0.15	0.15	0.15	0.13	0.15	0.15
MB	0.01	0.03	0.02	-0.09	-0.01	-0.05	0.03
RMSE	0.09	0.11	0.08	0.11	0.06	0.06	0.11
GE	0.08	0.08	0.07	0.10	0.05	0.05	0.10
MNB	0.13	0.20	0.08	-0.37	0.30	-0.27	0.11

Year 2007

200704

depth	0.05 m	0.10 m	0.20 m	0.25 m	0.50 m	0.60 m	1.00 m
avg_obs	0.25	0.22	0.30	0.29	0.32	0.31	0.40
avg_pre	0.26	0.28	0.26	0.28	0.29	0.27	0.28
MB	0.01	0.06	-0.04	-0.02	-0.03	-0.04	-0.11
RMSE	0.05	0.06	0.09	0.07	0.04	0.10	0.11
GE	0.04	0.06	0.07	0.05	0.03	0.07	0.11
MNB	0.09	0.26	-0.07	0.00	-0.11	-0.06	-0.28

200705

depth	0.05 m	0.10 m	0.20 m	0.25 m	0.50 m	0.60 m	1.00 m
avg_obs	0.27	0.17	0.29	0.30	0.29	0.31	0.38
avg_pre	0.28	0.27	0.29	0.28	0.28	0.28	0.28
MB	0.02	0.11	0.00	-0.03	-0.01	-0.03	-0.10

RMSE	0.08	0.12	0.07	0.08	0.02	0.07	0.10
GE	0.06	0.11	0.05	0.06	0.02	0.06	0.10
MNB	0.18	0.93	0.06	-0.03	-0.04	-0.05	-0.25

200706

depth	0.05 m	0.10 m	0.20 m	0.25 m	0.50 m	0.60 m	1.00 m
avg_obs	0.26	0.20	0.26	0.31	0.30	0.27	0.37
avg_pre	0.27	0.26	0.27	0.27	0.28	0.27	0.27
MB	0.01	0.06	0.01	-0.04	-0.02	0.01	-0.10
RMSE	0.07	0.07	0.05	0.09	0.03	0.06	0.10
GE	0.05	0.06	0.04	0.07	0.02	0.05	0.10
MNB	0.09	0.36	0.06	-0.07	-0.07	0.08	-0.27

200707

depth	0.05 m	0.10 m	0.20 m	0.25 m	0.50 m	0.60 m	1.00 m
avg_obs	0.23	0.25	0.24	0.31	0.32	0.24	0.40
avg_pre	0.27	0.28	0.26	0.29	0.29	0.28	0.29
MB	0.04	0.03	0.02	-0.02	-0.03	0.04	-0.11
RMSE	0.07	0.04	0.05	0.08	0.04	0.13	0.11
GE	0.06	0.04	0.04	0.06	0.03	0.10	0.11
MNB	0.26	0.15	0.10	-0.01	-0.11	0.15	-0.27

200708

depth	0.05 m	0.10 m	0.20 m	0.25 m	0.50 m	0.60 m	1.00 m
avg_obs	0.19	0.18	0.21	0.27	0.30	0.23	0.38
avg_pre	0.23	0.27	0.23	0.25	0.28	0.23	0.28
MB	0.04	0.09	0.02	-0.02	-0.02	0.00	-0.10
RMSE	0.07	0.09	0.09	0.06	0.02	0.14	0.10
GE	0.06	0.09	0.06	0.04	0.02	0.11	0.10
MNB	0.39	0.52	0.17	-0.02	-0.06	0.04	-0.25

200709

depth	0.05 m	0.10 m	0.20 m	0.25 m	0.50 m	0.60 m	1.00 m
avg_obs	0.24	NaN	0.30	0.25	NaN	0.21	NaN
avg_pre	0.21		0.22	0.23		0.20	
MB	-0.02		-0.08	-0.03		0.00	
RMSE	0.07		0.13	0.00		0.12	
GE	0.05		0.11	0.03		0.09	
MNB	-0.03		-0.16	-0.08		0.03	

200710

depth	0.05 m	0.10 m	0.20 m	0.25 m	0.50 m	0.60 m	1.00 m

avg_obs	0.21	NaN	0.23	0.26	NaN	0.17	NaN
avg_pre	0.20		0.19	0.22		0.17	
MB	0.00		-0.04	-0.05		0.00	
RMSE	0.06		0.06	0.05		0.09	
GE	0.04		0.05	0.05		0.07	
MNB	0.07		-0.14	-0.17		0.05	

Appendix G Isoprene calibration standard comparison

We compared an isoprene standard obtained in 2010 from Apel-Riemer Inc., FL, to a new one obtained as part of this project in 2014 from Scott-Marrin, Inc, CA. The comparison calibration lines, shown in Figure F1, are indistinguishable.
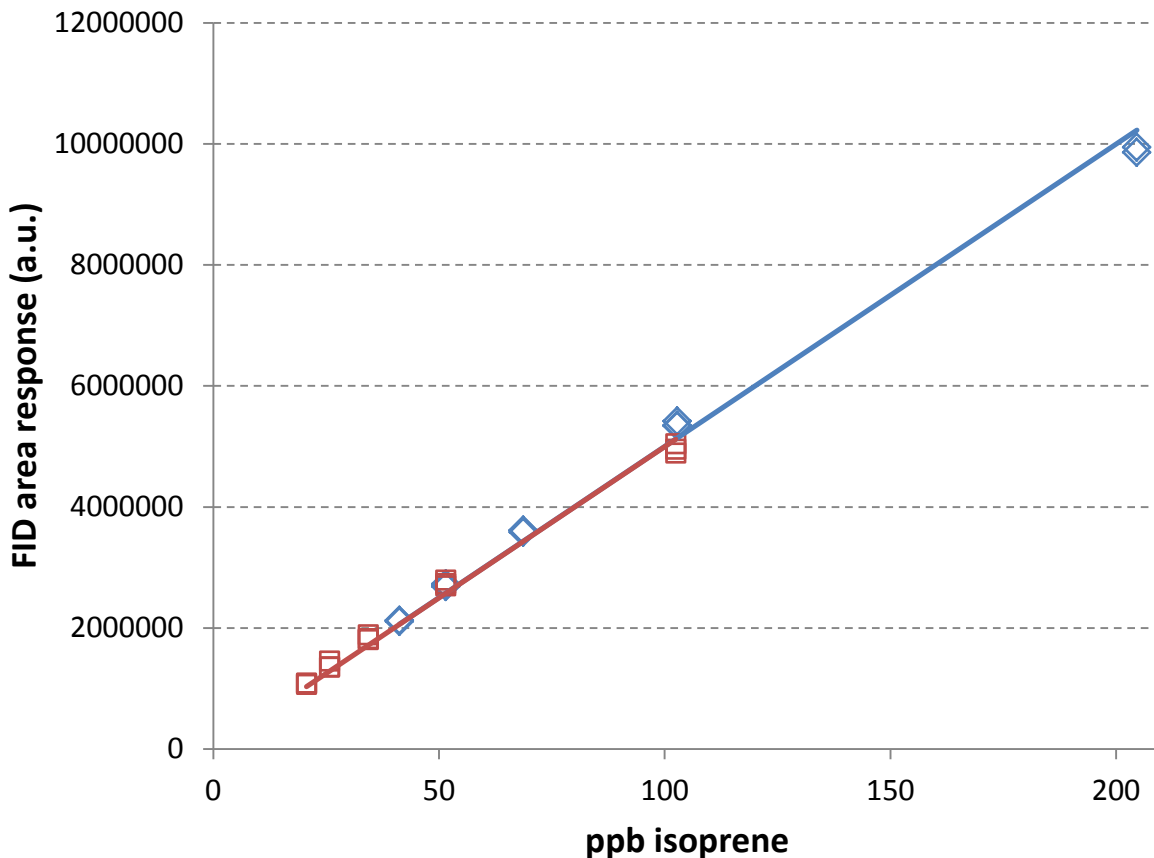

Figure F1. "Old" (2010) versus "new" (2014) isoprene calibration curve as obtained from dynamic dilutions of the gas standards with humidified zero air in early 2015. The regression coefficients r^2 were >0.99 in both cases and the slopes are virtually identical (approx. 50000 are units per ppb). Most sample isoprene concentrations obtained in this work were between 10 and 100 ppb.

Appendix H Greenhouse PAR, preliminary photosynthesis (µmol m^{-2} s^{-1}) and isoprene emission rate mid-September through early December
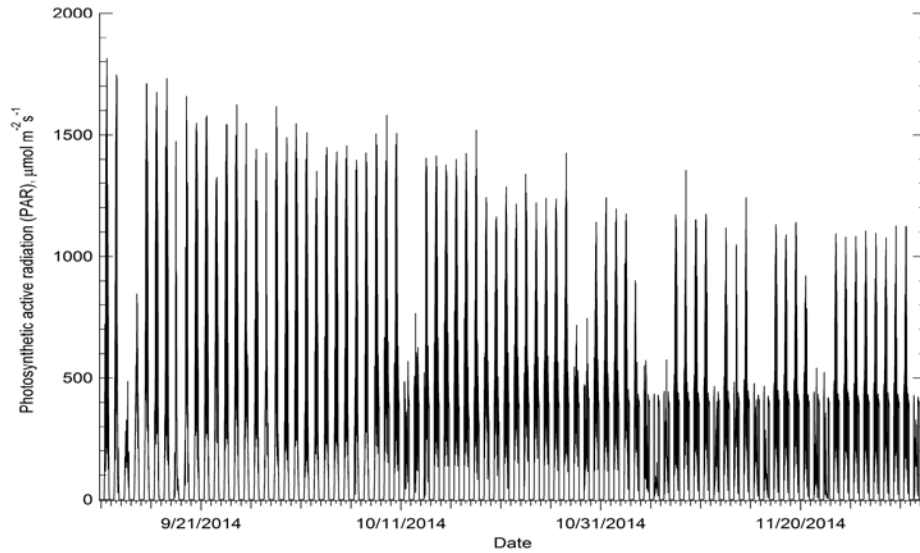
Greenhouse PAR mid-September through early December. Note decreasing light levels but maintenance of levels in November up to 1000 PAR units due to light supplementation.
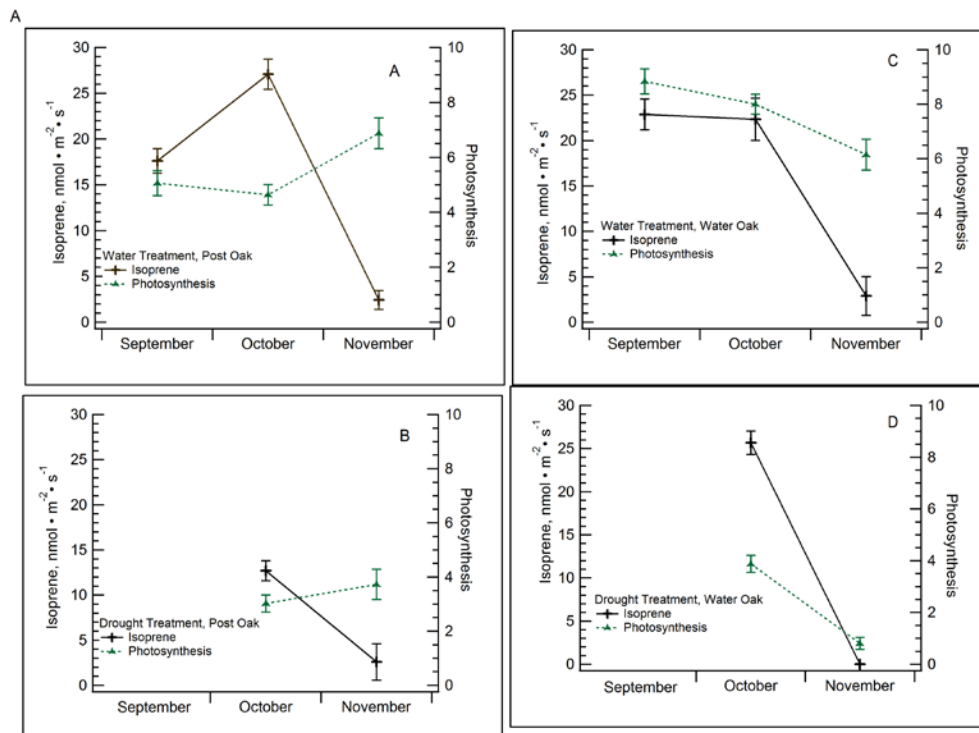
Preliminary photosynthesis (µmol m^{-2} s^{-1}) and isoprene emission rates from the greenhouse-based oak seedlings over time. Error-bars show variability (standard error, se).
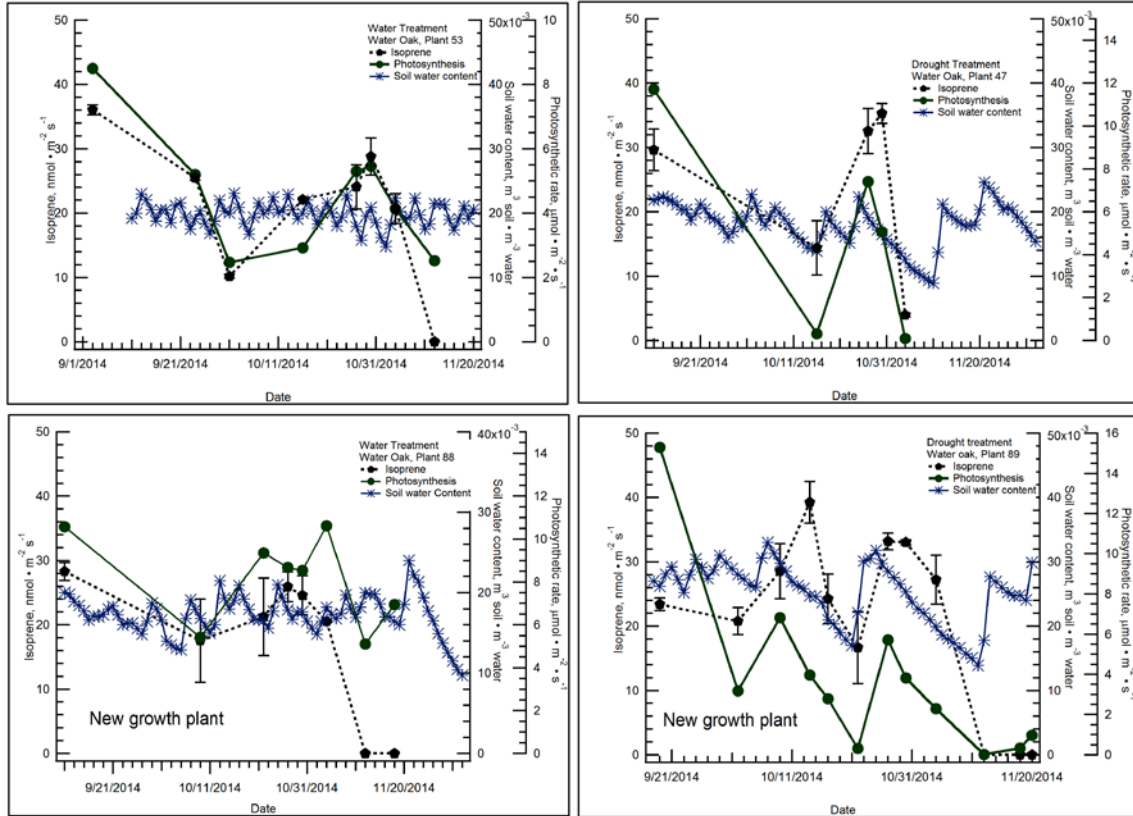
Preliminary photosynthesis and isoprene emission rates from four water oak seedlings investigated, two each per treatment group. Error-bars show variability (standard error, se).

Appendix I Basal emission rates from Texas oak species based on field measurements

Table G list several oak species and sweetgum we have measured isoprene emissions from under field conditions when no drought stress was present. The basal emission rates documented here were obtained during several field seasons as indicated, not necessarily covered by the 2014 AQRP grant.

Table G: Basal emission rates in microgram carbon per gram dry leaf mass per hour (μg C g^{-1} dw h^{-1}) plus/minus one standard deviation (using only pre-drought, May-June measurements for 2011).

year / species	post oak	water oak	southern red oak	southern live oak [1]	Texas live oak [2]	sweetgum
2011	74 ± 9	80 ± 11	87 ± 12			
2012				33 ± 8 [3]		
2013				48 ± 14 [4]		68 ± 14 [4]
2014					59 ± 16 [6]	
reference [5]	73	81	112	46	NA	68

[1] *Quercus virginianna* (at sites in the Houston metro area)

[2] *Quercus virginianna* var. *fusiformis* (at the Freeman Ranch in San Marcos)

[3] average of Dec 2011 and March 2012, 2011 leaves

[4] average of July and August 2013 field measurements

[5] Geron et al., 2001 (no error range given)

[6] only August values; reduced to 50±7 by October, possibly affected by late season; overall average: 55